ABSTRACT

Title of Document: DETECTION METHODS FOR COMMON PROBLEMS IN SOLAR HOME SYSTEMS

Mark Lomaskin, Rebecca Mahony, Lindsay Mooney, Ryan Robinson, Adam Teitelbaum

Directed By: Dr. Peter Chang, Ph.D
Civil and Environmental Engineering

Solar power is a valuable source of electricity for users in the developing world, yet many solar home systems are working at marginal capacity or not functioning at all. This study has two purposes: (1) to determine how common problems afflicting these systems affect the voltage output, and (2) to use patterns in voltage as a means of detecting these problems, via diagnostic tools. Team SHINE simulated common problems on experimental systems, collecting voltage data from the batteries and panels. Using these data, we created computer algorithms to detect the problem affecting the system. After testing several detection methods, it was found that the most successful performed at 86.5% accuracy. The algorithms can be used in future research to create a device for detecting these problems, allowing them to be addressed earlier.

DETECTION METHODS FOR COMMON PROBLEMS IN SOLAR HOME SYSTEMS

By

Team SHINE
(Students Helping to Implement Natural Energy)
Mark Lomaskin
Rebecca Mahony
Lindsay Mooney
Ryan Robinson
Adam Teitelbaum

Thesis submitted in partial fulfillment of the requirements of the Gemstone Program University of Maryland, College Park.
2009

Advisory Committee:
Dr. Peter Chang, Ph.D, Mentor
Fanny Missfeldt-Ringius, PhD, Discussant
Kaye L. Brubaker, PhD, Discussant
Jungho Kim, PhD, Discussant
Prakash Narayan, PhD, Discussant
Chrsitopher Davis, PhD, Discussant
Lindsay Madeira, Discussant

Acknowledgements

Team SHINE would like to recognize the numerous individuals and organizations who have assisted in making this research successful: The Gemstone Program, Dr. Wallace, and the remaining staff for their assistance, advising, and funding; Dr. Reinhard Radermacher, Ms. Mary Baugher, and the Center for Environmental Energy Engineering for the generous resources provided; B.P. Solar and Mr. Jay Miller for providing insight into photovoltaic production and the donation of experimental materials; our discussants, Dr. Fanny Missfeldt-Ringius, Dr. Kaye L. Brubaker, Dr. Jungho Kim, Dr. Prakash Narayan, Dr. Christopher Davis, Ms. Lindsay Madeira, Dr. David Lovell; our librarians, Nedelina Tchangalova and Damon Austin, for providing guidance during our research; and finally, our mentor, Dr. Peter Chang, for his continuous encouragement, enthusiasm, skilled guidance, and dedication to our project.

Table of Contents

List of Figures

List of Tables

List of Symbols

V	Voltage
I	Current
T	Temperature
σ	Standard Deviation
μ	Sample Mean
κ	Curvature
V_g	Gassing voltage
ΔT	Temperature deviation from 25 degrees Celsius
V_{fc}	End-of-charge voltage

Chapter 1 Introduction

1.1 Team SHINE

The Gemstone Program at the University of Maryland, College Park is a unique undergraduate research opportunity that allows students to participate in a three-year multidisciplinary team research project. Under the guidance of mentors and the Gemstone staff, Team SHINE (Students Helping Implement Natural Energy) consists of five undergraduate members of the Gemstone Program. The team was formed in the spring of 2006 driven by a common interest in the use of solar-powered electricity in developing nations. The team is performing its research under the guidance of Dr. Peter Chang, a professor of Civil and Environmental Engineering at the University of Maryland's A. James Clark School of Engineering.

Team SHINE's research goals arose from the group's concern about the quality of life in developing nations and the astounding failure rate of solar home systems in these regions. Team SHINE chose to focus on how common problems associated with photovoltaic systems affect the systems' voltage output. By collecting and analyzing voltage data, Team SHINE aimed to construct a diagnostic tool to be used in detecting these problems in implemented systems.

1.2 Context

Approximately two billion people in the world do not have access to the electrical grid, and ninety percent of these people reside in developing nations (Himann, 2008). Those living in such regions are limited in many aspects of daily life, including cooking, food preservation, cleaning, reading, purifying and

heating water, and many other activities common to those living with electricity. The majority of individuals not living on the electrical grid currently use hydrocarbon fuels or biomass, which includes wood, grass, and animal waste, for needs such as cooking (Solar Electric, 2008). However, the use of biomass as a main source of fuel not only depletes the environment, but gathering these resources also wastes hours of daylight that could be used more productively. Additionally, much of the developing world uses kerosene lamps for nighttime light. The problem is that kerosene emits cancer-causing smoke and causes approximately 20,000 injuries and house fires each year from spills (Solar Electric, 2008). Also, each home burning a kerosene-fueled lamp emits an average of six tons of carbon dioxide into the atmosphere in a 20-year period and is the primary source of greenhouse gases emitted from developing nations (Solar Electric, 2008, Himann, 2008).

Solar power is a proven solution to this problem that meets the needs of many citizens in the developing world who do not have access to the electrical grid. Solar power provides efficient, steady light that is safer for users and the environment when compared to traditional energy sources (Solar Electric, 2008). In fact, numerous rural communities in developing nations have been able to successfully implement solar powered systems as a source of steady electricity (Niewenhout, 2001, p.455). Access to electricity improves many aspects of users' lives in these rural communities. For instance, villagers are able to work after sunset, increasing their productivity beyond daylight hours (Solar Electric, 2008). Light helps to modernize the village and gives students the opportunity to read

and complete their homework at night. This bolsters education and literacy rates since school children are able to pursue academic interests beyond the daylight hours (Solar Electric, 2008). The installation of solar home systems at Myeka High School in the province of KwaZulu-Natal in South Africa created enough electricity to power a computer lab donated by the Dell Computer Corporation. Within a year of this installation the pass rate for students jumped from thirty to seventy percent, a clear example of how solar power can help to improve education (Solar Electric, 2008). Health clinics previously without lighting and certain medical equipment now have the ability to treat patients at night and use more sophisticated equipment. Additionally, clinics are able to refrigerate vaccines that are essential for survival in tropical regions (Solar Electric, 2008). Although lighting is certainly still considered a luxury for many developing communities, it is understood that the availability of light plays a major role in improving the quality of life for some developing areas (Gustavsson, 2005).

Solar powered systems are a solution to the lack of electricity for those unable to access the electrical grid; however, there are prominent issues to be considered with its use and implementation. Approximately 1.5 million solar home systems have been implemented in the developing world, yet 23% are only working at partial capacity while 15% are not working at all (Nieuwenhout et al., 2004, p.20). Solar power systems can incur a variety of problems which either decrease performance or cause system failure (Mapako, 2005). When these problems occur, members of the rural communities are often completely unaware the system is malfunctioning. In some instances the users alter systems to fit their

needs without knowledge of the effects on their systems. In other cases, the systems malfunction without any apparent cause and users are not equipped to recognize the problems (Instituto, 1998). Both of these scenarios lead to systems functioning at a lower capacity, ultimately leading to complete failure if the problem is not addressed (Energy, 2002). Projects also fail over time because of a lack of follow-up and poor capacity building by the implementers (Nieuwenhout et al., 2004, p.9). Additionally, systems are frequently installed in developing areas by implementers who lack full knowledge of how the systems work. Therefore, these implementers often offer inadequate information (usually limited to daily cleaning or maintenance procedures) to the future users of the systems. If any information is provided to the daily users of the systems, it is frequently limited to the basics, such as how to use the system or how to clean it (Energy, 2002). This gap in knowledge available to users of the technology leads to a disturbing lack of effective and efficient use of the panels. Even with extensive daily maintenance of the panels, there are still many common problems that plague the solar home powered systems, resulting from the implementation, user interaction, or other factors (Energy, 2002).

The problems affecting photovoltaic systems can be effectively separated into two groups: problems with the photovoltaic panel and problems with the battery. Problems affecting the solar panel include corrosion and dust accumulation on the panel. Problems affecting the battery include overcharging, deep discharging, use of a less effective type of battery, and a lack or misuse of a charge controller.

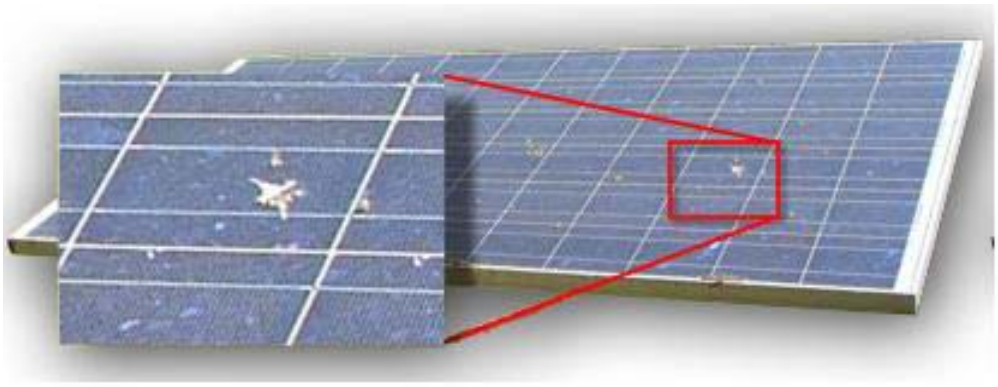

Figure 1: A panel with residue on surface

Overcharging and deep discharging of the batteries can degrade the batteries and cause a reduction in performance (Pearce, 2007). Another major factor in battery failure is the use of improper battery types. Most rural solar power systems use car batteries or "solar batteries" which are car batteries modified to have thicker plates to help with deep discharge (Van der Plas, 1998.). Car batteries or modified "solar batteries" typically will not last as long as a deep cycle battery, which is the type of battery better suited for photovoltaic systems. Incorrect battery use results in decreased system performance (See Appendix A).

Charge controllers are a crucial aspect of solar home systems as they regulate the flow of current to ensure a photovoltaic system's battery stays within a healthy range of voltage based on the type of battery. However, local users often believe the use of a charge controller is unnecessary. In one study, a survey of different solar power systems in Kenya found that only 10 percent of systems utilized charge controllers. Additionally, 18 percent of the systems with charge controllers had been altered to bypass the controller (van der Plas, 1998.). Although an isolated example, this is a common problem observed in developing

areas. Charge controllers are bypassed so that the user can draw more energy from the battery, even though this has serious consequences for the entire system. The controller prevents overcharging and deep discharging, both of which seriously reduce the life of the batteries. This potentially explains the high failure rate of batteries found in systems without charge controllers (van der Plas, 1998). A potential solution to a lack of charge controllers is the regular replacement of batteries in systems. However, continuous replacing of batteries can cause substantial financial strain on owners in developing areas; therefore, many owners continue to use poorly functioning batteries, thus having systems that work under capacity (van der Plas, 1998.).

In order to increase the effectiveness of the photovoltaic systems, the problems affecting the systems must be understood and easily identified. Table 1 presents these five previously described common problems, from their prevalence to their causes and effects. A detection tool for these common problems would provide considerable help to users with limited knowledge of how the systems work. Ideally, any problems affecting a system could be detected before permanent damage occurs. This would eliminate potentially expensive, long-term damage to the solar home systems, since the problem could be identified and addressed early. In order to identify the problems plaguing solar powered systems quickly and accurately, the development of a simple method for the detection of these problems is undertaken.

Table 1: SHS Common Problems

PROBLEM	PREVALENCE	CAUSES	EFFECTS	LONG-TERM DAMAGE
Overcharge	5-15% of solar home systems	Lack of proper charge controller; Poor user load management	Create excess heat production; increased corrosion on battery electrodes	Significantly decreases overall battery lifetime
Deep Discharge	5-15% of solar home systems	Lack of proper charge controller; poor user load management	Battery plate's active materials being utilized more than normal; high lead-sulphate presence in plates; formation of corrosive layer at the positive grid-active mass interface	Battery suffers from overall capacity loss; battery ages more quickly
Car Battery	5-30% of solar home systems	Mislabeling of batteries; choice of cheaper battery	Contain thinner battery plates, as are meant to be used for starting an engine	Shorter lifetime in PV applications
Lack of or Malfunctioning Charge Controller	~33% of solar home systems	Faulty equipment; User bypass	Can result in either overcharge or deep discharge of the battery	Ageing of battery; overall loss in battery capacity
Dirty/Dusty Panel	< 3% of solar home systems	Use of PV panels in arid, sandy, and windy climates near the equator	Less sunlight can reach the panel surface	If not cleaned, permanent loss in panel efficiency

1.3 Team Objectives

Although research has been conducted on solar home systems and problems affecting them, there are issues not fully addressed in the literature. The vast majority of existing research comes in two main forms. The first is aimed at either describing or identifying the causes of the common problems prevalent in solar home systems of developing countries. The second type of research aims at improving the existing technology of solar home system components. This is where a large amount of money is invested (e.g. improving solar panels, charge controllers, etc.). While improving solar panel efficiency is important for the future viability of solar power, a more immediate problem of detecting problems in the field needs to be addressed. There is a significant lack of research into the field of detection methods for common problems that are resulting in the failure of these systems. When many systems are failing or not functioning to full capacity, improvements in efficiency of components are all for naught.

The existing research concerning detection schemes is based in theory versus actual application and is limited in outlining effective methods for implementation versus providing immediate advice for users. In order to add to the current body of research and fill the significant research gaps surrounding detection methods, this project seeks to identify unique voltage output signatures for common problems in solar home systems. These patterns will then be utilized to effectively identify similar problems in other systems. The fundamental research question driving our project is:

- Is it possible to create a tool that efficiently and effectively diagnoses common problems on affected solar home systems using unique voltage data gathered from problem simulations?

Chapter 2 Background

This paper analyzes several common causes of solar home system failure, as well as methods for their accurate detection. A comprehensive literature review was performed in order to demonstrate the need for a detection tool, outline the major causes of system failure, and describe potential methods for problem identification.

Team SHINE's research adds to the existing literature by concentrating on an issue yet to be addressed by prior research. This study is unique as there has been little research performed to address a way to use patterns from obtainable measurements, such as panel and battery voltage, in order to create a detection tool that informs users of the causes of reduced performance in their photovoltaic system. This detection tool will identify the causes of reduced performance in solar power home systems of the developing world and alert the user so the problem may be addressed.

The first part of this literature review is an examination of the research previously conducted on each component of the system: the charge controller, the battery, and the panel. These three parts are where the majority of problems arise with solar home system. Then, past studies that have attempted to solve these problems concerning solar home systems will be discussed.

2.1 Potential Problems of Photovoltaic Systems

2.1.1 Charge Controller

Charge controllers are important elements in photovoltaic systems. The controllers regulate the flow of current from the solar panel to the battery to ensure the battery is not overcharged or deeply discharged (Dunlop, 2001). Misuse or lack of a charge controller in a photovoltaic system may cause significant damage to the battery; therefore, proper use is vital to system health. Battery manufacturers often provide recommended charge regulation set-points so the battery can be kept at an adequate state of charge, avoiding the degrading effects of incorrect charging (Dunlop, 2001). The literature has established charge controllers are an essential part of the solar home system, and their misuse or failure is a significant problem in the developing world.

Charge controllers, as their name suggests, regulate the amount of charge to the battery. There are two main types of controllers: "series" and "shunt": since they have both proven to be equally effective in practice, the minor differences are not important for this study's purposes (Instituto de Energia Solar, 1998, p.20). For more information on type and quality of charge controllers, see Appendix B. The battery guide for solar applications published by the International Energy Agency lists several positive effects of utilizing a charge controller. First, for a flooded lead-acid battery, a charge controller lessens the amount of water loss in the battery (meaning it has to be topped off less often) (International, 1999). Additionally, by limiting overcharge periods, the charge controller allows less acid to deposit in the battery's electrodes (International,

1999). This makes the battery easier to maintain, and will help the battery last longer.

Previous research demonstrates the negative effects absence of or malfunctioning controller can have on the photovoltaic system. A review of the literature on the subject shows about one-third of all solar home systems experience problems with the charge controller (Nieuwenhout et al., 2004, p.36). In one study, fourteen stand-alone photovoltaic systems were tested to determine the importance of charge controller set-points on preventing overcharge and deep discharge (Woodworth, 1994). For two of these systems, the charge controller malfunctioned. In the first case, the controller did not regulate the system at all, and it tried to charge the battery until sunset on clear days, ultimately overcharging in the battery. This severely corroded the positive grid (Woodworth, 1994, p.940). In the other malfunctioning cases, the controller had no low-voltage disconnect, equating to a lack of protection against deep discharge. Therefore, after a cloudy period, the controller could no longer function properly, which locked the overall system into a non-functioning state (Woodworth, 1994). This study demonstrates how a malfunctioning charge controller can drastically alter system health.

In another study where photovoltaic batteries were treated over several years, authors found that when items with operating motors (such as refrigerators or pumps) are hooked up to a system, they can falsely trigger charge controller set-points (International, 1999). These set-points are meant to keep the battery in the correct state of charge; if they are falsely triggered, the controller itself

becomes useless. This results in similar effects as if the charge controller is absent completely. In one study, 83 rural solar-powered communities in Mexico were surveyed and 555 batteries used in their system were tested. One of the most significant findings was that malfunctioning charge controllers frequently result in battery failure. For example, in one case, a battery cracked open because of the combination of a malfunctioning controller and the use of wrong battery caps (Huacuz, 1995, p.287).

One of the most alarming issues with charge controllers can be completely controlled involves user interaction. Approximately one third of solar home systems experience problems with the charge control. From this group, half of these systems are either missing the charge controller or it has been bypassed. One of the startling findings of the above Mexico study was that 21% of users utilized an override switch available on their charge controllers making the charge controllers pass the designed regulatory set points (Huacuz, 1995, p.292). In Indonesia, 58% of respondents to a survey admitted they would bypass the charge controller after the low voltage disconnect went into effect (Nieuwenhout et al., 2004, p.35). Essentially, when the load should have been cut off to protect the battery from deep discharging, the users overrode this in order to continue to drain power from the battery. This type of activity drastically affects the heath of solar home systems overall.

We aim to build upon this literature by creating a system to detect when a charge controller is not working properly, whether due to user interaction or malfunctioning equipment. It has been shown that the controller is essential in

maintaining the health of a photovoltaic system, and therefore can be detrimental when the charge controller is not present or malfunctioning. Because this is a common problem in systems implemented in the developing world, its detection would be beneficial although bypassing of the charge controller may remain a problem.

2.1.2 **Photovoltaic Panel**

The photovoltaic panel is the means by which the sunlight is captured to feed the solar home systems with needed power. The solar panels are positioned at a near-horizontal angle to take advantage of the sun's position in the sky at many locations close to the equator. These environments can be arid and dusty, and they are sometimes prone to sandstorms. This low panel angle and atmosphere causes sand or dust to accumulate on the surface of the photovoltaic panel, blocking out the sunlight. Past research has shown that this can have several negative effects on the system as a whole.

One study aimed to correlate the sand dust accumulation on the panel with loss of panel efficiency (Al-Hassan, 2005, p. 187). The authors did this by installing a system on the roof of a building in Kuwait and measuring the current-voltage characteristics between a panel that was cleaned and another allowed to accumulate dust (Al-Hassan, 2005, p.190). The authors found the short-circuit current and the maximum output power decrease significantly as the amount of sand dust particles accumulated on the module surface increases (Al-Hassan, 2005, 196). They also estimated the decrease in photovoltaic module efficiency due to dust accumulation on module surface was approximately equal to 33% for

each 1 g/m^2 of sand or dust accumulation (Al-Hassan, 2005). They have shown dust on the panel significantly degrades the panel's efficiency, thus affecting the overall system's efficiency as well.

In a similar study in Egypt, the effect of dust accumulation was measured, but this time using different tilt angles of the panels (Hegazy, 2001, p. 525). Nine glass plates were set up at different angles, and each was weighed after certain time periods to measure dust accumulation (Hegazy, 2001, p. 529). The authors discovered the general level of solar transmittance decreased as the number of days of exposure to the environment increased (Hegazy, 2001, p. 531). Additionally, the tilt angle was found to be a factor. Hegazy concluded the more horizontally oriented the panels were, the more dust accumulated. A horizontal panel accumulated nearly double the amount of dust as a panel at 45 degrees (Hegazy, 2001, 529). This study further established the importance of tilt angle and environmental considerations.

When solar home systems are implemented, users are commonly instructed to clean the panel. A survey in Chile reported that 91% of users were instructed to clean their panels when the systems were first implemented (Nieuwenhout, et al., 2004, p.11). Despite the instructions, the users did not perform this essential task. Many of the elderly members of the community were unable to clean the panels because the modules were too high to reach and some of the younger members even refused to clean them, as they did not understand the purpose (Nieuwenhout, et al., 2004, p.11). Studies have shown a large increase in efficiency if the panels are cleaned. For example, in Indonesia, 11

year-old photovoltaic panels that had not been regularly cleaned had an increase in power output from 32% to 57% of nameplate power once cleaned (Nieuwenhout, et al., 2004, p.11).

These studies have shown dust and sand accumulation to be an important factor in the effectiveness of a photovoltaic system. If the panel's efficiency is reduced, the full potential of the system is also being reduced. If users realize dust is accumulating early on, they can address the problem by cleaning the panel.

2.1.3 **Batteries**

Within the solar home system set-up, the battery is a crucial link between the solar panel and needs of the user. The battery serves as the storage device for energy coming from the solar panel, allowing users to utilize this radiation after the sun sets for light and other needs. However, due to the high demand placed on batteries in solar home systems, great care and awareness must be paid to this portion of the system. On a system lifetime basis, batteries contribute most to the life-cycle cost, and most of the serious problems with solar systems are battery-related (Nieuwenhout et al., 2004, p.36). There are a group of common problems affecting solar home system batteries due to their use, as well as the intrinsic nature of the battery. These problems can be alleviated through the correct regulation of the batteries, and with many studies aiming to explore the exact and best regulation process needed to achieve this. To better understand the overall health of the battery within a system, there has also been extensive research to determine the state of health of batteries.

The battery is a crucial component of the photovoltaic system as it is the storage point for all solar energy to be utilized. Many different types of batteries exist for this purpose including Lead-Acid, Nickel-Cadmium, and Nickel-Lead batteries. Each of these types of batteries has unique characteristics and components, as well as advantages and disadvantages. The most common form for photovoltaic systems is the Lead-Acid battery. It will be discussed at greater lengths due to its significant prevalence.

2.1.3.1 Types of Batteries

Batteries are divided into primary and secondary categories. Primary batteries can only be used once, as the chemical reactions that occur within them are irreversible and use up all active material (Linden & Reddy, 2002). These batteries are commonly used in applications such as flashlights, radios, and toys. Secondary batteries, also known as rechargeable, can be used, charged, and reused. This means the chemical reactions are able to be reversed for regeneration of the active materials. These batteries are used in a wide variety of applications, from cars to lighting to PV systems. In particular, PV systems utilize one of three types of secondary batteries: Lead-Acid, Nickel-Cadmium, of Nickel-Lead (Kiehne, 2003).

2.1.3.2 Lead Acid

Lead-Acid batteries are composed of plates, lead, and lead oxide. The system is set-up with a positive electrode, negative electrode, and electrolyte solution. The batteries work on the premise of a reversible chemical reaction involving the oxidation of lead. The battery needs all of the active materials, including those located at the positive electrode, negative electrode, and

electrolyte to function. The reaction of lead and lead oxide (located on the plates) with the sulfuric acid electrolyte produces a voltage (Linden & Reddy, 2002).

The positive electrode can be structured in various ways, including a pasted grid, tubular plates, or rod plates. The positive electrode's purpose is to supply electrons that allow charging of the battery. Pasted grid plates are commonly used in car batteries due to the high amount of energy, but low deep-discharge ability. The plate is a lead grid through which material passes. This is typically lower in price, however corrosion is common as material passes through the plates, meaning limited reliability and unknown lifetime. Tubular plates are another option, composed of a lead spine with plastic tubing around it with the active mass between these components. This format allows for high energy for a given volume and good deep discharge properties. Rod plates are the final common type of positive electrode, composed of vertical rods with the active mass around the rods in an enclosed pocket. These ensure thorough use of the active material, giving a high current ability and reliance (Berndet, 1926).

The negative electrode of Lead-Acid batteries is always made of a pasted grid plate, composed of spongy lead in comparison to the lead oxide of the positive electrode (Berndet, 1926).

The electrolyte of Lead-Acid batteries is diluted sulphuric acid. Throughout the reaction the sulphate ions are consumed as discharging occurs, while during charging the strong acid is regenerated at the surfaces of the electrodes (Berndet, 1926).

This basic structure to the Lead-Acid battery is kept throughout the three main types based on construction: Flooded, Gelled and Absorbed Glassed Mat. Each of these types of batteries has qualities which make them valuable for different applications. Lead-Acid batteries can also be divided into categories based upon application: Automotive, Marine, and Deep Cycle (Baxton, 2006).

2.1.3.2.1 Construction

2.1.3.2.1.1 Flooded/Open

Flooded Lead-Acid batteries, also known as Open Lead-Acid batteries or wet batteries, were the first type of battery designed in the category. These batteries are known as wet due to the liquidity of sulphuric acid solution. They have removable caps to allow topping off of the solution and small vents, making them open. During operation, hydrogen and oxygen are produced at the electrodes. These gases are allowed to vent from the battery through the small holes in the top (Baxton, 2006). In the case of over-charging, these batteries can lose large amounts of water via the vents. For these reasons related to the charge cycle, flood lead-acid batteries must have their solutions topped off frequently. They are potentially very dangerous due to the liquid electrolyte within them, making them difficult to use in some applications. They also must be kept in open, well ventilated areas to ensure the fumes are allowed to be expelled from the area. These batteries are relatively cheap, making them the most common in many rural implementations of PV systems where the disadvantages do not outweigh the need to be cost efficient (Crompton, 2000).

2.1.3.2.1.2 Gelled

Gelled lead-acid batteries are sealed batteries, with a few being valve-regulated. Valve-regulated designated the battery as a recombinant battery, where the oxygen and hydrogen generated during operation on the electrodes will recombine, eliminating the loss of water of other batteries. These batteries use gelled acid, where the electrolyte has been added to silica gel, resulting in a less hazardous battery that does not need to be maintained in a constant upright position. They are more resistant to temperature and movement problems. However, gelled lead-acid batteries need a slower charge rate to prevent excessive gassing and a lower charge voltage, as overcharging can leave holes in the gel matrix which reduces capacity of the battery (Crompton, 2000).

2.1.3.2.1.3 AGM/VRLA

Absorbed Glass Mat batteries, commonly known as dry batteries or valve regulated lead-acid batteries, are distinct due to their boron-silicate glass mats located between electrode plates within the battery. These batteries are also sealed completely against fumes leaving and do not leak any type of acid if broken. There is no continuous maintenance required and water loss is limited via the same mechanism found with the gelled lead-acid batteries. These batteries are very useful for PV systems because of their ability to be placed in almost any location without needing to consider venting or temperature. Their low self-discharge rate and sealed nature are also beneficial. These batteries are significantly more expensive than the alternatives, limiting their use (Anthony et al., 2004).

2.1.3.2.2 Applications

2.1.3.2.2.1 Car

The car battery, also known as the starting battery or SLI (Starting, Lighting, Ignition) battery, are batteries commonly used for the starting and running of engines. These batteries provide a surge of current for a short period of time, which works well for starting engines. The plates within these batteries are often very thin, porous (sponge-like), and very numerous. The design of the plates is to increase the overall surface area to allow for the large surge of current needed. In cars, once the initial ignition occurs, the alternator takes over as the power source. Starting batteries are never drained more than 20% of the total capacity. When this type of battery is put through deep cycles the porous plates are consumed and can no longer function. This leaves the battery working well below the initial capacity and, eventually not able to function at all (Dell & Rand, 2001).

2.1.3.2.2.2 Deep Cycle

The deep cycle battery is constructed of much thicker plates than the other types, which allows prolonged discharging. Unlike the other two types of batteries, deep cycle batteries are able to be discharged to as low as 20% of capacity many times with minimal overall capacity loss (Dell & Rand, 2001). Not only are the plates of the deep cycle battery thicker, they are usually made of solid lead. The main purpose of this battery is to deliver a sustained voltage to its load over time. Deep-cycle batteries are typically used in PV applications, as well as for backup power and other applications needing long, continued energy (Farret & Simões, 2006). Although, deep cycle batteries can be reduced by 80% of their full

capacity, it has been found that only discharging to 50% of capacity can double the lifetime of the battery.

2.1.3.2.2.3 Marine

Marine batteries can be considered a hybrid of the car and deep cycle battery. The plates of the marine battery are porous; however the material is coarser than that found in starting batteries. This ensures the battery will still generate considerable starting power, but will be able to function over a longer period of time, similar to a deep cycle battery (Payne, 2003).

2.1.3.3 Nickel Cadmium Batters

Nickel Cadmium batteries are a type of alkaline storage battery. These batteries consist of a positive active material of nickel oxide and a negative area containing cadmium. This type of battery boasts advantages such as low self-discharge rates, they are non-freezing and have a long life if not used with high frequency. However, there are disadvantages to these batteries that make them very difficult to use in PV systems. The disadvantages include low efficiency relative to lead-acid batteries and non-standard voltage and charging. From an economical standpoint, nickel cadmium batteries are also of limited applicability as they are very expensive and have a high disposal cost, as cadmium is very hazardous and has specific disposal procedures (Kiehne, 2003).

2.1.3.4 Nickel Lead

Nickel lead batteries are an alternative to the lead acid and nickel cadmium types of batteries for PV systems. Nickel lead batteries have anodes made of a steel wool substrate with the active material being iron. The cathodes in

this design are made of nickel plated steel wool with nickel as the active material. The electrolyte is potassium hydroxide (Gaters Energy Products, 1997). Although these batteries can be used in PV systems, their disadvantages far out weight any potential advantages. For instance, they are known to have very low efficiency, a high rate of self-discharge, high water consumption, high internal resistance (inconsistent voltage across cells which can cause lower capacity), varied output of voltage, and these batteries must typically be very large. Due to the high self-discharge rates, these batteries often necessitate a much large solar panel for charging to make up for the energy loss and are difficult to use for lighting as the changing voltage causes fluctuating light (Farret & Simões, 2006).

2.1.3.5 Cycles

Lead-acid batteries are most often used in PV systems, the cycling patterns of this battery will be further examined. The basic cycle consists of a charging phase and then a discharging phase. As a group the lead-acid batteries follow a similar pattern, with potential problems being examined at great length once the normal pattern has been established.

2.1.3.5.1 Charging

Charging of lead-acid batteries occurs in four distinct stages. The first stage is the main charge, where the battery achieves charging between 90% and 95% of full capacity. The next stage, top-off charge, will bring the battery to its full 100% charging capacity. The equalization charge is achieved when the maximum charge level has been reached by all cells within the battery, often facilitated by a special controller. Reaching the equalization charge will help ensure maximization of the battery's life. The final charge state is the

maintenance charge, the least frequent charging stage. Here the goal is to ensure the battery stays at full charge (Crompton, 2000). For lead-acid batteries, charging is known as "opportunity charging," because the battery may only be partially utilized between charging capable times, such as during the day, the battery is rarely fully drained and therefore the battery is partially charged very frequently (Baxton, 2006).

2.1.3.5.2 Discharging

Lead-acid batteries begin to discharge when a load is applied to them. A chemical reaction occurs between the sulfuric acid and the lead plates which generates a coating of lead sulfate on both the positive and negative electrode. This process is known as sulfation. The batteries voltage will drop as the sulfation continues, with the electrodes being covered in a very thick layer of lead sulfate. At this point the battery is completely discharged. Recharging will facilitate the reaction of lead sulfate back to sulfuric acid and lead (Gaters Energy Products, 1997).

2.1.3.6 Potential problems

The complex charging cycles of lead-acid batteries result in a few common potential problems that are frequently encountered in PV systems.

2.1.3.6.1 Overcharging

Overcharging occurs in PV systems when the battery is allowed to charge even when the battery is at full capacity. This situation can occur on very sunny days, where the PV panel absorbs a large amount of solar radiation, or if the battery has not been completely discharged (Lugue & Hegedus, 2003).

Overcharging can cause damage to the battery in several ways. For "wet" lead-acid batteries, the most common type in PV systems, overcharging can result in bubbling of the electrolyte fluid. As the acid is stirred, gas can form and be released. This is called gassing. The electrolyte fluid will become more acidic and begin to fizz, putting potentially harmful chemicals into the air. If not in a highly ventilated area, gassing can be extremely dangerous for people in the vicinity. Gassing is not healthy for the battery, and can result in lowered electrolyte levels in the battery. This will expose the electrodes to air and decrease the capacity of the battery permanently and can increase corrosion. The high temperature of the battery during overcharging will also increase the corrosion rate. Corrosion occurs at the electrodes. This can result in active material falling from the electrodes and severely decreasing capacity for charging over time (Farret & Simões, 2006). To eliminate this problem, a charge controller should be utilized to ensure overcharging is stopped. Levels of electrolyte should also be checked and re-filled as needed. If overcharging patterns are identified early, the user can implement changes to ensure this does not continue (Lugue & Hegedus, 2003). One possibility is covering the PV panel on especially sunny days if the battery has not been used frequently. Another possibility is discharging the battery on a nightly basis, by always leaving a light running. This will ensure the battery is drained by the next day's sun to make sure overcharging does not occur (Solar Energy International, 2004). Users should also stay aware of the noises and gases coming from the battery, and ensure it is in an open area where it can be observed.

2.1.3.6.2 Deep discharging

Deep discharging occurs when a lead-acid battery is allowed to discharge, then remains in a very low state of charge for an extended period of time. It is defined as discharging a battery below 20% of its full capacity (Lugue & Hegedus, 2003). This can lead to lead sulfate being left on the electrodes within the batteries, a condition known as sulfation. Sulfation slows down the charge and discharge reactions. It also causes longer charging times, incomplete charging, and excessive heat generation. Even with a charge controller, this slowing of the reactions can cause the controller to cut-off charge and discharge cycles at inappropriate times. In this way the battery will lose capacity earlier and age quickly (Bergveld et al., 2002). If lead sulfate is allowed to stay on the electrodes, lead sulfate crystals can form. These crystals are very hard and impossible to remove from the electrodes in a safe manner by the average user. Therefore, it is known as irreversible sulfation. Deep discharge can also be avoided by using an appropriate charge controller (Lugue & Hegedus, 2003). However, once irreversible sulfation has occurred on a battery's electrodes, the battery can never regain full capacity and should be replaced. If a PV system is being used frequently and/or for long periods of time, the user may want to find alternative ways to provide electricity or try to lower the use (Solar Energy International, 2004). This is a hard process to monitor as the voltage changes primarily occur within the battery, however decreased capacity coupled with high usage would indicate a deep discharge problem.

2.1.3.6.3 Correct Battery Use

2.1.3.6.3.1 Overcharge

Overcharging of the battery is a common contribution to the failure of photovoltaic systems in rural applications. Widespread literature has shown overcharging can damage the battery in several ways, and several previous studies have attempted to simulate the effects.

Overcharging has been documented as one of the main causes of decreased performance in the most common battery types utilized with photovoltaic systems, Valve-Regulated Lead-Acid batteries (VRLA batteries). Within this larger category of batteries, there are several subsets including flooded lead-acid, gelled electrolyte, and Absorption Glass Mat batteries, with the latter two being classified as sealed lead-acid battery devices. One study utilized batteries post mortem from photovoltaic systems to discover the impact of over-charging on the VRLA batteries. The batteries were first run in a standard solar home system, with a variety of different VRLA batteries being used under varying conditions. The battery was allowed to cycle through the charge-discharge process, just as they would in real life applications. It was found recrystallization of the positive electrode of the battery during discharge was the primary cause of problems with the battery. This recrystallization build-up decreased the batteries ability to recharge over time, resulting in poor performance of the battery overall (Mattera et al., 2003).

When a battery is overcharged, there is an increase in gassing (Dunlop, 2001, p.276). The acid in the battery cell is stirred and gas evolves because of chemical reactions taking place inside the battery, concentrating strong acid and

thus increasing the corrosion of the battery electrodes (Yang, 2006, p.286). Overcharging can also create excess heat production, which can further accelerate the ageing of a battery (Spiers, 1995, p.246). The charge controller attempts to restrict overcharging for these reasons, but as shown in an earlier example, the controller cannot always be relied upon. In one study, a battery without overcharging protection was tested to see how the lifetime of the system was affected (Yang, 2006, p.284). It was found if overcharging occurs in about six months out of a year, then the lifetime of the battery is about half the expected lifetime after two years of this pattern(Yang, 2006, p.286).

Batteries are especially susceptible to overcharging in photovoltaic applications. First, many of the batteries used in these systems are valve regulated lead-acid batteries. Electrolyte cannot be added to these batteries (unlike flooded lead-acid batteries), thus, their tendency for overcharging increases (Dunlop, 2001, p. 276). Overcharging can occur during the summer because batteries are overcharged during periods of intense sunlight (Yang, 2006, p. 285).

Overcharging is a serious problem that affects the ageing of the battery, and it is especially common in photovoltaic applications. By analyzing this along with other problems in our study, we aim to detect overcharging early, so as to lessen its harmful effects.

2.1.3.6.3.2 Deep Discharge

Deep discharge has also been established as a major cause of ageing for batteries in photovoltaic applications (International, 1999, p.8). Deep discharge

occurs when the battery is drained below an adequate state of charge, and it can result in a permanent loss of charge capacity as well as poor rechargeability.

In one study, tests were conducted on lead-acid batteries for a six-year period under simulated photovoltaic conditions (Spiers, 1995, p.247). The researchers found that after a long period of deep discharge, batteries suffer from some overall capacity loss (Spiers, 1995, p.251). This capacity loss results in the battery being unable to fully charge. Additionally, a deep discharge at a low rate means that the battery plate's active materials are being utilized more than normal due to the extended time and lower charge state. If this occurs (e.g. during a period of very cloudy weather), the battery can be very slow to fully recharge (Spiers, 1995, p. 246).

In another study, batteries used in photovoltaic systems were examined post-mortem (Mattera, 2003, p. 248). For batteries used in stand-alone domestic applications, the following problems were discovered: (1) Irreversible sulphation, as evidenced by a high lead sulphate presence in the charged positive and negative plates, (2) Electrolyte stratification, in which the lead sulphate gradient between the top and the bottom of the positive plate and negative plate indicates the presence of electrolyte stratification in both plates, (3) Formation of a corrosion layer at the positive grid-active mass interface, and (4) Textural change of the active mass- decrease in the porosity of the positive active mass (Mattera, 2003, p.250). These are all factors that cause a battery to age. Similar to previous studies, this study found poor rechargeability results after a long period of deep discharge. This occurs because the deep discharging causes a distribution of new

crystals on battery plates leading to poor electronic contact making recharging more difficult (Mattera, 2003, p.256).

These studies have shown that deep discharging can cause serious problems in photovoltaic systems. Batteries suffering from deep discharge become unable to charge completely and lose their effectiveness over time. We will take this research a step further by aiming to create a way to detect deep discharging aiming for early changes in the system functioning to prevent long-term negative effects.

2.1.3.7 Regulation of Battery

2.1.3.7.1 Need for voltage cut-off

Many studies have considered how to best eliminate the overcharging of VRLA batteries. In fact, a variety of studies went about this in a similar format to our study. In one study, researchers took batteries attached to simulators to mimic typical patterns in charging and induced overcharging on a portion of the batteries. Through evaluation of parameters over time, including porosity, electrode balance, acid compensation, and other factors, it was found some sort of protection was needed to ensure batteries stayed within specific ranges of charge, ensuring overcharge did not happen. In many instances, it was also noted temperature compensation needed to be factored into these limits as well. The research indicates that with protection and temperature factors, there could be limits set to regulate the batteries to best prolong life and avoid unhealthy charging cycles (He et al., 2001).

2.1.3.7.2 Finding correct cut-off

The need for exact limits on voltage for batteries led to an increase in research investigating how to find appropriate cut-off points for batteries. These voltage cut-offs are a necessity to prolong life and health of VRLA batteries in use. One study looked to supply this information, using previous data and mathematical simulations to find cut-off voltages for a given group of common VRLA batteries, looking for both the gassing voltage and end-of-charge voltage. An equation was determined whereby batteries could be regulated within a given range of voltages (Vela & Aguilera, 2006):

$$V_g = \left(a_g + b_g \ln(1+I)\right)\cdot\left(1 + c_g \Delta T\right) \tag{2.1}$$

$$V_{fc} = \left(a_{fc} + b_{fc} \ln(1+I)\right)\cdot\left(1 + c_{fc} \Delta T\right) \tag{2.2}$$

In which, V_g is the gassing voltage, I is the charge current, ΔT is the temperature deviation from 25 degrees Celsius, and *a, b,* and *c* are empirical parameters to be determined for each battery. In the second equation, V_{fc} is end-of-charge voltage. These equations factor in current rate and temperature to better approximate what these cut-offs should be. However, this was impossible to apply to a wide range of batteries consistently due to their design differences, but still established a means for finding these voltages experimentally for maximizing operational efficiency in regulation (Vela & Aguilera, 2006).

2.1.3.7.3 Floating Charge Regulation

The ability of a system to cut off voltage when a battery is charged completely has been established as crucial to prolong battery life. Regulation of batteries was taken a step further with research examining the concept of floating

charge regulation, where the regulatory set points for charge control change dependent on the circumstances. Due to the complex nature of batteries, there were a variety of floating charge schemes proposed to account for the changing environment of a battery and the changes within the battery itself. In one study five of the most common floating charge regimes were analyzed: constant voltage charge, constant current charge, constant current-constant voltage charge, intermittent charge, and interrupted charge control. Temperature was also considered within this floating charge, as temperature has proven to have a drastic affect on VRLA batteries. Ultimately, the study found the interrupted charge control regime was most effective in regulating batteries' end voltages, lowering the amount of overcharging and deep-discharging occurring within the batteries (Wong et al., 2008).

2.1.3.8 Incorrect Type of Battery Used

Another problem affecting photovoltaic systems is the use of car batteries, as opposed to the appropriate deep-cycle batteries. Though some batteries are made specifically for photovoltaic purposes, car batteries are often used because of local availability and lower costs (Huacuz, 1995, p. 287). They are the the cheapest to purchase in terms of nominal capacity. Additionally, because they are produced locally, these batteries can be recycled; this can reduce possible negative environmental side effects of batteries being disposed incorrectly (Instituto de Energia Solar, 1998, p.12).

Nonetheless, automotive batteries, specifically designed to provide cranking power to motor vehicles, are problematic in photovoltaic applications. The plates in car batteries are not as thick as in a deep cycle battery, as they are

only meant to provide short periods of output (for starting the vehicle), whereas deep cycle battery provide long continuous output. Therefore, they are very sensitive to deep discharge, and have a short lifetime in photovoltaic systems (International, 1999, p.14). For this reason, deep cycle batteries are recommended for photovoltaic applications, since they have a much larger battery lifetime and therefore reduce costs in the long run. Another possible alternative are modified car batteries. These batteries are altered so that their plates are thicker and they include a larger quantity of acid solution. This provides for a battery that is still relatively inexpensive and has a longer lifetime than conventional automotive batteries thought still lower than deep cycle battery (Instituto de Energia Solar, 1998, p.13).

Due to the common incorrect use, part of our project was designed to simulate the use of a car battery for a photovoltaic system. Because these are used often, especially in systems implemented in the developing world, we have further studied the effects of the use of these batteries on the health of the systems.

2.2 Solutions

2.2.1 Maintenance Changes

Implementing solutions to these common problems can be both burdensome and time consuming, varying by location. When the systems are located closer to metropolitan areas, solutions may be more widely available as there are more resources present. In remote areas, implementation can become very costly and difficult to arrange. This difficulty can stem from a lack of

understanding of the solutions as well as overly complex regulations that may limit the movement of the materials necessary for these solutions (Zahedi & Hallenstain 2007, 108). A major hindrance is associated with the very high cost of getting information back to a location to be processed (Mapako 2005). Some systems use satellites to monitor and then send information to centralized locations to allow recognition of problems arising with panels, though this is expensive and mainly used in grid-connected photovoltaic systems (Drews, 2007, p. 563). Perhaps a more efficient and effective method for monitoring off-grid systems would be a device to diagnose problems via direct attached to the systems.

2.2.2 **Educational Solutions**

Solar home systems require regular maintenance, as previously explained, to stay highly functional and effective. This maintenance must be continuously assessed and adopted to the demands of the system. Beyond simple maintenance, the system must be treated in a manner it was designed for, including use of a charge controller, correct charge controller set points, and correct battery usage. These aspects must all be clearly explained to the user to maximize system performance. Unfortunately, in a considerable portion of photovoltaic systems implemented in rural communities, implementation occurs by groups (non-profit organizations, etc.) visiting for a short time only to implement systems and then vacate the areas (Mapako 2005). This leaves many of those with the new systems lacking a clear understanding of the types of services needed on the system. The systems begin to degrade over time due to a lack of adequate information

provided to users (Gustavsson 2005, p. 557). Educational solutions have been implemented with the systems in some cases, and in other situations these solutions are implemented at a later date. These solar home systems are meant to be sustainable without continuous replacement of components. User training models have been developed to address the lack of educational resources upon implementation and aim to rectify the current problems (Adiyabai, 1982, p. 2272). However, problems will still arise regardless of the educational system put in place due to the complex nature of the systems. An efficient tool is still needed to quickly diagnose problems with the photovoltaic systems and provide the user instructions as to what step are needed to rectify the problem.

2.2.3 **Testing Battery Health**

Although a system for regulating voltage of VRLA batteries has been established, testing must still occur to indicate the health of a battery and to understand what parameters may be affecting it. Assessment of battery health can be achieved by a variety of means, ranging from a purely experimental in lab approach to a system designed based data from batteries in the field. The estimation of lifetime based on state of health for batteries has become a very important field as batteries are the weakest link in the photovoltaic system.

2.2.3.1 Basic Model

Basic equations for understanding the state of health of a VRLA battery have been established, with small variations in the equations dependent on the number of parameters factored into the original design of the experiment. One study was designed to consider a rather large number of parameters, such as electrode

morphology, electrode porosity, and acid concentration. During a simulation using batteries in a controlled setting, these factors were all monitored on a variety of VRLA batteries to ensure the model would not be extremely limited to one type of battery brand. From these data, a model was designed to test the state of battery health, and then tested against additional data from other laboratory experimentations. The model uses measurable temperature and voltage data to predict things such as reaction rate, porosity, acid concentration, and water dry-out. It is a good representation of the type of variable used to evaluate systems in the field, although its applicability is limited due to the large number of measurements which must be taken to fill all the variables within the equation (Tenno et al., 2002).

2.2.3.2 Changing model for temperature

The complex nature of solar home systems makes it vulnerable to many factors possibly affecting the functioning of these systems. Temperature, as discussed previously, can have dramatic effects on the degradation of VRLA batteries. Temperature has been proven to change the discharge and charge rates of the batteries, as well as overall battery functioning. Therefore, temperature must be factored into the health test of a battery. One study achieved this by applying a wide range of temperatures to batteries running through the charging cycle within the lab (Tsujikawa et al., 2009). From the current and voltage output of these systems, as well as a previously established equation for the health of a battery, the study was able to establish a deterioration degree to be applied as an addition to the original equation of health. This deterioration degree allows one to

factor in varying temperature on the average life of a battery, making the health equation more valuable to those using systems in areas where the temperature can reach extremes (Tsujikawa et al., 2009). It is recommended other studies be conducted to find an understanding of how varying parameters affect the systems.

2.2.3.3 Using Voltage to Diagnose

Voltage of photovoltaic systems is an important indicator of the health of the system overall. There are typically normal voltage ranges designated by the manufacturers for both the battery and the panel. In a healthy solar home system, the recorded voltages will be in these ranges when the system is first implemented; if the new system is not within these ranges, it is an indication the photovoltaic system is malfunctioning in some manner.

In one study, it proposed to use battery voltage to diagnose the health of a battery in solar home systems. In this research, the problems studied were similar to the ones we analyzed (dirty panel, lack of charge controller). These researchers created a method of early detection based on comparing expected battery voltage versus actual battery voltage. For the "expected voltage," they created a model that estimated a healthy battery's voltage over time; this could be compared to the voltage of a solar home system battery in actual application. Then, if there was a discrepancy between this expected voltage and actual, a problem could be detected (Lorenzo and Labed, 2005). Our experiment is similar, except that we are measuring voltage between systems with problems and controls where all data is actually collected and not theoretical. It was suggested in the article, as the authors mention that rather than using expected voltages, one could use voltages

from a newly implemented system to collect data (Lorenzo and Labed, 2005, p. 258). These authors were limited in only proposing a detection system, no method was created. We intend to pursue this recommendation by identifying what problems are actually occurring, as opposed to simply determining whether the system is healthy or not, and designing a potential tool for detection.

2.2.3.4 Central Lab Testing

Often the problems exhibited by the systems stem from incorrect battery maintenance. Lack of, or incorrect maintenance can be a cause of overuse of the battery or overall neglect of the battery. To attempt to diagnose some of these battery problems, laboratories have been built to serve as test sites for rural communities. Users bring failing or malfunctioning batteries to this central site, and tests are conducted to determine the problem. Causes of battery failure or inefficiency are determined by putting the batteries through a multitude of elaborate tests designed by engineers; these tests consider several aspects of the battery's condition, including voltage and current (Diaz, 2001, p. 363). Although this central lab concept does offer advantages to those with solar home systems and malfunctioning batteries, there are significant disadvantages. The overall maintenance of such an operation proves very costly and once the problem is identified, it can often be too late to fix the battery (Diaz, 2001, p.373). This leaves those who operate the labs with high operating costs and those who use the services with the burden of bringing their batteries to the locations. Additionally, since the battery often cannot be repaired, this can be a waste of time and resources (Diaz, 2001, p. 374). Overall, this shows the system to be inefficient on

both ends of its use, for those running the laboratories and the user. Our system aims to alleviate this burden from both ends by designing a system that does not require movement of any portion of the photovoltaic systems, but rather allows the technology to come to the system to assess the batteries in the community setting. Our diagnostic tool has the potential to prove more efficient and effective in dealing with battery problems in these systems overall.

Chapter 3 Methodology

The purpose of this research is to improve the detection of problems affecting solar home systems in developing countries. Team SHINE designed algorithms which utilize patterns in voltage output as 'fingerprints' for five common problems. The research aimed to answer the following question: Is it possible to create a tool that efficiently and effectively diagnoses common problems in small solar home systems?

Team SHINE answered this question by using a true experimental design. The experiment employs photovoltaic systems with five artificially induced problems which represent common issues observed in solar home systems including dirty panel, overcharging the battery, deeply discharging the battery, lack of a charge controller, and use of a car battery. These five problems are commonly observed in solar home systems in the developing world.

3.1 Preliminary Experimentation

The purpose of the preliminary experiment was to demonstrate the visible effect dirt buildup had on the voltage output of solar home systems, using a small scale example. This was essentially a preliminary version of the full scale dirty panel test. The system was assumed to be healthy, as it was new at the beginning of the trial run. Two solar garden lights were placed outside for approximately 48 hours (9:21 PM, 21 September to about 11 PM, 23 September) with no intervention in Annapolis, Maryland. One was left as normal and the other was made artificially "dirty" by sprinkling flour onto clear adhesive tape and then placing the tape over the solar cells. The voltage for both lamps was recorded

every two minutes utilizing a small data logging device connected to the light's battery terminals. The results are displayed in Figure 2.

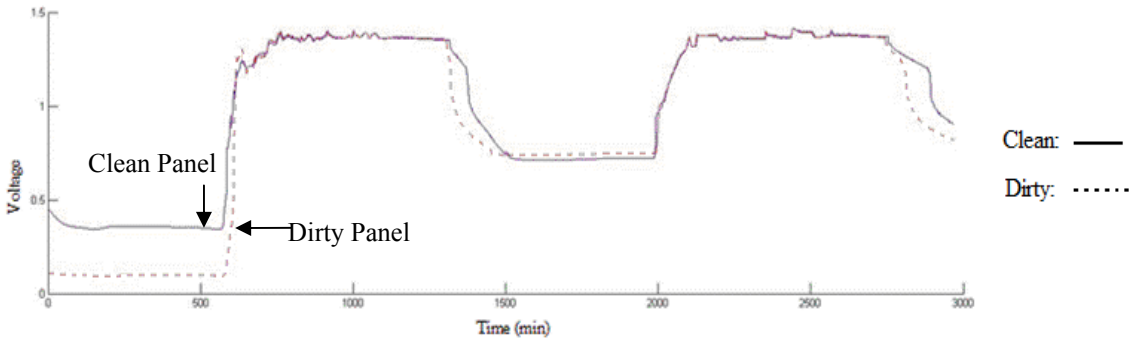

Figure 2: Voltage of a clean vs. dirty panel for two solar garden lights

Both lamps follow approximately the same voltage curve while they are exposed to the sun, but when the sun sets, the voltage of the battery in the lamp with the "dirty" panel drops more quickly than the "clean" lamp. The light was visibly much dimmer as well. Perhaps even though the panels are at the same voltage during the day in full sunlight, the "dirty" panel isn't able to supply as much current to the battery, and thus the battery loses its charge more quickly when subjected to the same load at night. The results of the preliminary experiment were important to our research because it demonstrated that the induced problem caused detectable changes in voltage output when comparing the clean and dirty panels.

3.2 Location and Mounting of Panels

The solar panels for Team SHINE's experiment were placed on the roof of the Glenn L. Martin Engineering building on the University of Maryland, College Park campus (Figures 3 through 7). This location was chosen for a few key reasons. First, the location of the building allows for unobstructed sunlight during

the day, minimizing the need to consider shade in the final results. The building is oriented in an East-West direction which allowed the panels to be mounted so that they faced south, where they would receive the most direct sunlight. The building's roof also allowed for access to an office closet where other necessary equipment for the experiment was placed including; batteries, charge controllers, and a laptop computer for data collection and processing.

Figure 3: Team SHINE members mount solar panels on the roof of Martin Hall.

The angle of the panels was the next consideration in the mounting process. After researching past experiments involving solar panels and other documented set-ups similar to that of our research, it was decided to use the following equation for the angle (θ) of the solar panels: θ = Latitude + 15º (Landau, 2002, Robinson). The location of the testing, College Park, Maryland, is at 38.9839 º of Latitude, meaning that the angle of the panels was found to be

53.9839º, which was rounded to 55 º. This equation maximizes the average exposure of the panels to sunlight throughout the entire year. Although changing the angle of the panels throughout the year would yield the highest amount of sun exposure, this technique was not employed because it is not commonly recommended in developing countries. This is due to the fact that manually changing the angle would require additional work and would risk damaging the modules. Additionally, there is a risk of losing additional energy if the angle is set improperly (Instituto de Energia Solar, 1998, p.10). Another reason for limiting the systems to one angle is the limited knowledge of the average user. Finally, this is also the best way of simulating solar home systems in developing countries, where the angle is usually fixed after implementation.

Once the angle and location for the panels was decided, the mounting was designed. On the roof of The Glenn L. Martin Engineering Building there are several rows of anchored metal hooks that are oriented in an East-West direction. These hooks served two purposes. They provided a line along which to orient the panels once mounted to other support. They also acted as a strong anchor into the building, ensuring limited movement of the mounted panels.

Figure 4: Team SHINE members build mounts for the panels.

Eighteen small panels were mounted on a structure made of plywood and 2” x 4” supports. The basic design of the structure is a long triangular tube, consisting of 2” x 4” wood right triangles with angles of 55, 35, and 90 degrees.

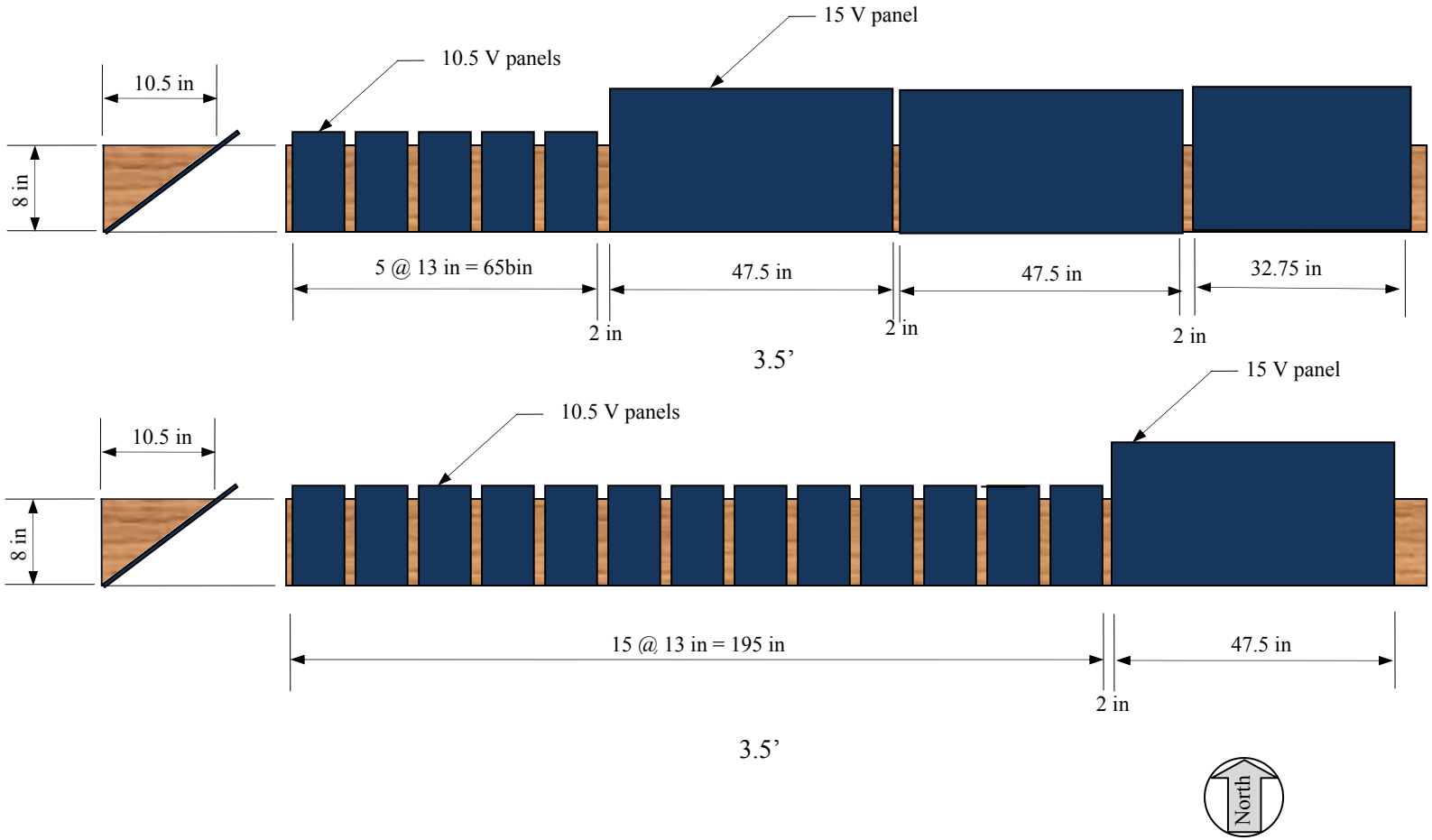

Figure 5: Birds-Eye View of Mounted Solar Panels

Figure 6: Panels mounted on the roof of the engineering building.

The plywood frames were then anchored to the hooks on the roof using pipe straps and screws. The frames were further held down by weights placed throughout their length, to ensure that no lifting force from wind could move the structure.

Figure 7: Team SHINE members fasten mounts to the hooks on the engineering roof.

3.3 Simulation of Problems on Systems

In order to gather data for training and testing our detection algorithms, we constructed a set of small solar home systems similar to those found in the developing

world. Our test set consisted of eighteen systems, divided into six groups of three. Each group represented one of the six conditions for which we are testing: Healthy (control group), Dirty Panel, Overcharged Battery, Deeply Discharged Battery, No Charge Controller, and Car Battery. For each condition, we altered the systems to induce the problem. Each problem was induced on three systems simultaneously in order to mitigate variations that might have occurred in each individual system.

3.3.1 **Control System**

The “Healthy” or control system was the standard by which the systems with induced problems were compared. These systems were constructed with 6.4W 10V thin film silicon solar panels, 12V 5Ah sealed lead acid batteries, charge controllers, load switching circuitry, and a 35Ω load. The specifications for this design are based on those of systems installed by the Light Up The World Foundation (LUTWF) in rural villages in the developing world (Solar Electric). Figure 8 shows a schematic diagram of the control system's construction.

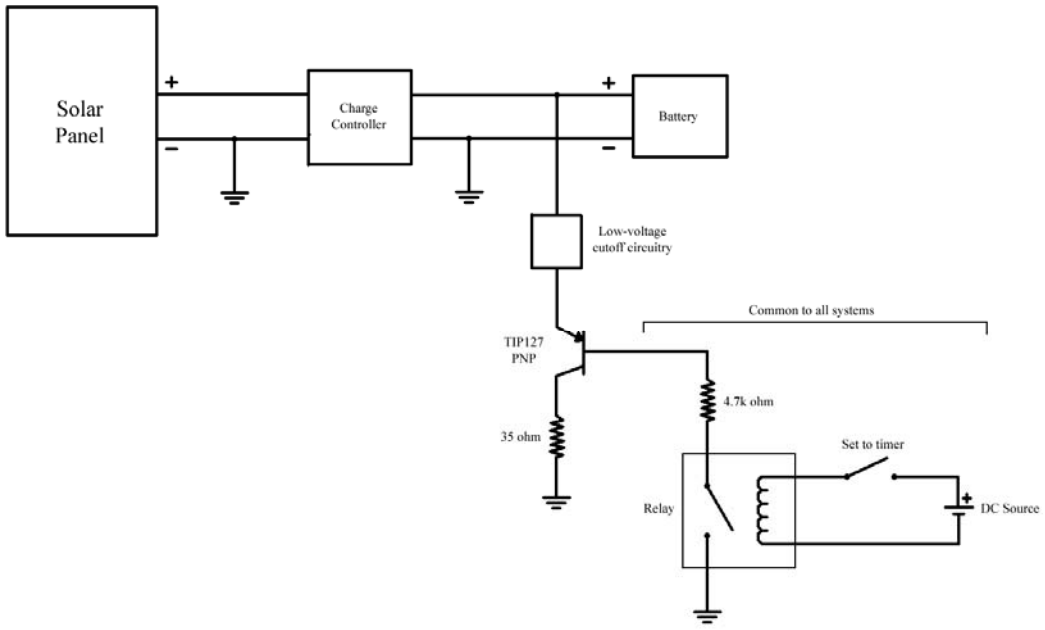

Figure 8: Control (Healthy) System

During the day, the charge controller regulates the flow of current from the solar panel to the battery in order to prevent overcharging. At night, a timer switches on, causing the power transistor to conduct, and allowing current to flow through the load. By Ohm's law, the current through the load will equal the battery voltage, minus a small drop across the power transistor, divided by the load resistance. Assuming 12.6V for a fully charged lead-acid battery, about 1V for the transistor drop, and a 35Ω load, the current will be about 330mA, reasonably close to the 300mA current specification for the 1-watt white LEDs used in LUTWF's systems.

To protect against deep discharge, either the charge controller or a comparable external circuit of our construction interrupted current flow to the load when the battery voltage fell below 10.5V. The low voltage cutoff circuit is described in Section 3.3.7.2.

3.3.2 **“Dirty Panel” System**

Systems intended to simulate charging a battery with a dirty panel were electrically identical to the control system. We chose to simulate the problem by applying a thin coat of spray paint to sheets of clear acrylic glass holding the spray paint can approximately 18 inches away from the glass. The acrylic glass was then fastening these over the appropriate solar panels. The paint simulated dust and dirt, permanently blocking light on the panel’s surface.

3.3.3 **“Overcharged Battery” System**

We attempted to simulate overcharging the battery by making three modifications to the control system scheme. First, the three 6.4W solar panels were replaced with a single larger 80W panel, supplying the batteries with more current than a control system. Secondly, the charge controller was replaced with a diode, allowing current to flow unregulated to the battery during the day, but blocking the battery's discharge through the panel at night. Lastly, the load resistance was doubled, causing the current flow during the discharge cycle to be cut in half. These changes would cause the battery to receive more charge during the charging cycle, and to lose less to the load during the discharge cycle, resulting in a net gain in charge over time. The schematic diagram in Figure 9 depicts these changes from the control system setup.

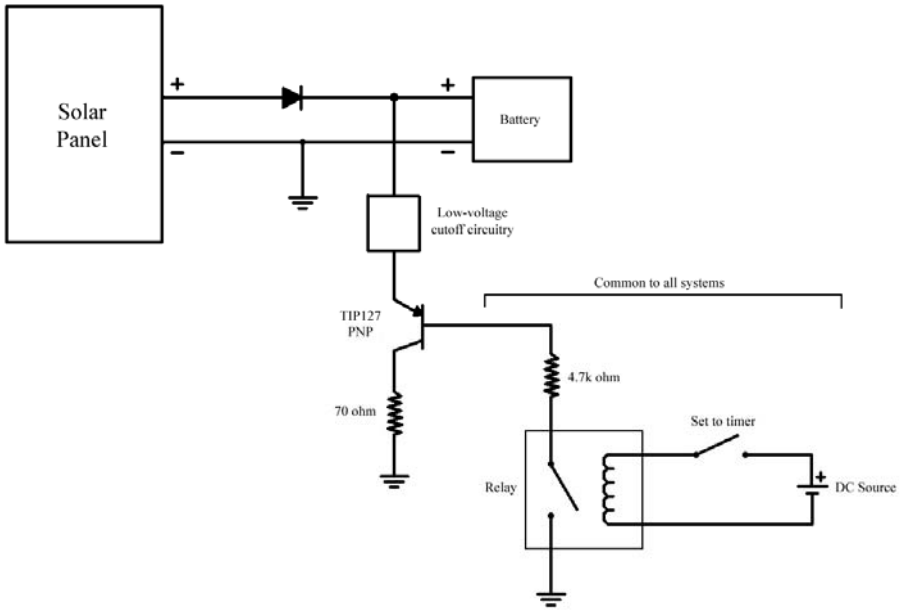

Figure 9: Overcharge System

3.3.4 **"Deeply Discharged Battery" System**

To simulate discharging the battery below the recommended minimum threshold, two modifications were made to the control system scheme. First, the low-voltage cutoff circuitry was removed (while still maintaining the charge controller's protection against overcharge) in order to let the battery drain to damagingly low states of charge. Second, the load resistance was reduced to one third that of the control system, causing the current during the discharge cycle to be three times the original quantity. These modifications would cause the battery to lose more charge during the discharge cycle than is gained during the charging cycle, resulting in a net loss of charge over time. The schematic diagram in Figure 10 reflects these changes from the control system set up in Figure 8.

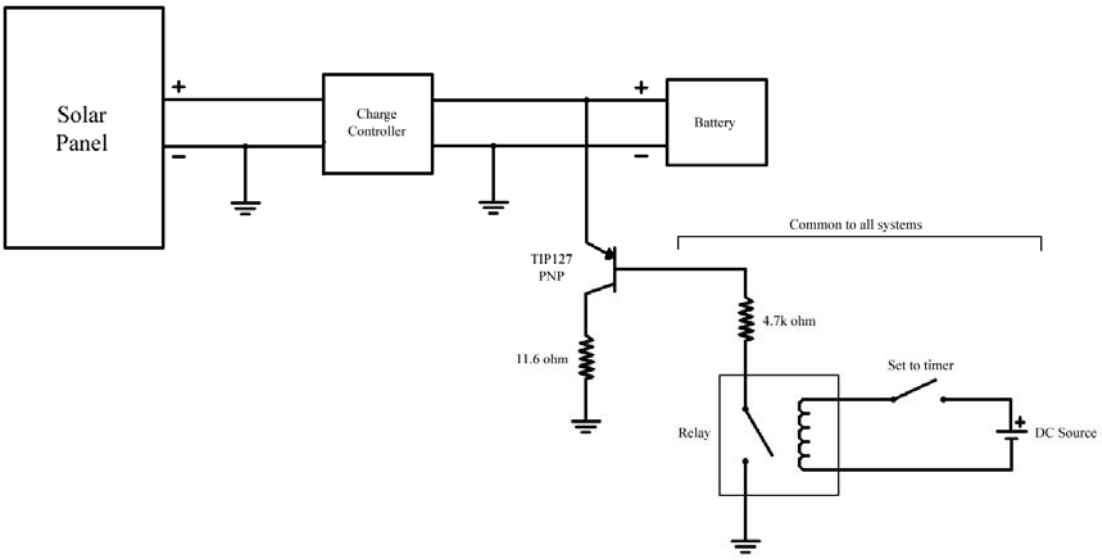

Figure 10: Deeply Discharged System

3.3.5 **"No Charge Controller" System**

We simulated the lack of a charge controller by omitting it from the circuit, and instead connecting the panel directly to the battery. This allowed completely unregulated flow of charge from panel to battery during the day, and from battery to load at night. Thus, the battery was allowed to both overcharge and discharge too deeply. The schematic in Figure 11 depicts this configuration.

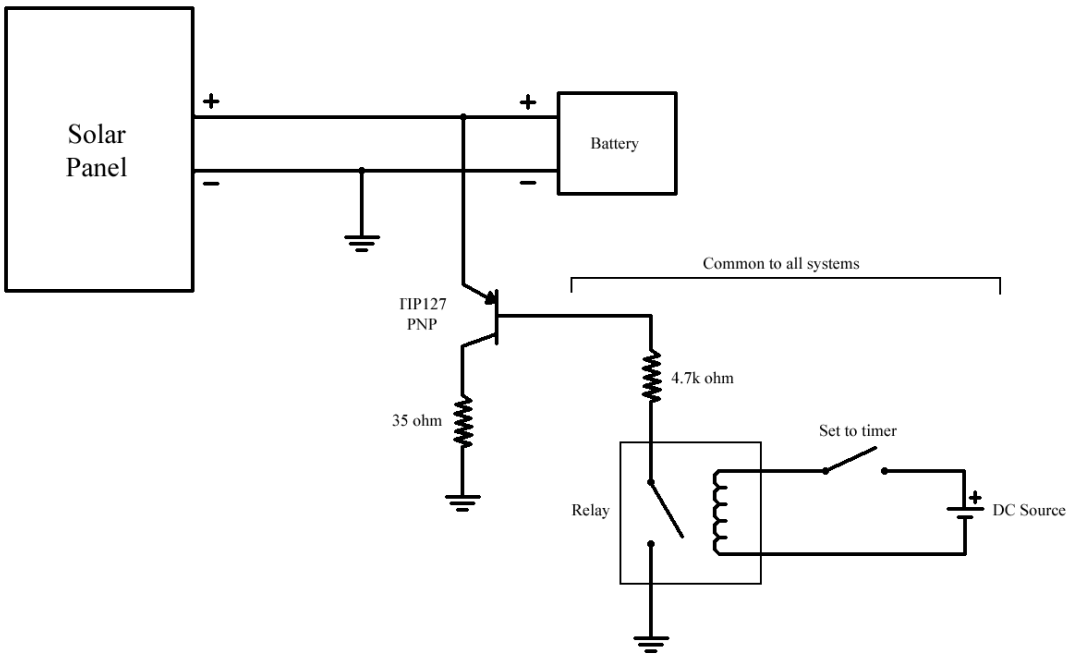

Figure 11: No Charge Controller System

3.3.6 **"Car Battery" System**

Simulation of the use of a cranking/car battery instead of the proper deep-cycle battery was achieved by replacing the battery in the "No Charge Controller" scheme with a car battery. The supporting circuitry is otherwise identical the control system set up depicted in Figure 8.

3.3.7 **Supporting Circuitry**

3.3.7.1 Panel Voltage Correction

Due to the unexpectedly low open circuit voltage of our solar panels, we were concerned that the charge controllers, intended to be used with 12V panels, would not function properly. Since the panels only generated about 10.5-11V open circuit (lower when loaded, as when charging a battery), we decided to add 2V by inserting a power

supply between ground and the common (-) node of all eighteen panels. In the interest of time and cost, we accomplished this by using a computer power supply which was rated for 32A on its 5V line, and regulating the 5V down to about 2.1V using LM317 voltage regulator ICs (integrated circuits). Because we expected to need to pass as much as 500mA x 18 systems = 9A of current, we used ten of these ICs in parallel, since each is capable of passing 1.5A. The Figure 12 shows our implementation.

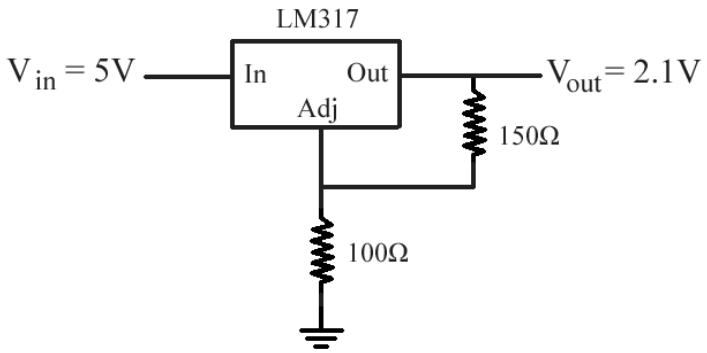

Figure 12: 5V to 2.1V Regulation

Using the formula given in the datasheet for the LM317, the output voltage is 1.25V*(1+ (100Ω/150Ω)) = 2.1V (3) giving an open circuit voltage of 12.6-13.1V. One important point which we did address is whether the addition of the power supply would disturb the normal operation of the solar panels other than to increase their voltage. Such a disturbance could have potentially led to unrealistic results, for example if the "dirty" system were able to charge batteries fully, when we expect that this should not be the case. However, in addition to supplying their own current, solar panels also limit the amount of current that can pass through them due to their electrical properties. Thus, we

believe that the panels in our experiment are behaving very similarly to panels with an inherent open circuit voltage of about 13V.

3.3.7.2 Low Voltage Cutoff

The set of charge controllers used for this experiment was not uniform. Several charge controllers were donated to our project, but we had to purchase a different model for the remaining three. The three Silicon Solar charge controllers offered protection against discharging the battery too deeply, while the Morningstar charge controllers did not. Some of our tests did not require such protection, but we did not have enough of the Silicon Solar charge controllers to otherwise fulfill our needs. Our solution was to construct circuits which would automatically disconnect the load when the battery voltage fell below a certain level. Based on the specifications of the Silicon Solar charge controllers and our research on batteries, the threshold was set to 10.5V. The following schematic in Figure 13 shows the circuit.

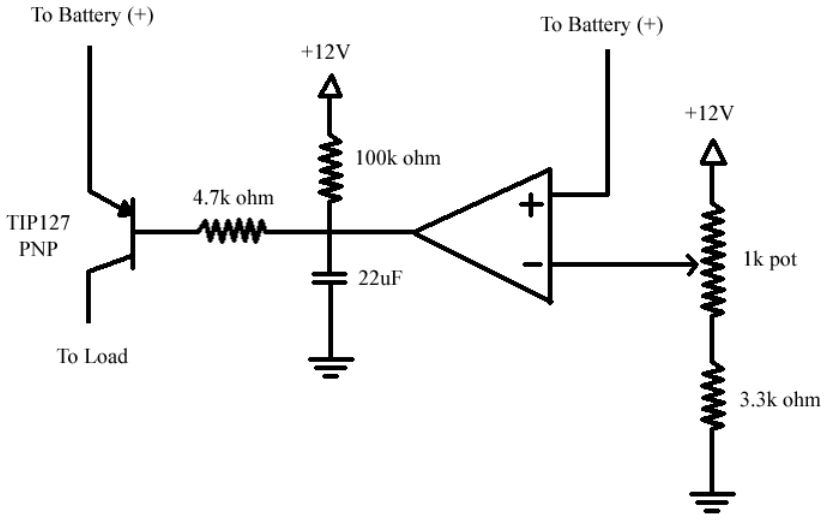

Figure 13: Representation of low voltage cutoff circuit.

Its operation is as follows: the battery voltage is compared with a reference voltage (10.5V), set manually by the potentiometer as a fraction of the 12V supply. When the battery voltage is above the reference, the output of the comparator is "low," providing a path to ground for the base of the PNP power transistor, in turn allowing current to flow to the load. If the battery voltage falls below the reference, the comparator's output goes "high," causing the transistor to cut off, and the battery to cease to drain. The capacitor connected to the comparator's output prevents oscillation when the battery voltage is nearly the same as the reference.

3.4 Data Acquisition

In order to record data from the solar home systems, hardware and software from National Instruments (NI) were employed. An NI data acquisition module (DAQ), version USB-6008 and NI LabVIEW software were purchased for this purpose. LabVIEW is a versatile icon-based virtual interface used to create and control programs for the NI hardware.

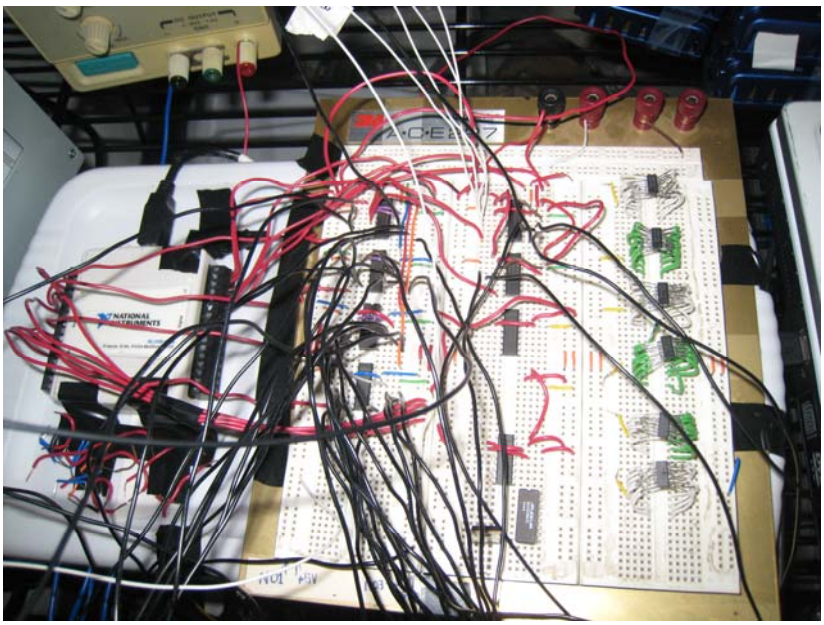

Figure 14: Image of the LabVIEW data acquisition module (DAQ) and related circuit.

The LabVIEW program gathers voltage and current data by employing analog inputs and digital outputs on the data acquisition module, or DAQ. However, the DAQ has only four analog inputs; in order to collect the 40 different input measurements we required, a strategy was employed to switch between inputs. A system of multiplexers was constructed to cycle through all of the inputs (see Figure 15).

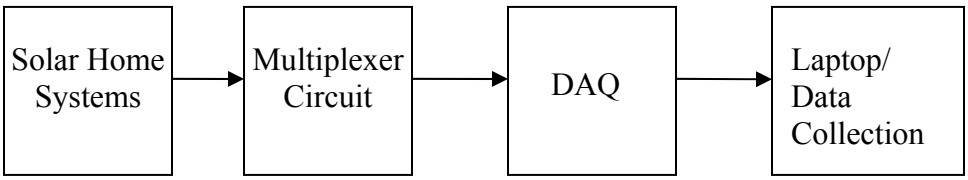

Figure 15: Diagram of Data Acquisition Circuit

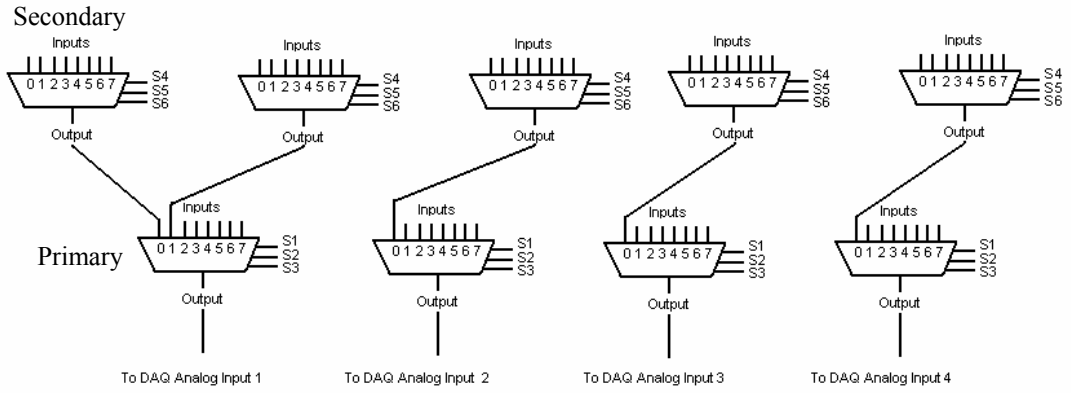

Figure 16: Setup of multiplexer circuit for Data Acquisition

The LabVIEW program outputs digital signals to sequentially select each of the multiplexers' input channels. The digital output component on the DAQ consists of six ports (S1, S2, S3, S4, S5, S6). These ports each output a binary signal (0V low or 5V high), which are toggled between high and low throughout the duration of the program.

Each unique combination of three signals (low-low-low, high-low-high, etc.) indicates which input port on the multiplexer to activate. There are eight possible combinations. This allows for the selection of one of the eight channels (voltage measurements) on each multiplexer; the measurements are then sent to the analog inputs of the DAQ. When a selected channel has been measured, the DAQ will input the next signal combination in the sequence. The DAQ cycles through all eight signals, and then it restarts at the beginning of the sequence for a new set of measurements.

The multiplexers are divided into two tiers: primary and secondary. This was necessary because we needed to take more measurements than one tier could provide. The DAQ has 4 inputs and each multiplexer has 8 channels. That adds up to 32 measurements, but we needed 40+ measurements. The two-tier setup was convenient and easy to implement. The four primary multiplexers have outputs directly feeding to the analog inputs on the DAQ, while the five secondary multiplexer outputs feed into some of the primary multiplexer input channels. Three of the DAQ digital output signals act as selectors that cycle through inputs for the primary set of four 8x1 multiplexers. The second set of three signals are select inputs for the secondary set of five 8x1 multiplexers.

The four analog input ports on the DAQ are able to measure voltages ranging from -20V to +20V. The analog inputs obtain voltage measurements from the outputs of the four primary multiplexers. As the DAQ cycles through output signals, so does the voltage measurement coming into these inputs. A LabVIEW program organizes and stores this information in order to accurately preserve the voltage patterns of the photovoltaic systems over weeks or months at a time.

3.5 LabVIEW: Data Collection and Organization

The LabVIEW program is necessary for the measurement of voltage and current data from the panels and batteries. The program can be split up into three major stages: (1) initialization of digital output channels, (2) output of high or low digital signals, and (3) acquisition of voltage measurements.

The first stage within this data collection program is the initialization of digital output channels. This stage initializes the digital output channels to which the DAQ will send binary signals. The program then transitions to the running state in which it indicates which signals the DAQ sends to the multiplexers. As previously mentioned, a group of three channels is used to select which input on the multiplexer is measured by the DAQ at a given time. The third and final stage in this program involves acquiring voltage measurements and saving the data to text files. The program acquires measurements from the DAQ, which measures the DC voltage coming from each of its four analog ports. The measurement data was written to several text files (see Appendix D) with eight columns of voltage and time data. It then saves the data to a specified file.

There are eight major 30 second loops that occur once the program is initiated. Within the first 30 second loop, a set of three low signals selects the first measurement port on each of the primary multiplexers. The program also toggles between the eight ports on all of the secondary multiplexers, utilizing the second set of three digital output channels, in minor three second loops. As each of these ports is toggled, data are collected and written to a text file. In the second 30 second loop of the program, the same process occurs, except using the second measurement port on each of the primary multiplexers. For the remaining six 30 second loops, the remaining six ports on the

primary set of multiplexers are measured. None of the ports on the secondary set of multiplexers are measured in the last six 30 second loops.

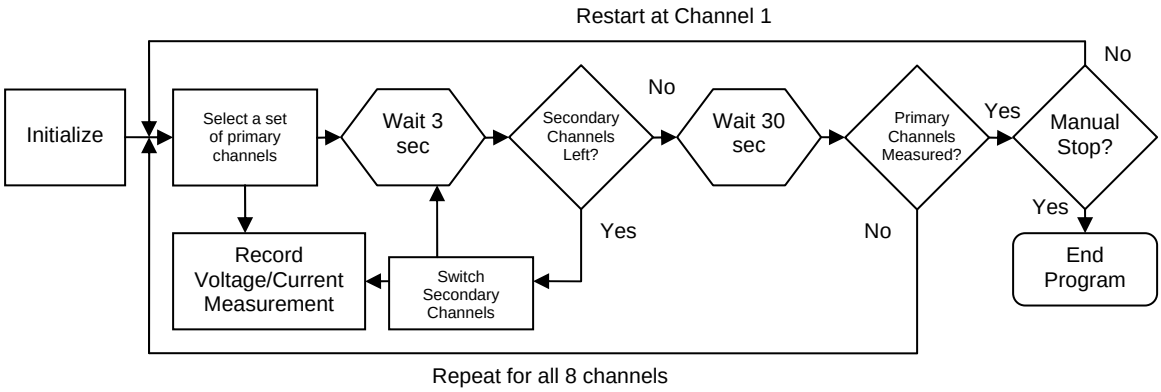

Figure 17: Block diagram of the LabVIEW Data Collection Program.

Table 2: DAQ Outputs and Corresponding Digital Signals

	Signal 1	Signal 2	Signal 3	Signal 4	Signal 5	Signal 6	Signal 7	Signal 8
Selection Port 1	low	high	low	high	low	high	low	high
Selection Port 2	low	low	high	high	low	low	high	high
Selection Port 3	low	low	low	low	high	high	high	high
Selection Port 4	low	high	low	high	low	high	low	high
Selection Port 5	low	low	high	high	low	low	high	high
Selection Port 6	low	low	low	low	high	high	high	high

3.6 Current Limitations

In order to gain a more complete picture of the charging cycles of the batteries, we attempted to construct current-sensing circuitry which would measure the current delivered to each battery during daylight hours. What follows is a description of the current sensing implementation we attempted.

The basic principle of measuring current is to insert a resistor with a value small enough so as not to significantly disturb the system in-line with the desired circuit branch, and then to measure the voltage across it. We chose 0.1Ω resistors for measuring current, so that the estimated maximum current of approximately 500mA would produce a voltage drop of only 50mV. However, the voltage resolution of our data acquisition equipment was such that directly measuring this voltage would not have yielded useful results. Furthermore, our data acquisition equipment was ground-referenced, and the measurement needed was a differential one—either two separate voltage measurements with respect to ground would be needed in order to take the difference between the two, or else we would have to use differential amplifiers.

Due to the somewhat limited availability of measurement channels, the better option was to use differential amplifiers. Initially, we attempted to use Maxim MAX4378 integrated current sensors, which required only to be connected to the high and low sides of the in-line resistors, and would output the differential voltage multiplied by some gain. However, we had difficulty finding these, or anything comparable, in a Dual Inline Package that we could use on our breadboards. Our attempts to adapt surface-mount versions were functionally successful, but failed due to poor durability.

The next option was to construct such differential amplifiers ourselves, using standard op-amps and resistors. These require many more components, and much more space than their integrated counterparts, so we were only able to construct a few. We used a version of the circuit shown in Figure 18, modified with R1 = R3 = 1kΩ, and R2 = R4 = 100kΩ, so that the gain was approximately 100 (yielding a full-scale output, with input 50mV, of 5V). The op-amps used were LM324 single-supply quad-channel units.

We were able to obtain reasonable current readings for a brief period from several systems, but the addition of the current sensors unfortunately caused erratic changes in many of the voltage readings for reasons which we were unable to discern. We decided to forego the current data in favor of consistent voltage data.

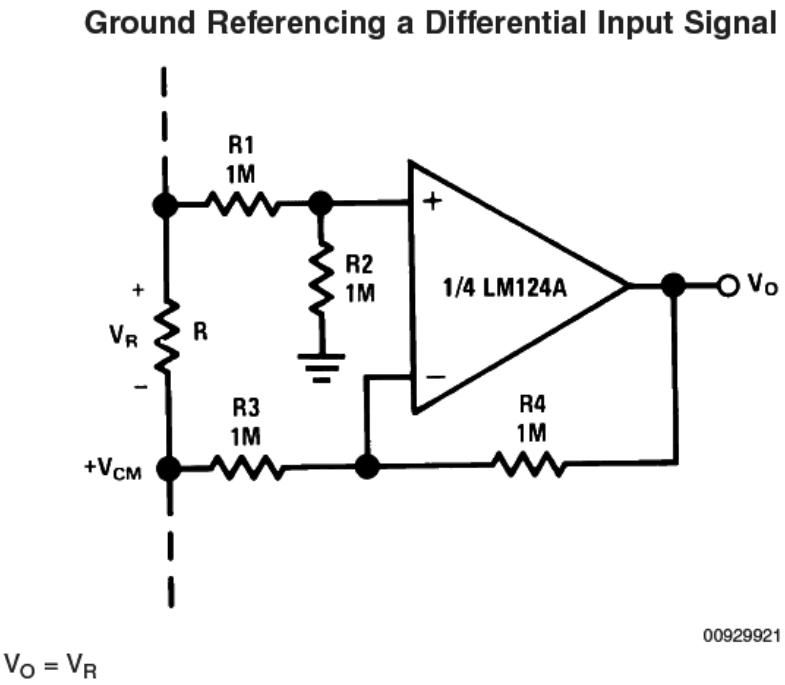

Figure 18: Circuit Employed to Ground Reference a Differential Input Signal. (Source: National Semiconductor datasheet for LM324)

3.7 Weather Data Collection

Weather conditions affect the voltage output on a given day; for example, the voltage from a panel on a rainy day is often significantly lower than on a sunny day. We have decided to take this factor into account by recording the general daily weather for each day of data collection. We coded each day into one of three weather categories**:** sunny**,** cloudy**,** or rainy. The weather data were obtained from WeatherBug, the world's largest weather network that provides users with neighborhood level weather reports. For this project, data from the WeatherBug Tracking Station located at Saint Hugh's Catholic

School in Greenbelt Maryland was used. The school is located only five miles away from the University of Maryland, where the photovoltaic systems are set up, which ensures that the weather conditions that are recorded are accurate. Additionally, the weather data were verified through the personal observations of one of the team members and by checking the National Weather Service's website. The weather data for the National Weather Service were recorded at Reagan National Airport which is approximately fourteen miles from the University of Maryland. We considered weather when we analyzed the data, as will be discussed in Section 4.2.1.

3.8 Limitations

In the data acquisition phase, three months of panel and battery voltage data for the 18 systems were obtained. The data ranged from October 13th, 2008 to December 21st, 2008. Our initial goal was to capture six months of data, with special attention to data in the summer, which would most closely represent the data of solar home systems in equatorial countries. Problems arose, however, with the system setup that delayed the data acquisition.

These problems occurred over the span of Summer 2008 and were not fully resolved until October. With the removal of current sensing as a requirement for data acquisition and analysis, voltage from the panels and batteries was able to be reliably measured and recorded.

The delays in data collection and the need to begin extensive data analysis in 2009 provided only a three month window of opportunity for data collection. This placed major limits on observing differences in voltage patterns due to seasonal change. It also hindered the analysis of long-term effects of each problem. For instance, the voltage

pattern of a system with a deep discharge problem would have changed much over time, devolving from a healthy system to a system with low voltage during the nighttime, to a system with relatively low voltage in the daytime and nighttime (indicating a dead battery).

Although data were collected in fall and winter, and cannot be directly related to solar home systems in equatorial countries we believe the detection algorithms proposed could be applied to these systems by simulating systems using similar procedures from this research to develop baselines. The algorithm structure would be the same, but the baselines would be changed to more closely replicate systems in countries near the equator, where sunlight is abundant year-round.

With a constant load, the current reading during the discharge cycle is not of much interest. In fact, the discharge current for each battery could be calculated very easily by simply dividing the voltage signal by the corresponding load resistance (Ohm's Law: $I = V/R$). Since the resulting signal is merely a scaled replica of the voltage, however, it would be of no additional use in detecting changes in voltage output. Measuring the current during the charging (daytime) cycle would add much more detail to the "picture" of the battery's health, since the voltages were largely constant during that part of each day.

Having access to the rate at which the battery is able to accept charge and how that rate varies with time can provide insight into the battery's function that voltage alone cannot. For example, a battery which ceases to accept new charge very early in the day and then discharges quickly at night is likely suffering from internal damage which reduces the active surface area of the metal plates. One situation in which this can occur

is in car batteries which are deeply discharged repeatedly, causing parts of the thin plates to crack and disconnect. A battery in this state could appear to be healthy with a very small number of voltage readings, since it would reach and maintain a normal voltage once charged and may settle at a similarly normal voltage when discharged. Current readings for this battery would quickly reveal a current which falls to zero shortly after the beginning of the charging cycle as the battery runs out of available metal surfaces to react, therefore ceasing to retain further charge.

Unfortunately, current is more difficult to measure than voltage for two main reasons. First, it requires breaking an existing connection to insert a resistor, which may be inconvenient depending on the system's construction. Second, it requires a differential voltage measurement (often with amplification), which adds to the complexity of the data acquisition hardware. As previously explained, the latter reason was the main obstacle which prevented us from measuring current in this experiment.

Chapter 4 Diagnostic Tools

4.1 Pre-processing

The raw data output from our solar panels and batteries is subject to noise from a number of sources, including clouds passing overhead and electromagnetic radiation. In order to make valid comparisons, it is necessary to remove the effects of such random noise from the signals. Because these disturbances have high frequency compared to our sample rate of once every 10 minutes, a low pass filter sufficiently suppresses the noise without distorting the important features of the signals.

4.1.1 Data Formatting Program

We created a data formatting program to transform the text files written by LabVIEW into named vectors containing the voltage for each panel and battery over a select period of time. This was a necessary step, as it transformed our data into a standard format that could be easily read by our diagnostic programs. This dramatically simplified the testing and comparison of our pattern matching algorithms.

This data formatting program was created using the tools found in MATLAB. First, the program selects one of the 16 text files from the panel and battery voltage data collected using LabVIEW. Each of these text files contains eight columns of time and voltage data (four columns of voltage and four columns of time). Using the "textread" MATLAB command, our program deletes the first 21 lines of the text file, which contain an unnecessary header. The remaining text is then converted into a matrix with eight columns and a number of rows corresponding to the number of measurements collected since the beginning of data collection. This "textread" command is employed once for each of the 16 text files.

We then designed the program to simplify the data further using several steps. First, because the program cycles from one panel-battery pair to the next, the number of measurements may not match from one pair to another. For example, one vector may have 143 measurements, while another has 144. Therefore, we find the shortest vector length and set all of the vectors to that length, so that there are the same number of data points for each panel and battery. Additionally, every odd column of every matrix (1^{st}, 3^{rd}, 5^{th}…) is a vector of time corresponding to the voltage data in every even column (2^{nd}, 4^{th}, 6^{th}). Since the data were collected across these panels/batteries over the same time period, all columns of time data beyond the first were redundant, and were therefore removed.

The next step involved the organization and naming of the vectors. We used MATLAB to convert each of the individual voltage columns into its own vector, so that we would be able to compare or plot one individual panel or battery's voltage over time. After this, we gave each of these voltage vectors a name identifying problem it represents (e.g. deep discharge, dirty panel), whether it is from a panel or battery, the assigned number for each set of systems (since there are three systems for each problem), and the assigned number out of all 18 panels. An example of a name of one of these vectors would be "Drt_B1_2," meaning "Dirty Panel," Battery 1 (of 3), System 2 (of 18).

4.1.2 **Data Parsing**

For both our experimental training data (the "known" sets) and for any input ("unknown") data, it is necessary to divide large blocks of data into segments that our algorithms can use. While it is possible for a human to look at the data and determine where each day starts, it is desirable to automate as much of the process as possible.

The separate24.m algorithm relies on the steep increase in solar panel voltage at sunrise to signal the beginning of each new day. Its input is a string of time-series voltage data of any length. Raw data is shown in Figure 19. The steps in the algorithm are as follows:

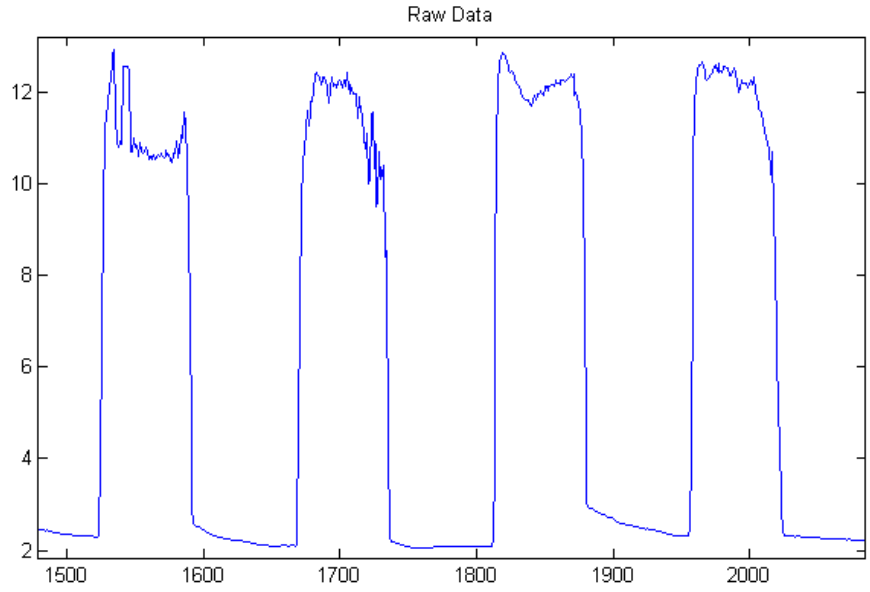

Figure 19: Graph of raw voltage data.

1. Filter with a 16-sample average: to remove noise, since sudden changes in voltage will be amplified in the next step, and could trick the algorithm into falsely detecting new days (Figure 20).

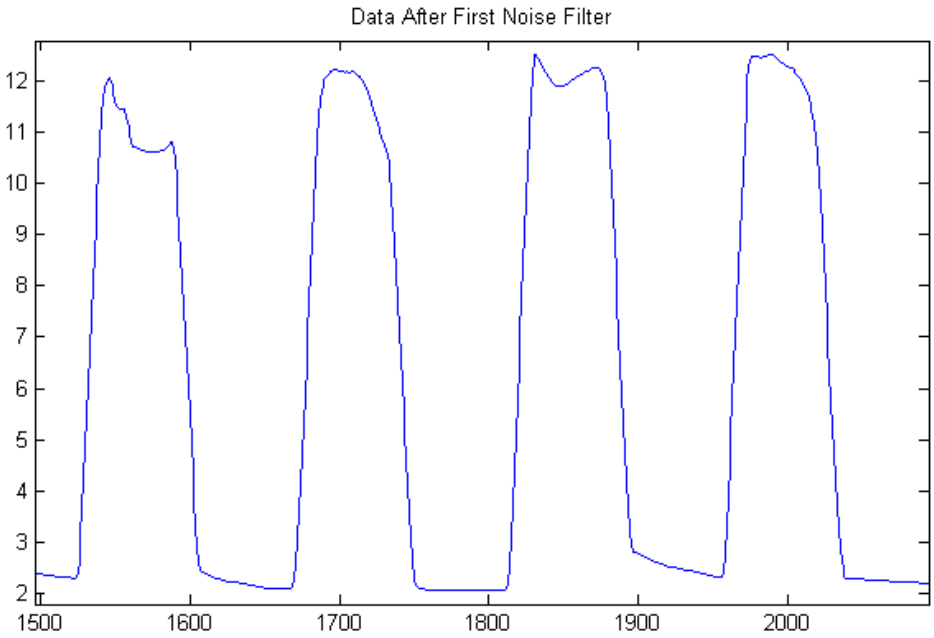

Figure 20: Voltage graph after the first noise filter.

2. Differentiate the signal: find the change between each point and the one before it. Steep increases and decreases such as those we are looking for will show up after this filter as large peaks above or below zero. The resulting data is shown in Figure 21.

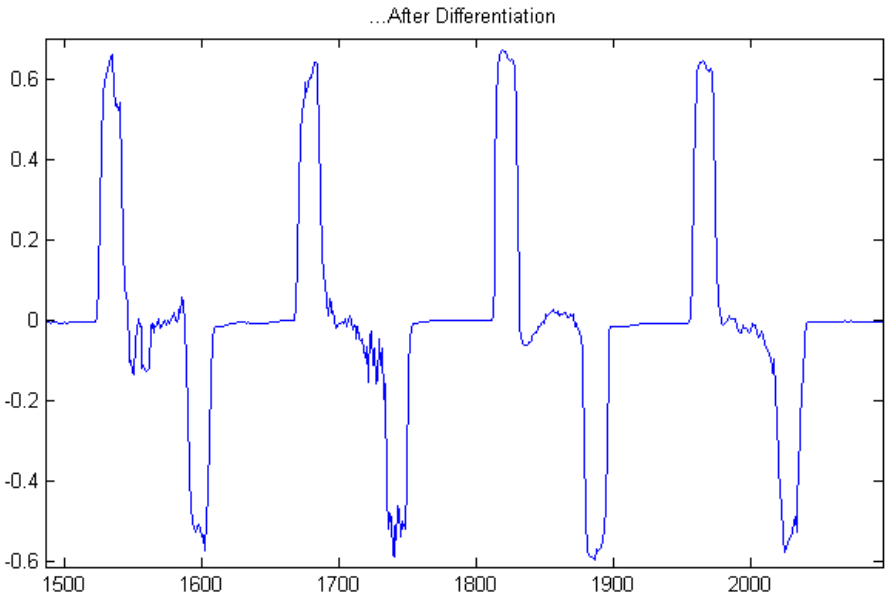

Figure 21: Voltage graph after differentiation.

3. Filter with 16-sample average again: the differentiation introduces new noise into the signal which must be filtered before we apply a threshold. Because the spike we want is the largest, it survives this second noise filter while smaller ones are suppressed. See Figure 22.

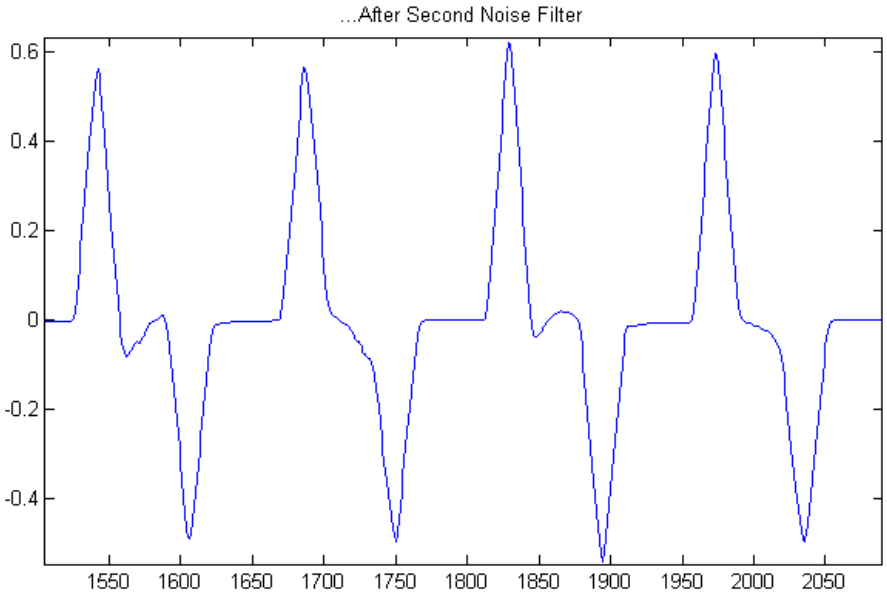

Figure 22: Voltage graph after the second noise filter.

4. Exponentiate each sample with a high odd power: this exaggerates the difference between any remaining peaks while preserving their sign, so that sunrise is not mistaken for sunset, and also in case we have a need in the future to divide day from night. See Figure 23.

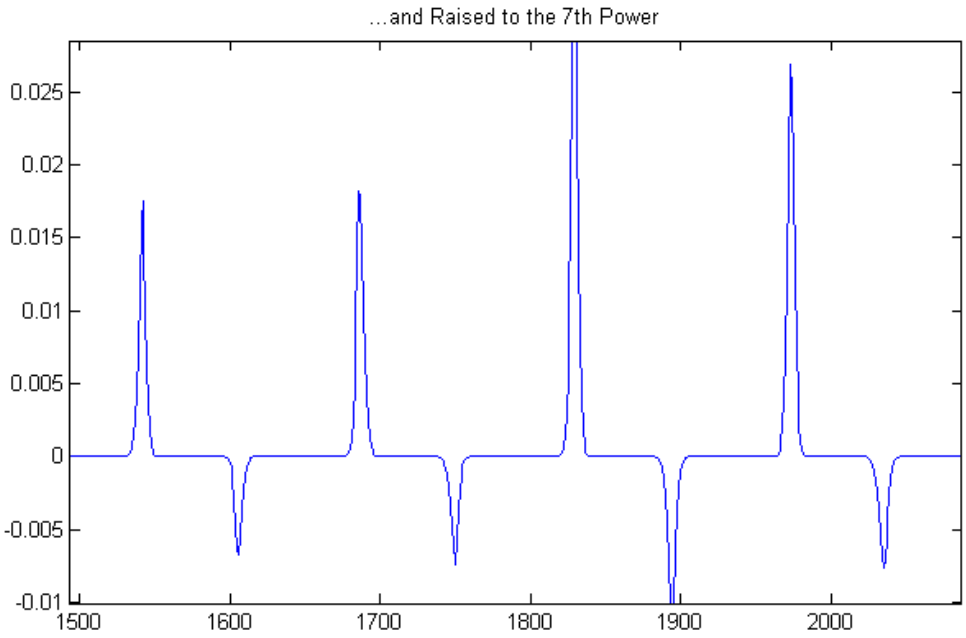

Figure 23: Voltage graph after exponentiated.

5. Subtract a threshold value and search for negative-to-positive zero crossings—find the indices where the data output from the previous step crosses some (experimentally determined) threshold in the positive direction. These indices are returned by the function as the indices where each new day begins. See Figure 24.

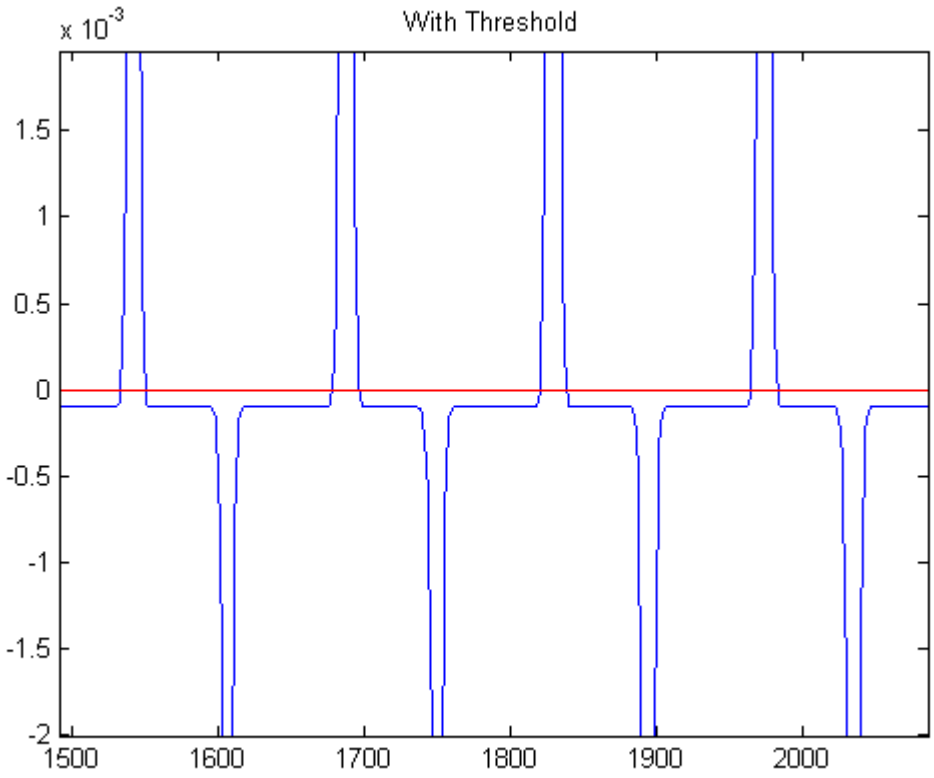

Figure 24: Voltage graph with threshold.

After testing with a few data sets to determine an appropriate threshold value, this algorithm is able to find the beginning of each new day with nearly 100 percent success. Its accuracy is affected by the weather, but it tends to err in favor of false negatives rather than false positives. A listing of the program is shown in Appendix G.

4.1.3 **Normalization**

It is clear from many of our voltage-vs.-time plots that regardless of weather conditions or problems afflicting the system, there is a distinct trend of voltage being higher during the day and lower at night—a pattern which repeats every 24 hours. Since we are limiting the scope of our matching algorithms to a fixed set of baselines, we can remove the component of the signal that is common to all six baselines. This has the

effect of exaggerating the differences between the signals, reducing the chance of misdiagnosis due to similarity with multiple baselines.

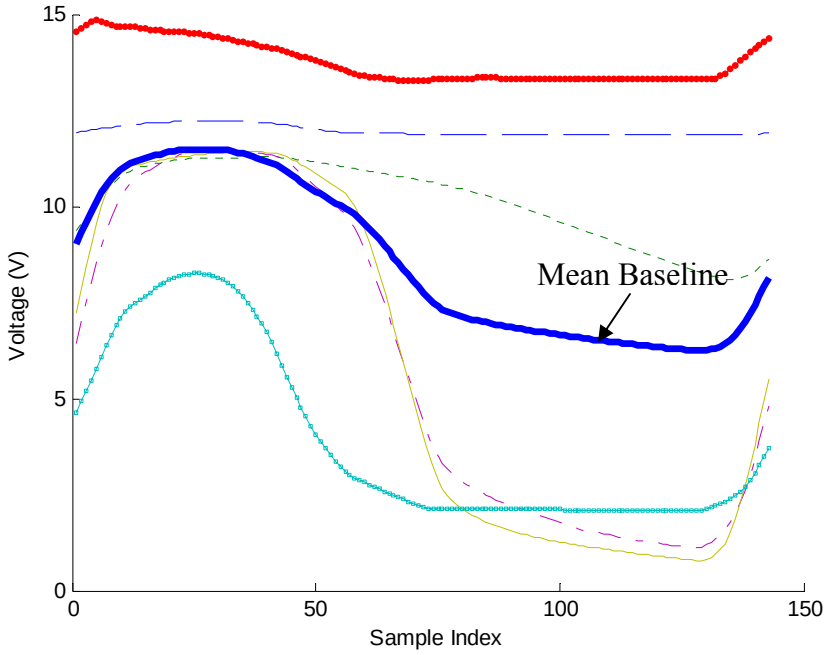

Figure 25: Baselines with Mean Baseline.

The fundamental equation used to create the mean baseline is given by:

$$v_{avg} = \frac{\sum_{i=1}^{N} v_i}{N} \tag{4.1}$$

In this equation, N is the number of baselines, v_i is the voltage of each baseline, and v_{avg} is the resulting average voltage point. The equation is used to calculate 143 baseline indices.

In theory, this signal contains the frequency components common to all six baseline signals. Figures 26 and 27 show the mean baseline and its Discrete Fourier Transform (DFT), a representation of the frequency content of the signal. The DC offset

has been removed (by subtracting the average value of the signal) to make the AC components more readily visible.

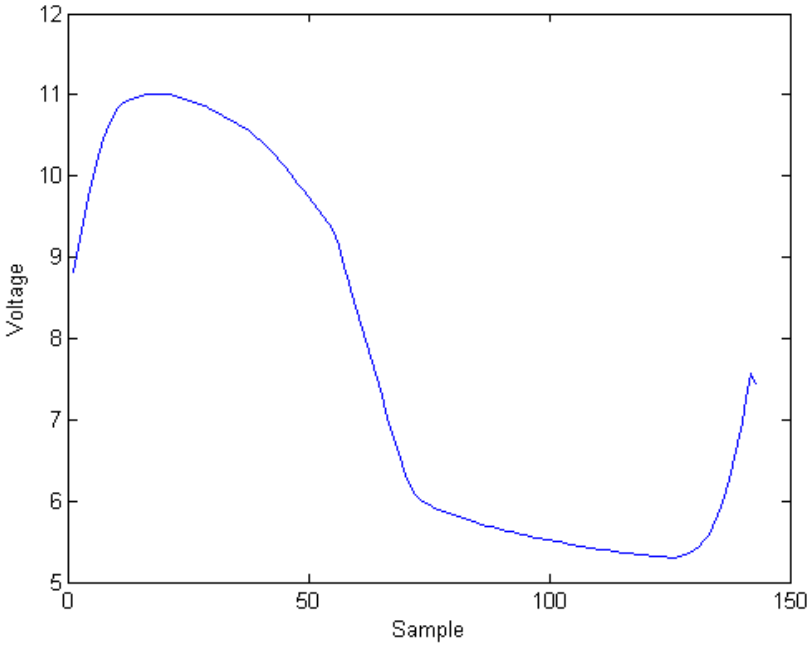

Figure 26: Mean Baseline

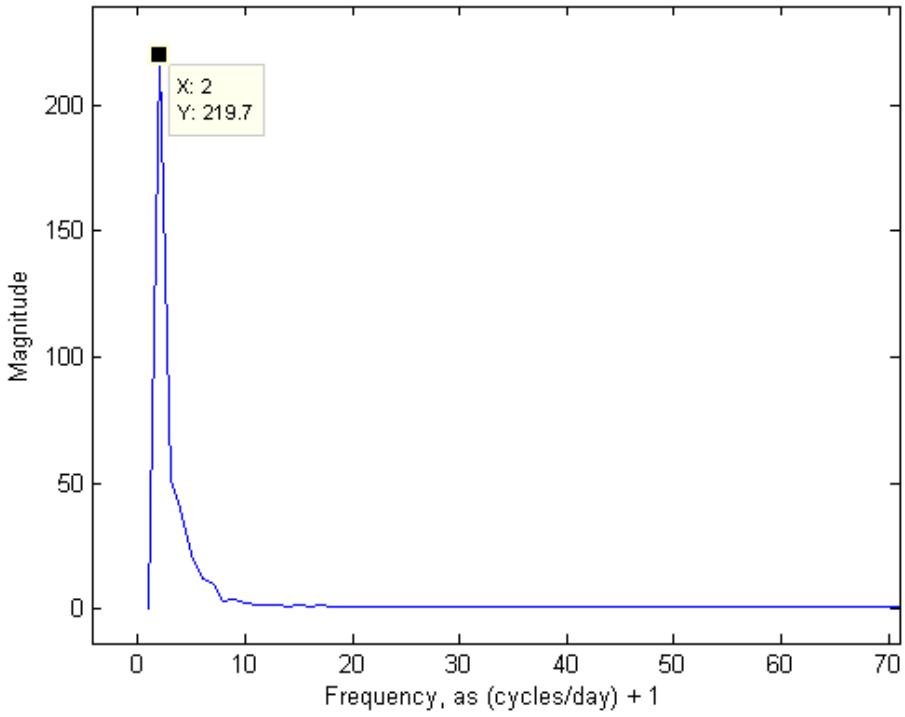

Figure 27: DFT of Mean Baseline.

The most important thing to note about the DFT of the mean baseline is the tall peak corresponding to the fundamental 24-hour cycle. This is the major "trend" in each daily cycle that we wish to eliminate. Ultimately, the "common component" is nothing more than the average of the baseline signals–a signal of the same length as each baseline, where each sample is the average of the baseline samples at the same time index. By subtracting the mean baseline from the six baseline signals as well as the input signal in question, we are therefore subtracting out the 24-hour trend that we set out to eliminate, as well as some other components which happen to be common among the signals. Figures 28 and 29 show the baselines before and after the mean has been subtracted. Note that the normalized data are centered about zero; the vertical axis now represents volts of deviation from the mean.

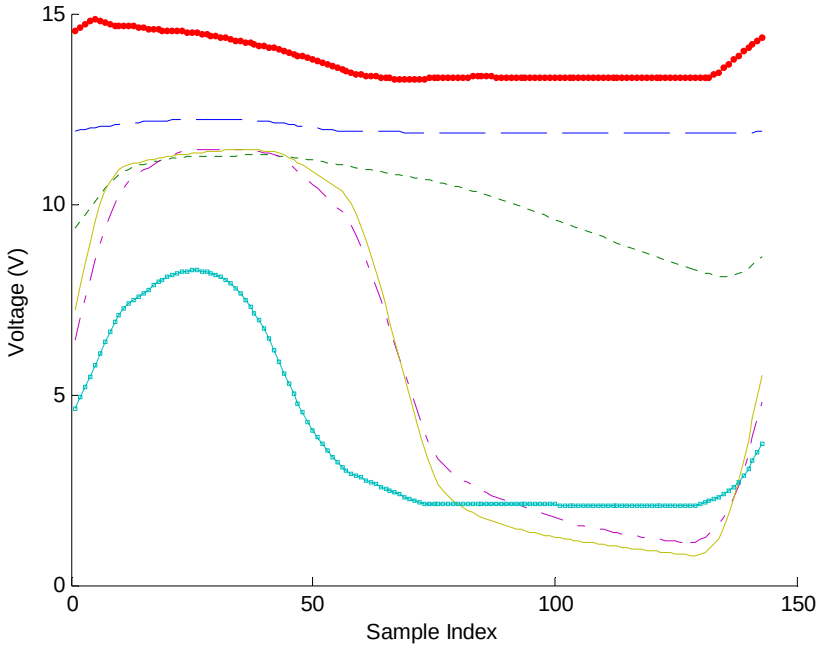

Figure 28: Baselines before Normalization.

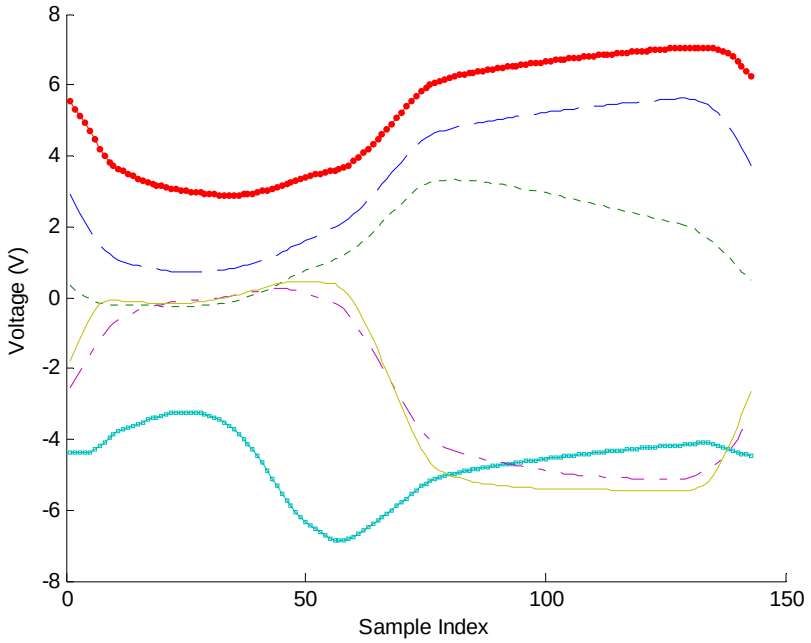

Figure 29: Baselines after Normalization.

Due to time and logistic constraints, we were only able to implement normalization in the Least Squares and Gaussian matching algorithms. The results for these sections reflect matching based on normalized data.

4.2 Diagnostic Tests/Algorithms

Our team designed several algorithms with the goal of detecting and accurately diagnosing problems in actual solar home systems. In order to develop and test the viability of the algorithms, we used data collected from the experimental systems. Part of the experimental data was used to develop the algorithms, while another part of the experimental data was used to assess their accuracy. The algorithms we developed are the Baseline Test, the Single and Combined Metric Tests, the Least Squares Test, and the Gaussian Test.

4.2.1 **Baseline Test**

The Baseline test is a pattern-matching algorithm that can be used to diagnose systems by means of a baseline, or pre-recorded set of voltage data. By comparing a working photovoltaic systems' voltage output data to these baselines we believed that the program can accurately diagnose the problem affecting the working system. The purpose for developing the Baseline test was to investigate the effectiveness of using pre-recorded data as a tool for detecting SHS problems. It also served as a benchmark for the more sensitive baseline test we used, called the Gaussian test.

The baseline test is analogous to a fingerprint in that it represents a known pattern, in this case, training data from the first phase of data collection. The data are used to make a baseline pattern that can be reliably matched by future data of the same type. The baselines are not exact replicas, but rather an envelope of the standard deviation of training data. An envelope is necessary because, realistically, voltage patterns will not be exactly the same from day to day. The fact that the patterns are similar from day to day, however, indicates that this test may be reliable.

The width of the envelope for the baseline test was an important parameter to set. If the envelope is too narrow, the true diagnosis may be rejected. If the envelope is too wide, the baselines would overlap too greatly, leading to a greater chance of misdiagnosis. The envelope for the baseline test was chosen to be within one standard deviation of each of the data points of the training data because this allowed for a statistical majority of points to be detected, while overlapping little with other baselines.

From the first two weeks of collected voltage data, a set of baselines was defined. The baselines, which represent the voltage pattern of an 'average day,' were used not

only in the baseline test, but in the Least Squares and Gaussian tests as well. These baselines were created from a two-week set of data, starting on November 11 and ending on November 23. First, using the data separation program created in MATLAB, the data were separated into 24-hour cycles. Data points corresponding to the same daily time in each 24-hour cycle were averaged, creating the baseline curves, shown below. The standard deviation for each time index was also determined. Dotted lines appearing above and below the central curves represent the standard deviation envelope that the baseline algorithm employs to determine matches between the baseline and sample data.

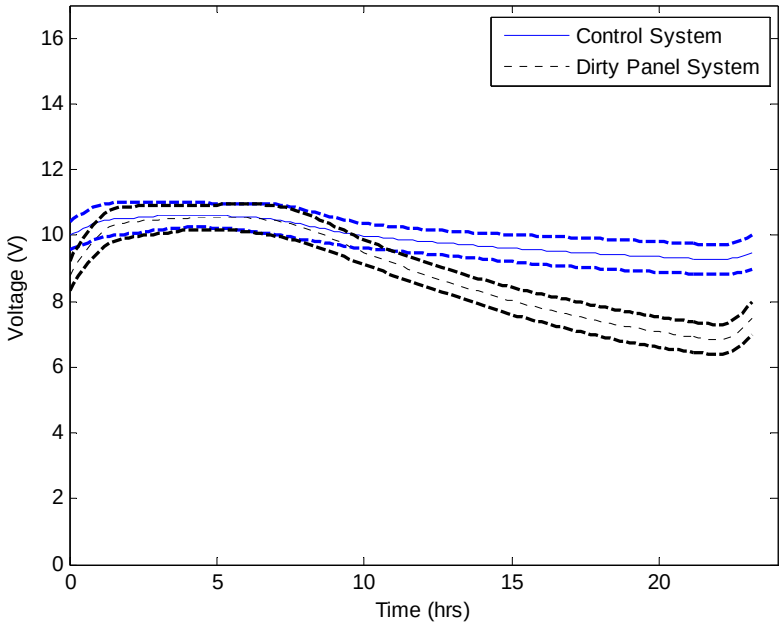

Figure 30: Baselines and Standard Deviation for the Control and Dirty Systems.

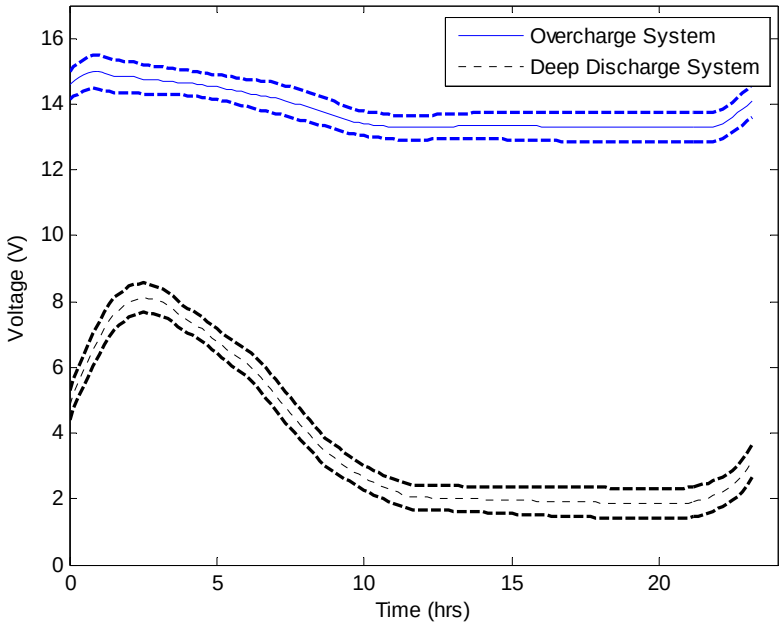

Figure 31: Baselines and Standard Deviation for the Overcharge and Deep Discharge Systems.

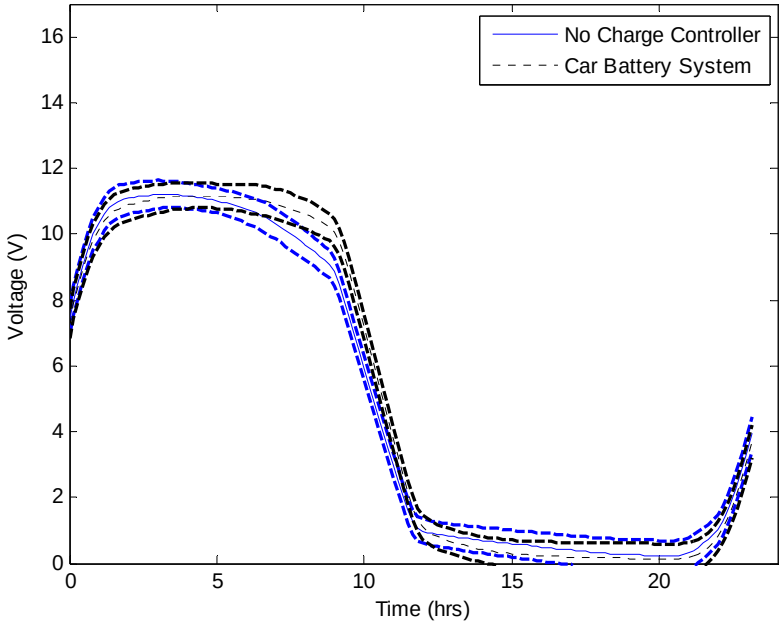

Figure 32: Baselines and Standard Deviation for the Malfunctioning or lack of a charge controller and Car Battery Systems

Furthermore, distinct baselines were created for different types of weather. These additional baselines were merited because cloudy and rainy weather significantly affected

daily voltage patterns, and the baseline envelopes created were too wide for accurate diagnosis. Baselines for sunny, cloudy, and rainy weather were incorporated in the baseline detection algorithm, but none of the other algorithms.

The baseline detection algorithm, created within MATLAB, was a function that required three inputs: (1) a vector of time (which was created in the data formatting program), (2) a vector of voltage data (also created in the data formatting program), and (3) a vector of new day indices (indicating the start and end of each day). The program created a matrix which contains the four columns: day number (the first day of collection being 1), start of day index (which indicates the first voltage reading of that day), end of day index (which indicates the last voltage reading of that day), and weather type.

The algorithm then compared one day of data at a time to the baselines in order to determine how well the sample data match each. The program calculated how many of the sample points of voltage lie within the standard deviation of each of the baselines. Whichever baseline had the highest percentage of matches was determined to be the program's diagnosis of which problem the sample data represents. Only a plurality of data points was necessary for a match, not a majority. For example, if Baseline 1 has 40% of matches, while Baselines 2 and 3 both have 30% of matches, Baseline 1 is chosen despite having less than 50% of the total matches.

Though this program can determine the closest-matching problem using a single day of data, basing any decision on a single sample is unreliable. Therefore, the process was repeated over several days. As previously explained, a problem was determined for each day; then the program determined which problem occurred most frequently during that period of time, which provided a more accurate diagnosis.

4.2.2 Single and Combined Metric Tests

The second diagnostic tool we created attempts to diagnose problems in a solar home system without the use of baselines. This program was instead based on identifying features in the data that can be measured quantitatively. These parameters were determined and each feature was given a weight to form a 'combined metric.' Each of the six identifiable problems was each given a target 'score,' predicted from training data. From any set of sample data, problems can be diagnosed by matching the score of the data with the problem score of nearest value.

4.2.2.1 Single Metric Tests

First, single metric tests were developed by choosing a single parameter out of a group of important parameters, such as average voltage, curvature, and slope. To build these programs, that parameter was averaged for each of the 6 sets of training data to set target values. The single metric test was performed on 6 sets of 'unknown' standard test data for diagnosis. For each day, the program first calculated the values of the parameter for each day, and finds the closest target value. The diagnosis is decided to be the condition corresponding to that target value.

In order to extract important features from each daily cycle, input data was separated into 24-hour periods. The program, written in MATLAB, evaluated several parameters from the curves in order to develop the metric. Each of the identifiable problems had distinct features that separated it from the other problems. For each 24-hour cycle, the following statistical parameters were extracted:

- Average Voltage
- Average Rotation
- Average Curvature
- Maximum Curvature
- Minimum Curvature
- Maximum Discharge Slope
- Average Discharge Slope

The average voltage parameter was used to distinguish normally high-voltage patterns (overcharge, control) from relatively low-voltage patterns (deep discharge, no charge controller). High average voltage indicates that the battery is being consistently charged to full capacity, while a low average voltage implies the battery is not being fully charged.

The "rotation" of a single point was determined by measuring the angle (in degrees) that an imaginary line between a data point and the origin makes with the horizontal axis. The rotation of the data points were averaged over each 24-hour cycle. Rotation does not directly correspond to any physical phenomenon in the voltage patterns; however, this parameter was used because rotation values remained fairly constant for each system over time, but were different for each simulated problem.

The average curvature parameter was used to accentuate the differences between voltage data that are highly curved and those that are mostly flat. Curvature is defined through the equation:

$$\kappa = \frac{\left|\frac{d^2V}{dt^2}\right|}{\left[1+\left(\frac{dV}{dt}\right)^2\right]^{\frac{3}{2}}} \tag{4.2}$$

where $\frac{dV}{dt}$ and $\frac{d^2V}{dt^2}$ are the first and second derivatives of the voltage, respectively. Minimum curvature and maximum curvature are also used for this purpose. Curvature depends on the type of system; for instance, there is a high maximum curvature for the car battery system because after dusk, the battery discharges from 12 V to 0-2 V very quickly, and thus curves from a flat horizontal line to a nearly vertical line in a short time period. On the other hand, there is a very low maximum and minimum curvature associated with the control system because it does not discharge much.

Finally, maximum and average discharge slope of the battery sending charge to the load were used. Discharge slope corresponds to the rate at which the physical phenomenon occurs. This parameter is important because the voltage profiles of certain problems exhibit higher discharge slopes than others.

4.2.2.2 Combined Metric Test

The combined metric test was adapted from a pattern matching technique used in "Discharge pattern recognition in high voltage equipment" (Gulski, 1995). Gulski used a 'centour score,' or the mathematical center of a combination of statistical parameters, from partially-discharging high voltage equipment to identify types of discharges. The score nearest to the sample score was diagnosed as the corresponding type of partial discharge.

Similarly, the combined metric test used for SHINE's research determined a 'score' through the summation of important statistical parameters to diagnose PV system problems. In order to set target scores of system problems for the combined metric test, training data were input into a preliminary program, which calculated the parameters and summed them to determine target scores. Weights for the combined metric test (shown in Table 3) were chosen based on forcing all the metrics to have the same order of magnitude. The average curvature weight is large because average curvature values were on the order of 10^{-3}. Next, the scores were multiplied by the weights, which separated problem target scores from one another. This was performed by maximizing the normalized standard deviation of the target scores.

The values were compiled for every day of the sample data, averaged over those days, and a score was determined using a weighted sum of the statistical parameters. The program then compared the score to the predicted scores for each simulated problem.

The parameters were weighted by the following factors:

Table 3: Weights for Selected Parameters

Average Voltage	Average Rotation	Average Curvature	Minimum Curvature	Maximum Curvature	Maximum Slope	Discharge Slope Avg.
-5	-0.3	800	4	3	5	5

The combined metric test algorithm summed the weighted parameters, which yields a value that usually lies between -100 and 100. The 'score' was then compared to predicted scores for each problem; an example is depicted on a number line in Figure 33. The predicted scores were determined from averaging scores of the first two weeks of collected data. The positive scores on the number line were voltage patterns characterized by high curvature and high discharge slope. The negative scores were

voltage patterns characterized by low curvature and low discharge slope. The algorithm determined which predicted score is closest to that of the sample system, and identified the corresponding problem.

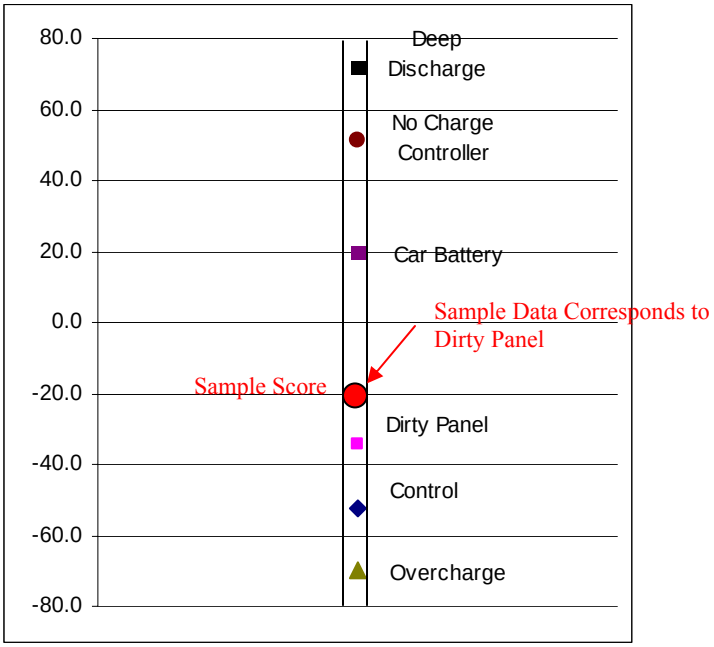

Figure 33: Representation of Combined Metric Test.

4.2.3 **Least Squares Test**

The Least Squares matching method is a much different approach compared to the previous two methods. Rather than treating the signals as a series of voltages in the time-domain, it treats them as points (or vectors) in high-dimensional space. The problem of matching signals then becomes a geometric one—each of our baselines represents a different direction in space, and when given a signal from a system with an unknown problem, we must find to which of the six directions it is closest. The algorithm accomplishes this by scaling and summing the "known" vectors to minimize the sum of the squared distances in each dimension to the "unknown" one. This is known as the

"least squares approximation" of the unknown vector. The method described in this section performs the task very efficiently with matrix operations.

The general principle of minimizing squared error between two signals is well suited to creating matching algorithms. It has been used for many years in the image recognition field; for example, as described by Bethel (Bethel, 1997). The paper describes an iterative process for transforming and matching small fragments of a grayscale image, in particular for application to stereo cameras. While the method described in the article calls for performing least squares approximation on the transformation parameters, we are assuming the signals to be uniform in phase and scale, so transformations are not necessary for our purpose. The "parameters" will instead be the time-series voltage samples of each signal. For background information on the mathematics employed in this algorithm, refer to a Linear Algebra text such as Introduction to Linear Algebra, 3rd Edition (Strang, 2003).

4.2.3.1 Applying Least Squares to Our Problem

Using six sets of data, each corresponding to a known condition, our goal is to identify the problem in an unknown set by finding its closest match among the known sets. Each "set" that we are working with is one day long, consisting of 143 voltage samples taken at 10-minute intervals. Using the vector interpretation described previously, each set of known data represents a vector in 143-dimensional space, and the set of unknown data is the vector we wish to approximate by linear combination of the known sets. Our coefficient matrix then consists of six columns with 143 elements each—an extremely over-constrained system. By the least squares method, we expect that the approximate reconstruction of the unknown data set will have one clear, strong

component in the "direction" of one of the known data sets, allowing us to diagnose the problem.

4.2.3.2 Least Squares Matching Algorithm

The least squares matching algorithm takes, as input, two series of voltage data—from the solar panel and battery—of any length, as long as the two are the same length. We had hoped to use battery current in the matching as well, but were unable to collect adequate current data. The solar panel voltage is fed to the data parsing (day separation) function to obtain the indices of each complete day within the input series.

The vector of new day indices is then checked for false positives by taking the difference between adjacent entries. If any of these intervals is less than some arbitrary "minimum day length" (we used 140 samples), the earlier time index is discarded. The remaining indices are then used to extract 143-sample blocks from the input data which represent the days to be tested. These are arranged into a matrix where each column is one day.

Least squares approximation is then performed on each column of this matrix individually, and the resulting coefficients collected into a matrix of a similar format—six entries per column, one for each of the conditions for which we are testing, and one column per input day tested. Because the coefficients are sometimes not well separated, we exaggerate the differences by dividing by the mean of each set of six, then squaring the values. After this, we have attempted to use two different methods to make a decision. The simplest is to force a decision by taking the maximum for each day. In order to account for cases where two or more coefficients are close together, however, we tried implementing a second method whereby exactly one coefficient from each set of six was

required to be above some threshold, or else the day was flagged "indeterminate." This is probably the better option in practice, due to the possibility of problems other than the six for which we are testing, but much more training data would be required to determine accurate threshold values. We therefore used the simple maximum for deciding the diagnosis.

In order to analyze the success rate of the algorithm, we use Matlab to display a bar graph of the total number of decisions in favor of each problem. At this point, in practice, either the software could automatically make a decision, or a human could decide the final diagnosis based on the bar graph.

4.2.4 **Gaussian Test**

Our final matching method is called Gaussian because it makes use of the Gaussian probability density function, commonly known as a "bell curve," to represent the baselines. It is very similar to the Baseline test discussed previously in that it evaluates the similarity between data sets based on proximity in voltage over time. However, where the Baseline test uses a strict "hit or miss" scoring for each point in time, the Gaussian test employs a smooth weighting function. During periods where the "unknown" curve matches a particular baseline more closely, a higher score is awarded. The result is a finer measure of similarity over all points in time, leading to greater accuracy than the Baseline test.

4.2.4.1 Background

The Gaussian probability density function is given by the equation:

$$P(x) = \frac{1}{\sigma\sqrt{2\pi}} \exp\left(-\frac{(x-\mu)^2}{2\sigma^2} \right) \tag{4.3}$$

where μ is the mean and σ is the standard deviation, which determines the spread (Knoke, Bohrnstedt, and Mee, 2002) . For a data set with N values, the mean is simply the sum of the values divided by N, while the standard deviation is given by the equation:

$$\sigma = \sqrt{\frac{1}{N}\sum_{i=1}^{N}(x_i - \mu)^2} \tag{4.4}$$

The use of the Gaussian density function implies that a substantial and representative set of data was used to create the distributions, and ultimately the baselines against which the input signal will be compared. Ideally, training data for our system would exhibit both of these qualities, but the training set used in our evaluations was unfortunately limited to several weeks during the fall. These data were enough, however, to obtain means and standard deviations, and we must simply make the assumption that they are representative of all systems with similar specifications.

We are interested in time-domain voltage signals, so when we refer to “mean” and “standard deviation” in the context of our baselines, it is not exactly in the same sense as for a single distribution, where there is only one mean and standard deviation. Rather, each baseline consists of one μ and σ for each sample in time. The time-series of distributions (in voltage) then comprises each baseline signal for this method. Figures 34 and 35 show example baseline distributions. Darker areas represent regions of higher density (meaning the training data were more consistent at those parts of the cycle). The thin line laid over both distributions represents the average of several days' of test data from a system with a dirty panel. Because the test data in Figure 34 closely follow the dense region of the distribution, the "dirty" diagnosis would receive a high score. In contrast, the test data in Figure 35 largely do not intersect the dense regions of the

baseline distribution, and a low score is therefore awarded. Figures 36 and 37 show example distributions with different μ values and large and small σ, respectively.

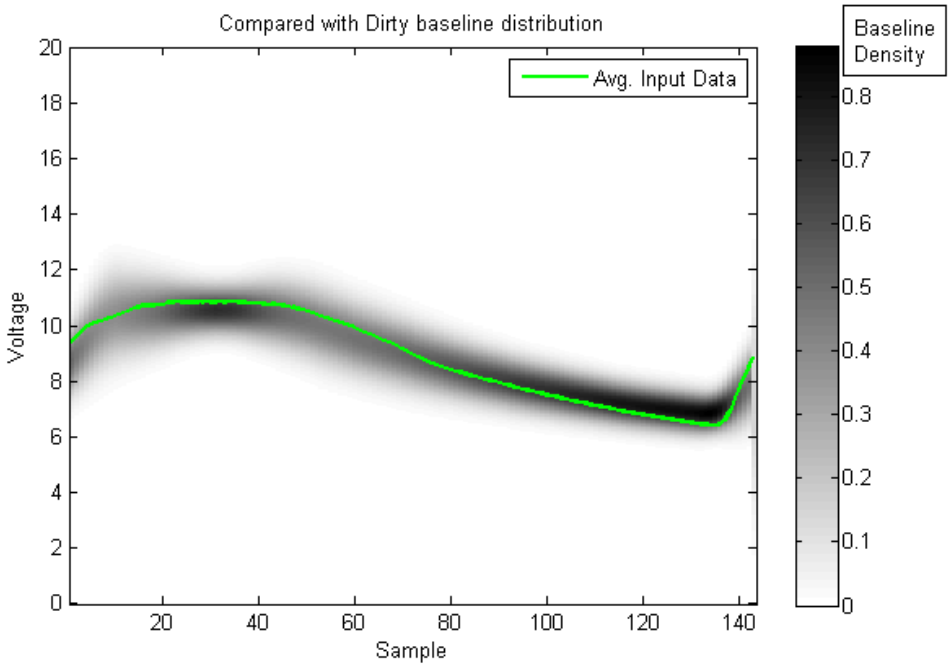

Figure 34: Gaussian Weight Field – Match

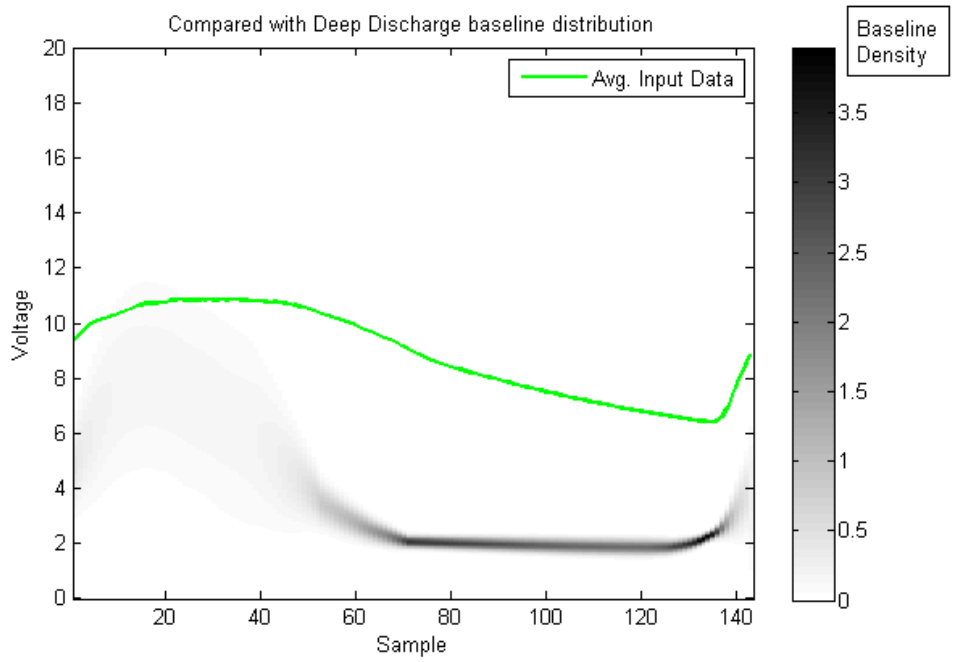

Figure 35: Gaussian Weight Field - Mismatch

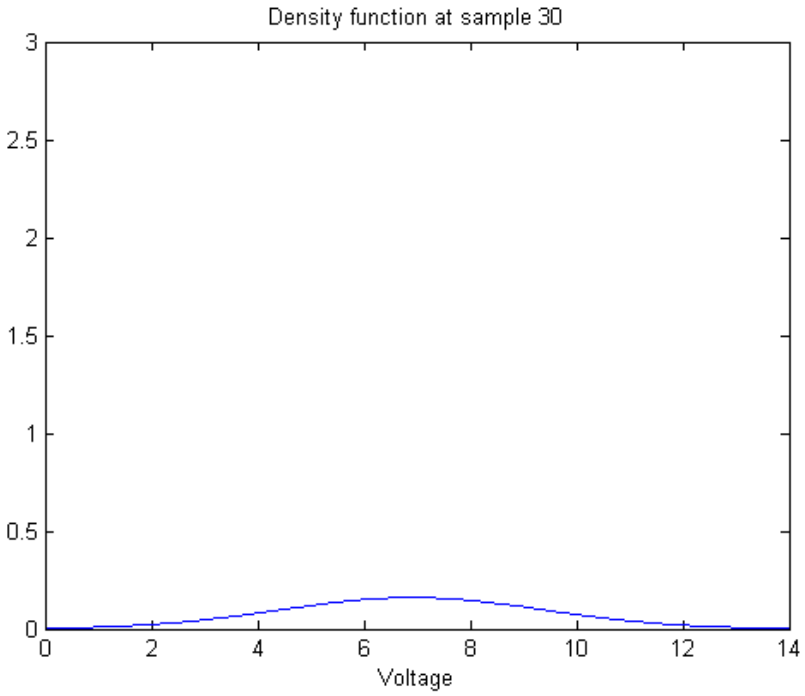

Figure 36: Density Function at Sample 30

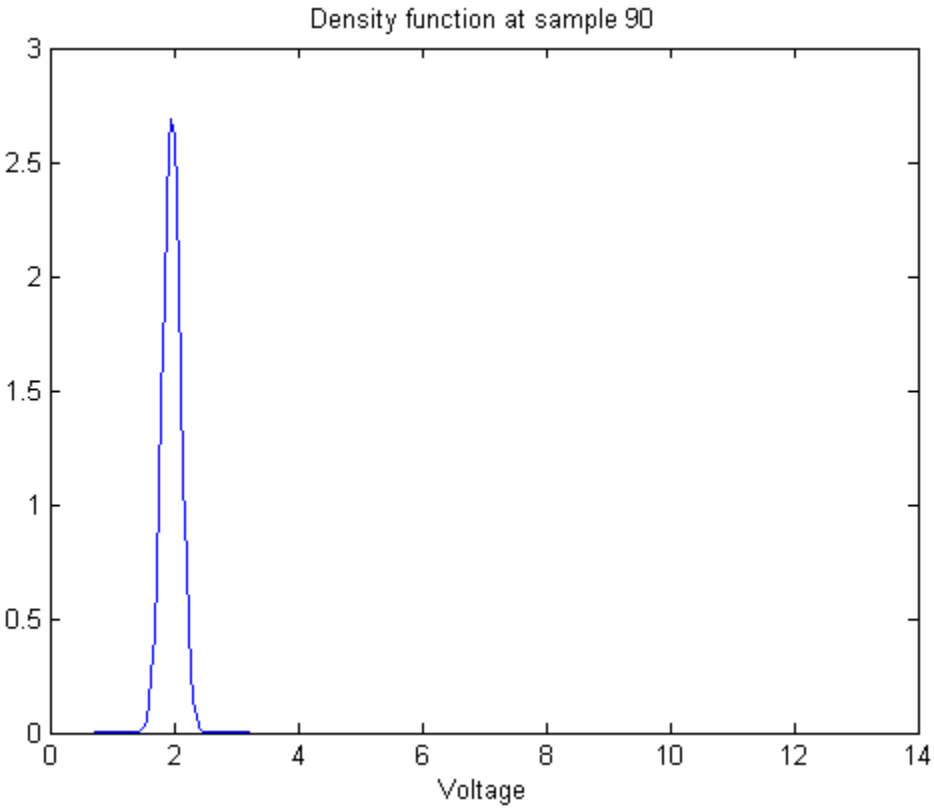

Figure 37: Density Function at Sample 90

An example of the Gaussian distribution applied in a signal processing and pattern recognition context comes from a paper titled “Gaussian Mixture Modeling… for Audio Fingerprinting” (Krishnan and Ramalingham, 2006). The paper describes an approach to the problem of “fingerprinting” audio signals for later recognition, a problem very similar to ours. One of the main ideas is to extract features from a set of training data and represent these as Gaussian distributions. This saves the algorithm from having to store the large amount of time-series data that constitute an audio signal. There are key differences, however, which render the methods described in the article not entirely applicable to our problem. First, our signals are very short compared to audio signals, thus we do not necessarily need the benefit of data compression. Secondly, much of the feature extraction described in the article is performed in the frequency domain, while our signals are very sparse in frequency content. Because of this, most of the feature extraction techniques (the entropy metrics, for example) would not give us useful fingerprints. Still, we found success with a method which treats the (relatively) small number of time-domain samples as independent features for matching.

4.2.4.2 Matching Algorithm

The matching algorithm's operation begins with a series of steps identical to the pre-processing performed for the Least Squares test. The raw input data are divided into 24-hour segments using the day separation function, and arranged column-wise into a matrix. Each day's data will be diagnosed independently.

The algorithm matches an input signal to one of the six conditions as follows. First, as in the Baseline test, training data are used to generate a mean and standard deviation signal for each condition. Each mean/standard deviation pair is then used to define a Gaussian probability density function. Because our standard baseline length is

143 samples in time (totaling 24 hours), there will be 143 Gaussian distributions per baseline. The concatenation in time of all the distributions for one baseline yields a two-dimensional density function which we call the "baseline distribution." There are six of these in total, one for each condition tested.

To diagnose one day's worth of data, the baseline distribution for each problem is integrated along the voltage curve for that day to obtain a score. In discrete terms, the score is the sum over all 143 time indices of the Gaussian distributions evaluated at the corresponding voltages in the input signal. More concisely:

$$Score = \sum_{i=1}^{143} P_i(v(i)) \tag{4.5}$$

where 'i' is the time index, P_i is the Gaussian distribution at time i, and v(i) is the voltage sample from the input data at time i. When all six conditions have been tested for, the condition with the highest score becomes the diagnosis. Figure 34 shows an example of a good match using this method, while Figure 35 shows a poor match.

A note on our usage of the Gaussian distribution: the typical statistical interpretation of the Gaussian distribution involves integrating the function over some interval to determine the probability that a random variable lies within that interval. Thus the probability of any single value is zero. However, because we are not performing any probabilistic calculations (making predictions, for example), only determining relative similarity between signals, we have found that an instantaneous evaluation of the function is sufficient.

Chapter 5 Results

Data were collected from October 13, 2008 to January 4, 2009. A typical forty-eight hour sample of filtered data is shown below for each system type of SHS problems simulated. Figures 38 to 43 illustrate the voltage patterns of each simulated problem. The first daytime cycle (0 hrs to 12 hrs) is a sunny day, while the second daytime cycle (24 hrs to 36 hrs) is a rainy day.

The voltage pattern of the solar panel in the control system is characterized by variations from about 12-12.5 V in the daytime to 2-3 V at night. The charging and discharging slopes are relatively high. The battery voltage reaches the same voltage as the solar panel during the day, and attains a charge capacity high enough so that nighttime discharge affects the battery voltage very little.

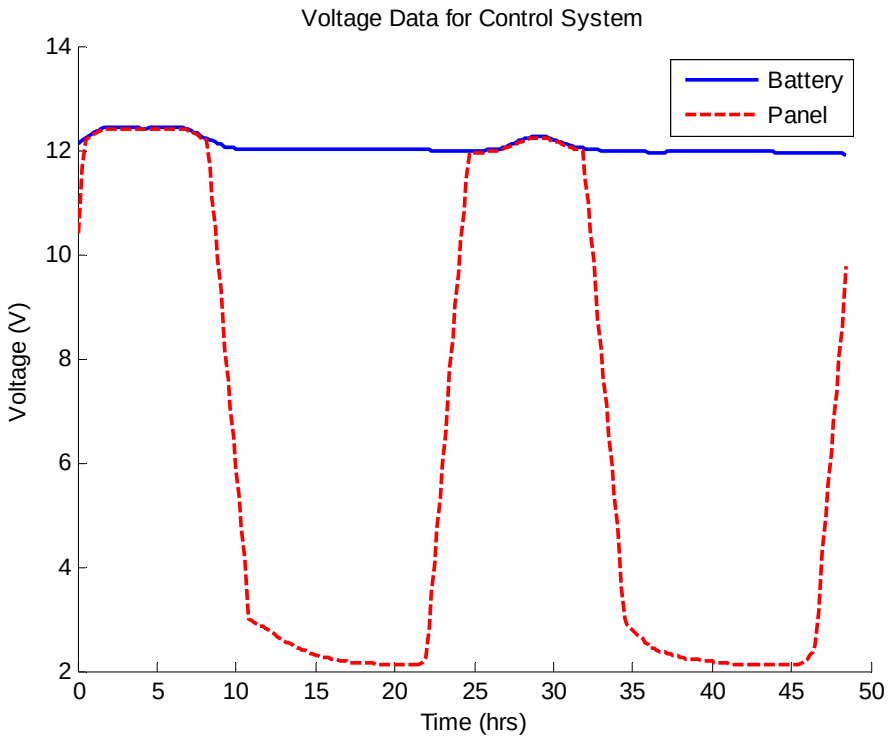

Figure 38: Average Graph of Voltage Output of the Control System (Nov. 12th to Nov. 14th).

The “dirty panel” system exhibits many features distinct from the control system. First, although the voltage from the solar panel itself reaches 12.5 V, the charging and discharging slopes are less steep than the control panel, meaning the system is not charging the battery as quickly, and is therefore less efficient than the control. Enough sunlight reaches the panel during the mid-day to produce the maximum 12.5V. However, some of the sunlight is blocked, which hinders the ability of the solar panel to reach the same voltage as the control panel as the sun rises and sets. This effect is most noticeable on the second day, which was a rainy day. The panel narrowly achieves full voltage at hour 30. The battery reaches a voltage slightly less than that of the panel during the day, and discharges considerably during the night. On the second day, because the system was charged less, the battery voltage dropped to a lower level during discharge than during the previous day.

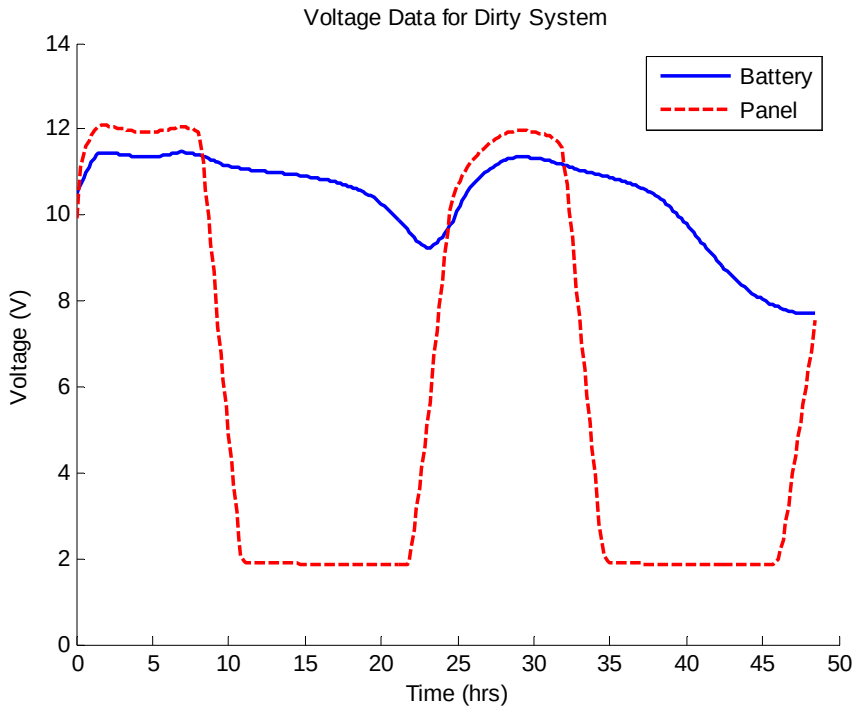

Figure 39: Average Graph of Voltage Output of the Dirty System. (Nov. 12th to Nov. 14th).

On an overcharged system, the larger solar panels reach a maximum of 16.5 V. The overcharged batteries exhibit a higher maximum voltage, averaging about 10% (~2 V) higher than the control. The batteries were also shown to charge to nearly the same level during the daytime, and remain at a high voltage during the night. Overcharging the batteries electrolyzes the water inside, which produces volatile hydrogen gas. Within a month, the overcharged batteries were noticeably bulging, and the systems were disconnected for safety reasons.

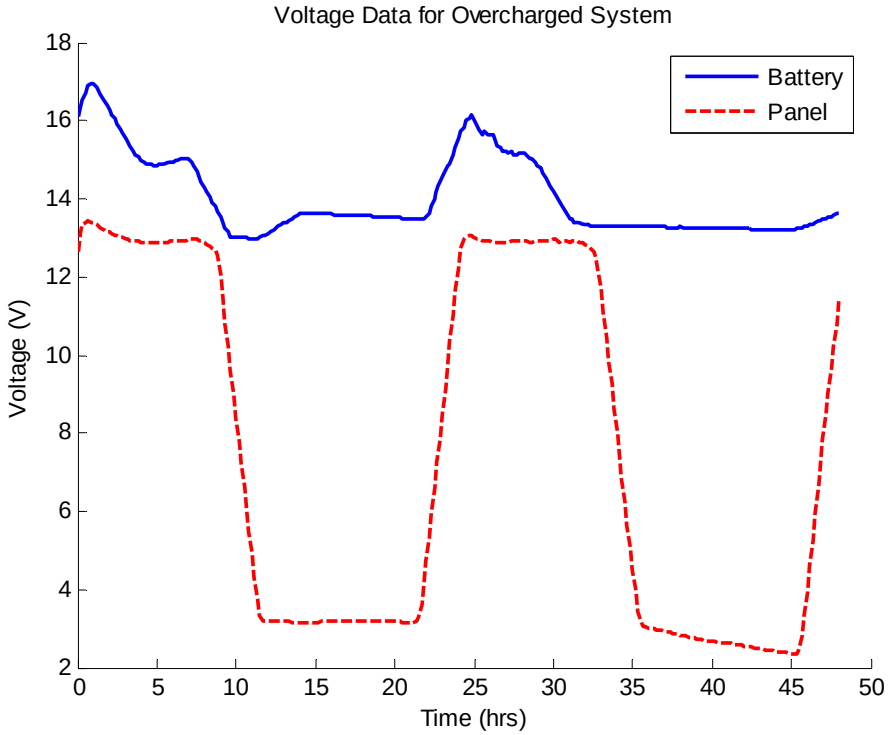

Figure 40: Average Graph of Voltage Output of the Overcharged System. (Nov. 12th to Nov. 14th).

Systems with batteries set to discharge deeply lost charge over a matter of weeks. In the data below, the battery is already deeply discharged, which seems to have affected the panel, possibly through corrosion. The panel now charges considerably less than a full 12 V and the voltage level is very susceptible to reduction in cloudy or rainy weather. The charging and discharging of this system is more gradual, as indicated by the slopes of

the charging and discharging periods. The panel is able to charge the battery to nearly its own voltage level during the day. For this system, the battery discharges to a voltage slightly higher than that of the panel voltage during the nighttime. In other cases, the battery was discharged so heavily that it could no longer hold charge, and the voltage hovered between 2 V and 4 V.

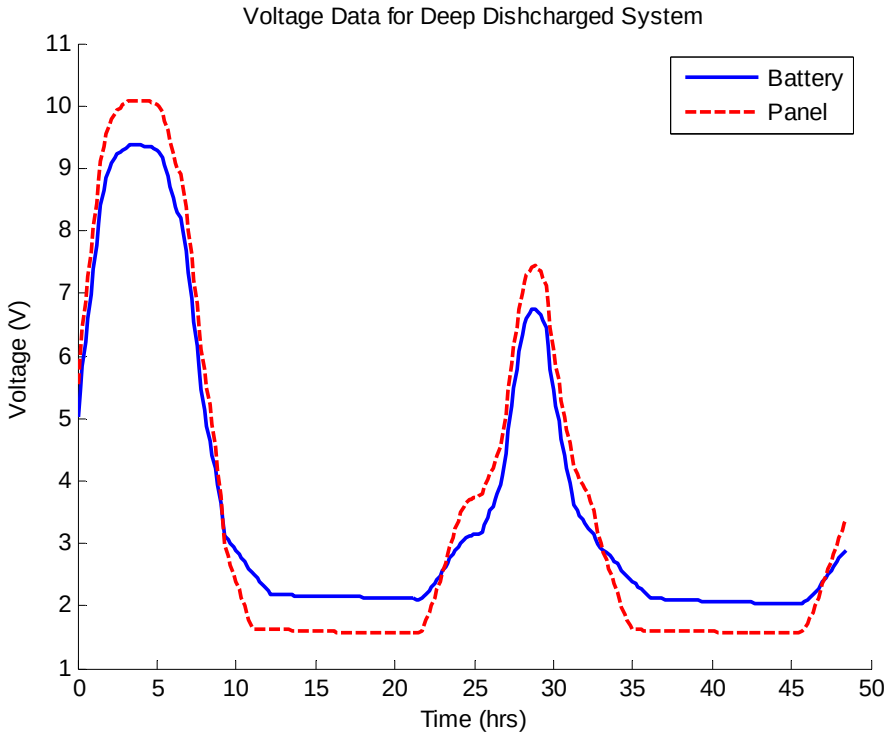

Figure 41: Average Graph of Voltage Output of the Deep Discharge System (Nov 12th to Nov 14th).

For systems lacking a charge controller, the battery and panel voltages are virtually equivalent because they share the same 'positive' and 'common' electrical nodes. Unfortunately, there is no simple way to automatically measure the panel and battery independently. As the system cycles between day and night, the voltage alternates from 12 V to 0.25 V. When the battery is disconnected, the battery voltage was measured to be 2.5 V during the day, meaning the battery actually holds very little charge during the day.

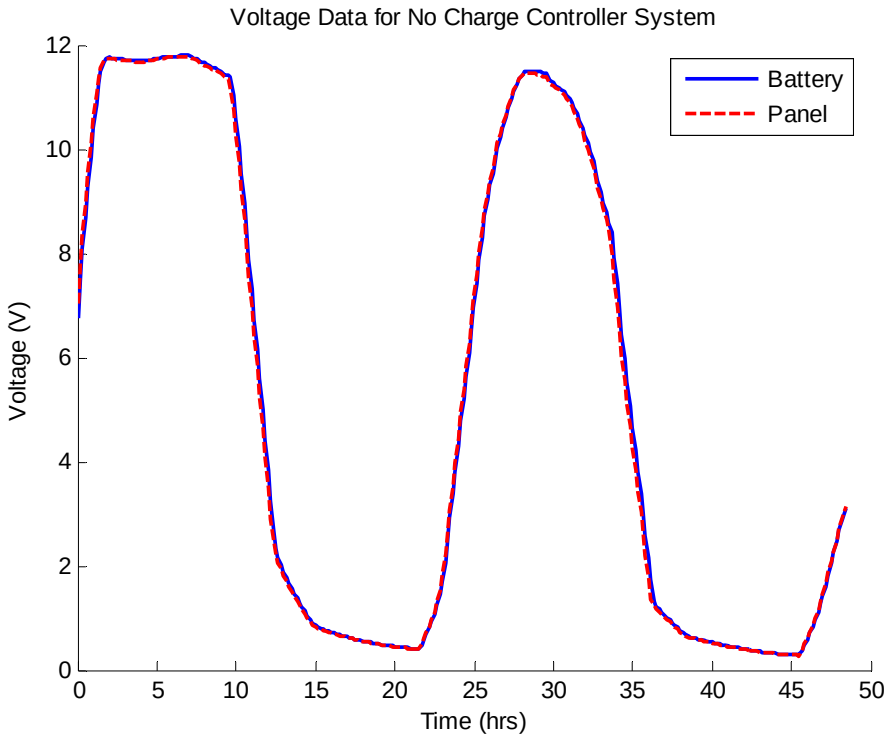

Figure 42: Average Graph of Voltage Output of the No Charge Controller System. (Nov. 12th to Nov. 14th).

Voltage data for the system using a car battery, which also does not include a charge controller, is shown in Figure 43. This battery, as opposed to a deep cycle battery, is designed to supply high current for a short time in order to start the combustion engine in an automobile, and is not ideal for use in solar home systems. After several cycles of deep discharging (significantly fewer cycles than a deep cycle battery of equivalent capacity), the system loses the ability to hold charge. Nevertheless, this type of battery is often used in the systems of villagers in developing countries due to their greater availability and lower cost. Again, the battery and panel voltage is virtually equivalent because the system is set up in such a way that the panel and battery voltages are

measured at the same points in the circuit. The features are very similar to the no charge controller test above.

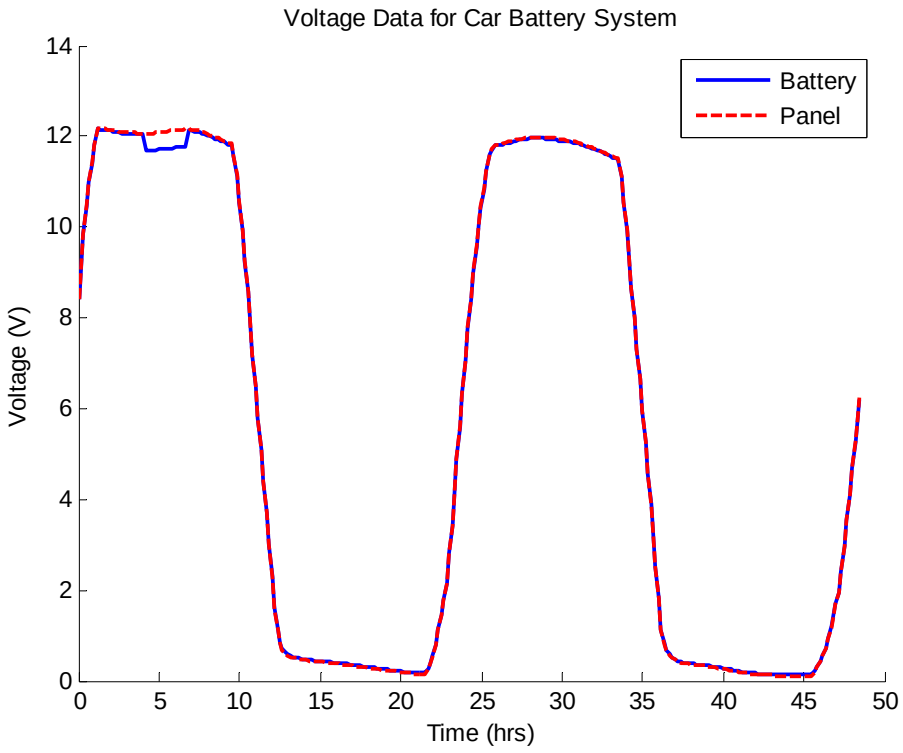

Figure 43: Average Graph of Voltage Output of the Car Battery System. (Nov. 12th to Nov. 14th).

5.1 Standard Test Samples

In order to compare the accuracy of the diagnostic algorithms employed, a standard set of sample data was selected. The data are composed of three weeks of panel and battery voltage measurements from December 1 to December 21.

Each type of system (control, dirty panel, etc.) is represented in the test set. First, each set of data is input into each detection algorithm. Next, the algorithms make diagnoses that should correspond to the type of system that the data comes from. Finally, the diagnoses are checked for accuracy and the accuracies of the algorithms are compared with one another. In this manner, it is possible to determine which algorithms are most

effective. The tests are also valuable in determining which problems are easy to identify, and which are most difficult.

The test data are from the same system, but from a different time period than the data used to create the baselines. The goal of this research is to determine if the detection algorithms can accurately identify problems from an arbitrary set of voltage data. Nevertheless, we assume that no significant changes, such as heavy battery degradation, occurred between the periods which would render the baselines unrepresentative.

Selected data, in Figure 44 illustrate the voltage pattern of the standard test data. It is important to notice the similarity between tests such as the control system and the dirty panel system. In Figure 44, data for the dirty panel is the dashed line because it discharges to a lower voltage than the healthy system; yet it would be more difficult for someone viewing the patterns to identify if only one pattern were depicted at a time. Likewise, the no charge controller and car battery systems have similar voltage patterns. Successful pattern-detection algorithms must be able to detect the small variability between these curves.

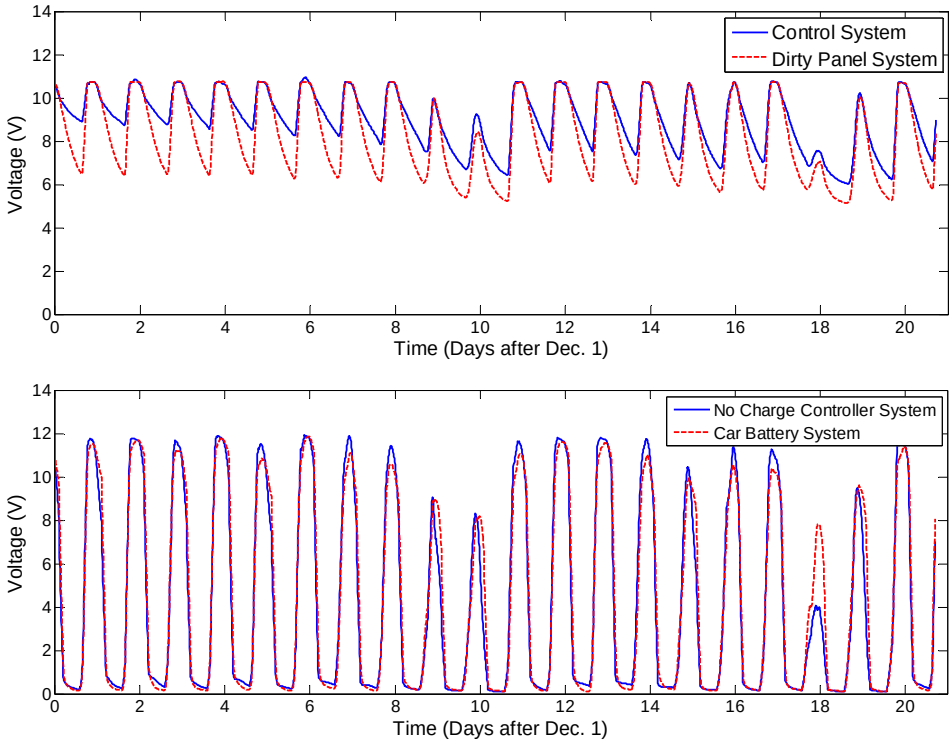

Figure 44: Standard Data from Selected Test Systems (Dec 1st to Dec 21st)

5.2 Comparison of Detection Algorithms

Team SHINE proposed several detection algorithms for system diagnosis. Using the standard test data, we tested and compared the detection algorithms. Each strategy has advantages and disadvantages. A detailed evaluation of the four detection algorithms is presented here.

5.2.1 Baseline Test

The six graphs in Figure 46 are a representation of the fraction of correct and incorrect diagnoses for each set of test data. Each graph may include a dark bar, which corresponds to the amount of positively diagnosed days of the test data. Light bars represent the misdiagnosed days and their respective fractions of occurrence. For example, Figure 45 is a results graph of a no charge controller system diagnosis. The test data was diagnosed correctly (dark bar) about 65% of test days, while it was

misdiagnosed as deep discharge (first light bar) 10%, and a car battery system (second light bar) 25% of the time.

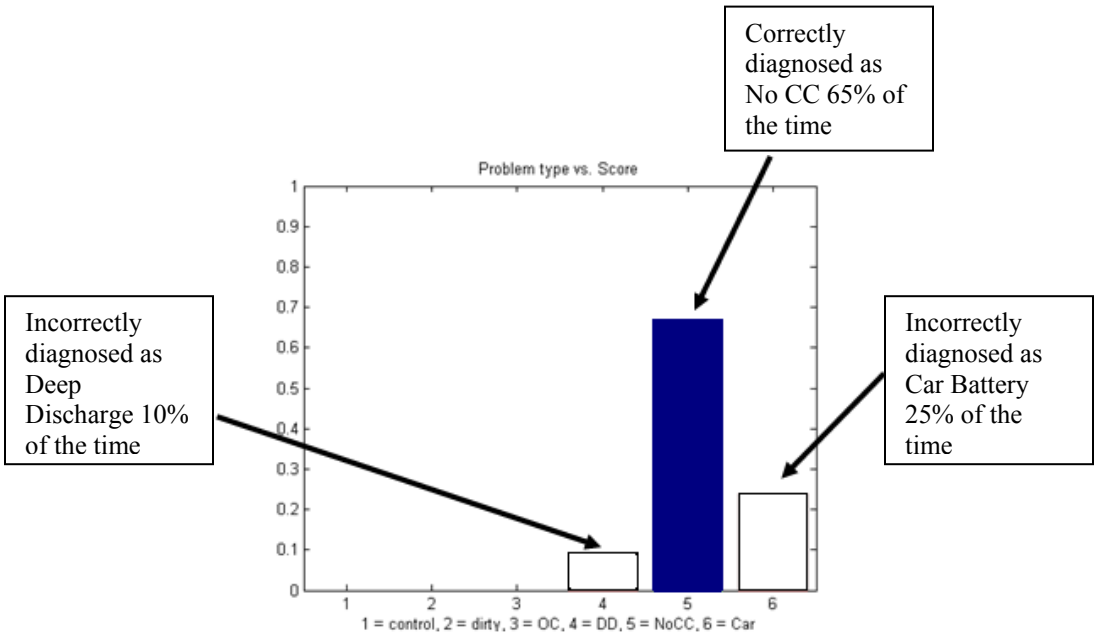

Figure 45: Example Graph of System Diagnosis

It appears that the control panel was diagnosed as a dirty panel system because of seasonal change. The amount of available daylight lessens near the time of the winter equinox. As winter approached, the amount of discharging for both the control and dirty panels continuously increased because there was less sunlight available and the battery may have not been charging back to full capacity during the daytime. Incidentally, the baseline data for the dirty panel system in November were very similar to the test sample data for the control system in December. The baseline algorithm was not sophisticated enough to account for this, and the control system was diagnosed as a dirty panel system. Further improvements could, however, take into account seasonal change and its effects on battery voltage. Nevertheless, the algorithm did identify that the control system was

discharging more than expected, indicating a smaller load should be used during the winter months.

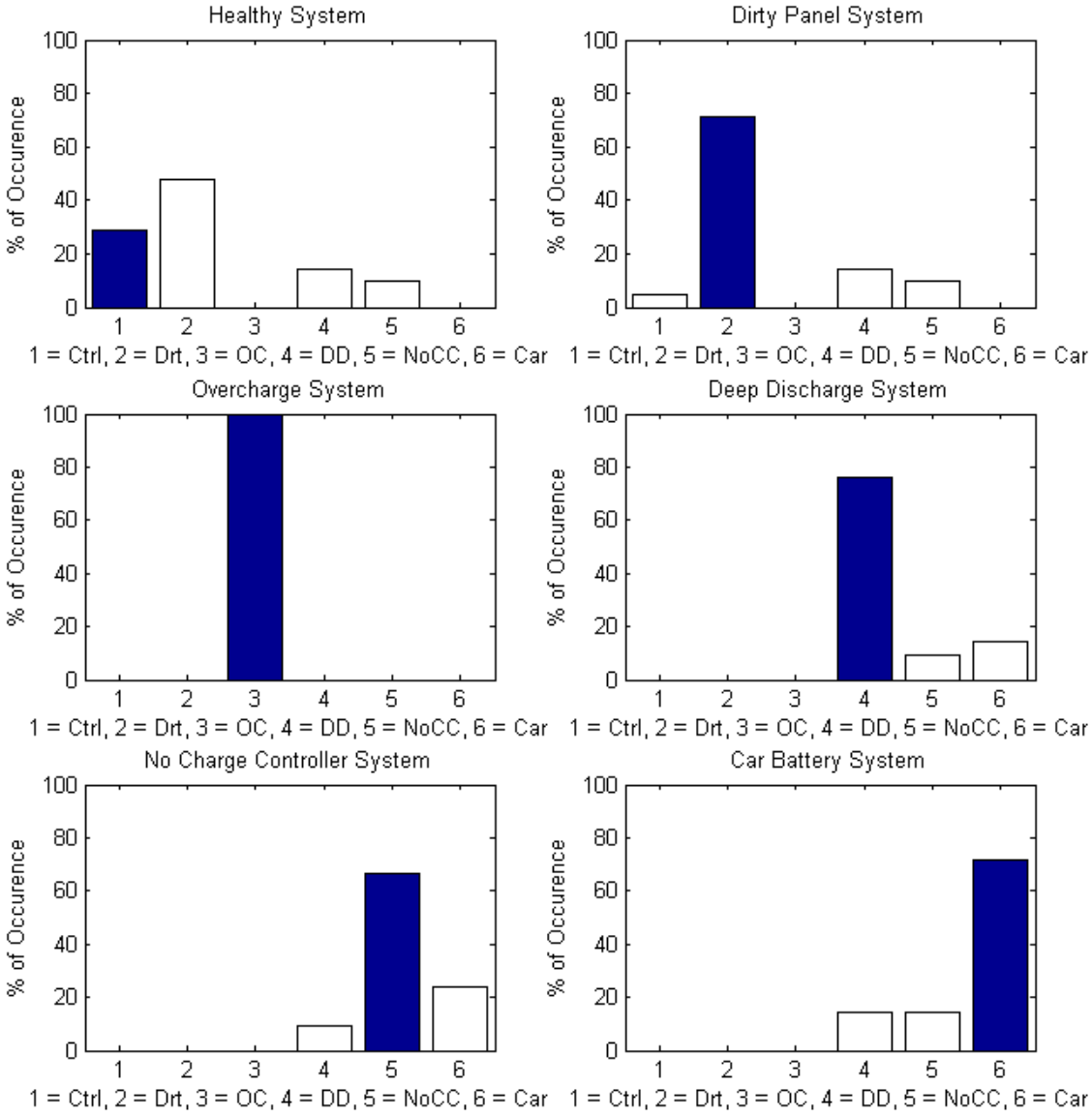

Figure 46: System Diagnoses using Baseline Test

5.2.2 **Single Metric Test: Average Voltage**

The first single metric test, which calculated average voltage for each day, correctly diagnosed 61.1% of daily voltage patterns overall. Average voltage was very accurate for the dirty panel system, overcharging system, and deep discharging system, which are

characterized by average voltages clearly separate from the other types of systems. This made the systems easy to diagnose.

As Figure 47 shows, the control panel, no charge controller, and car battery systems were misdiagnosed more often than they were correctly diagnosed. Daily average voltage alone cannot be used for high accuracy. This suggests that taking into account other parameters as well would allow for a stronger differentiation between each of the systems.

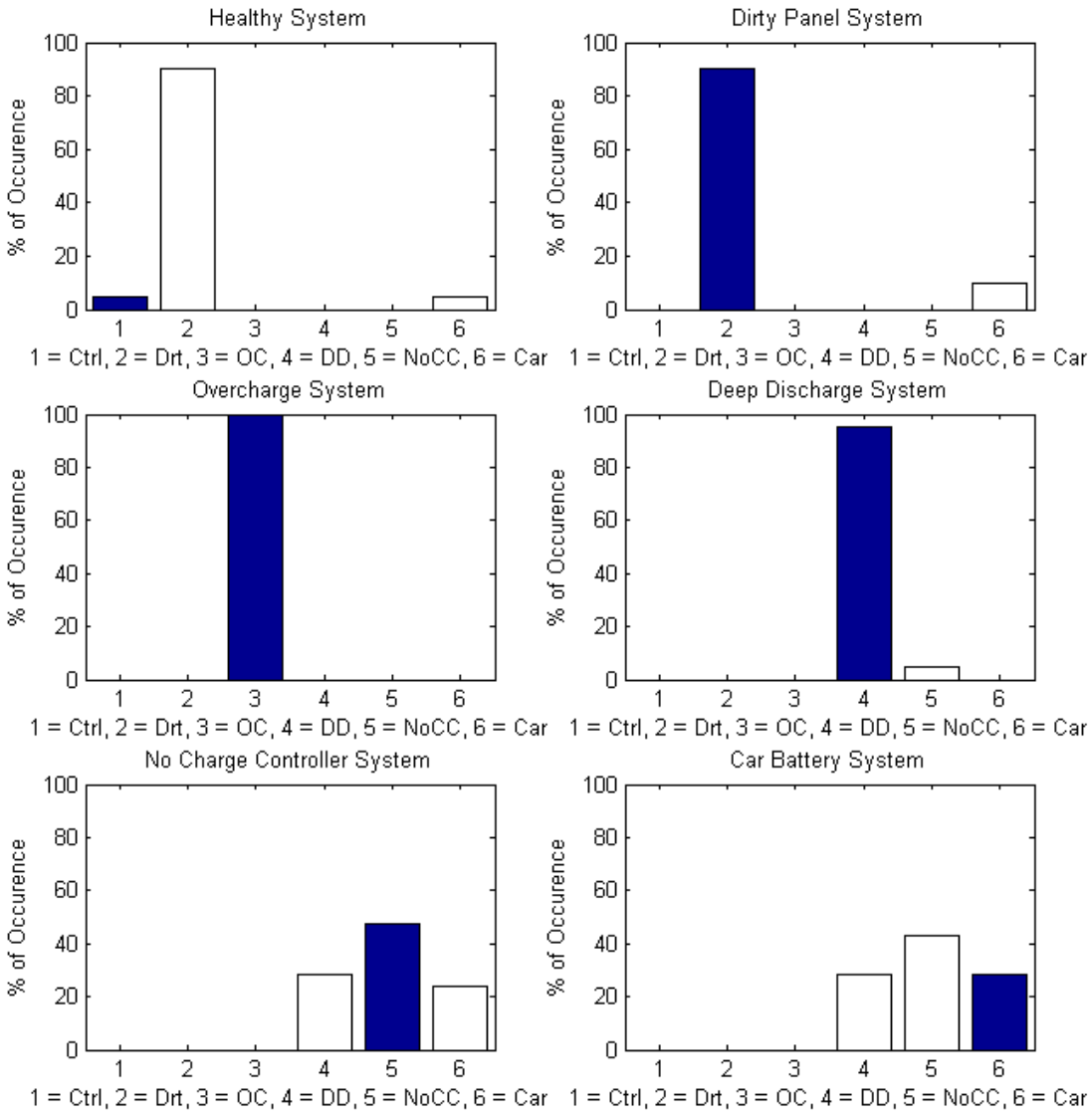

Figure 47: System Diagnoses for Single Metric Test: Average Voltage

5.2.3 **Single Metric Test: Average Rotation**

The measurements of average rotation were compared to those of the training data for diagnosis. The reliability of the average rotation test was equal to that of the average voltage test, with 61.1% of daily voltage patterns diagnosed correctly. This may be in part because average voltage and average rotation are related almost linearly. From Figure 48, this test diagnosed the dirty panel system and deep discharge system better

than the average voltage test, yet it diagnosed the no charge controller and car battery tests with lower accuracy.

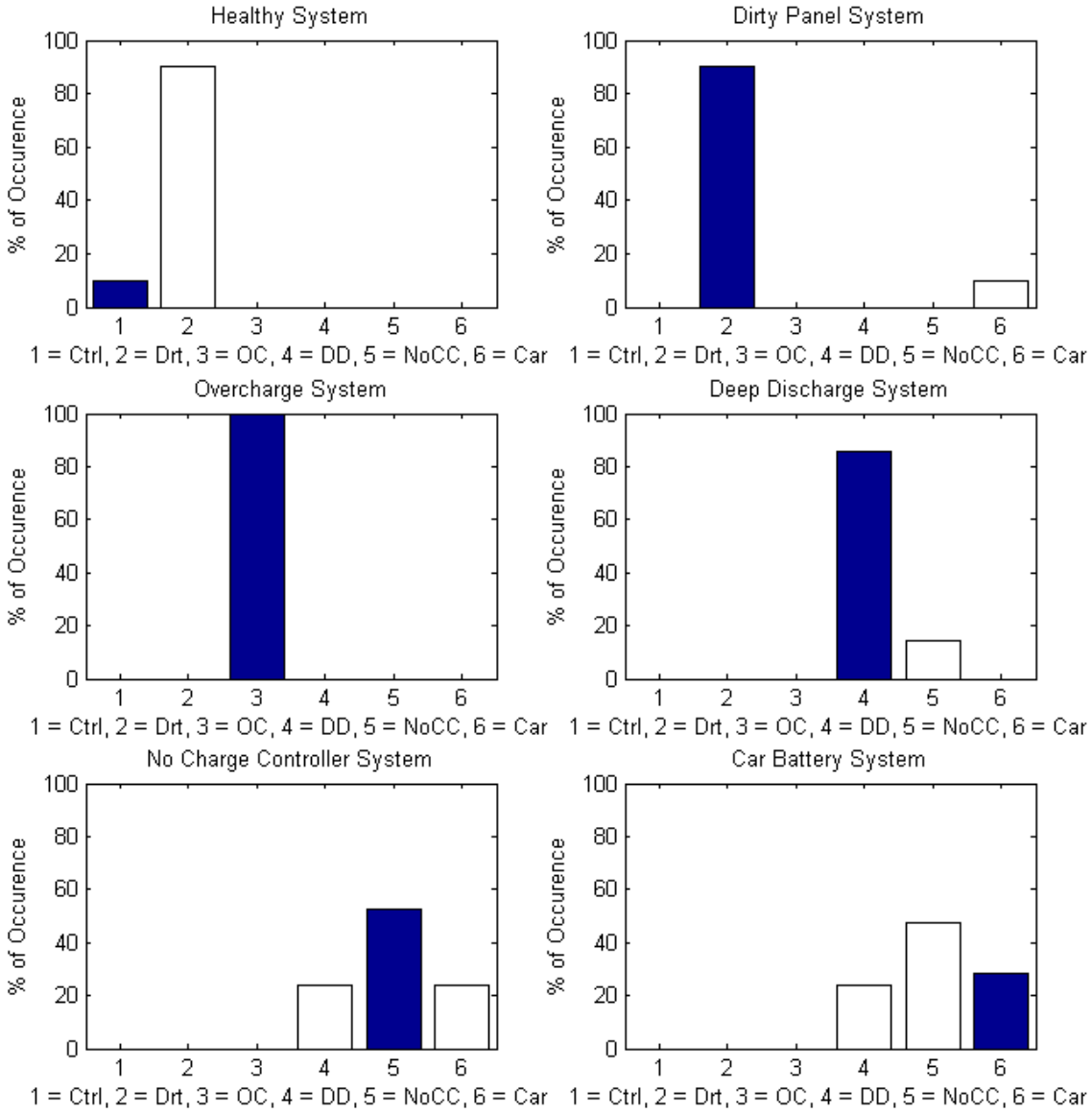

Figure 48: System Diagnoses for Single Metric Test: Average Rotation

5.2.4 **Single Metric Test: Average Curvature**

An average curvature version of the single metric test did not perform well, with an overall accuracy of 34.9%. As Figure 49 depicts, only the Control system and No Charge

Controller system were diagnosed correctly over 50% of the time. This leads to the conclusion that average curvature alone is not a reliable factor for the determination of system type. Although some system data are more curved than other data, the similarity between one pattern and at least one other are so close (e.g. the healthy and dirty panel systems) that the system misdiagnoses one of them. Also, due to daily fluctuations, curvature may be much different from day to day.

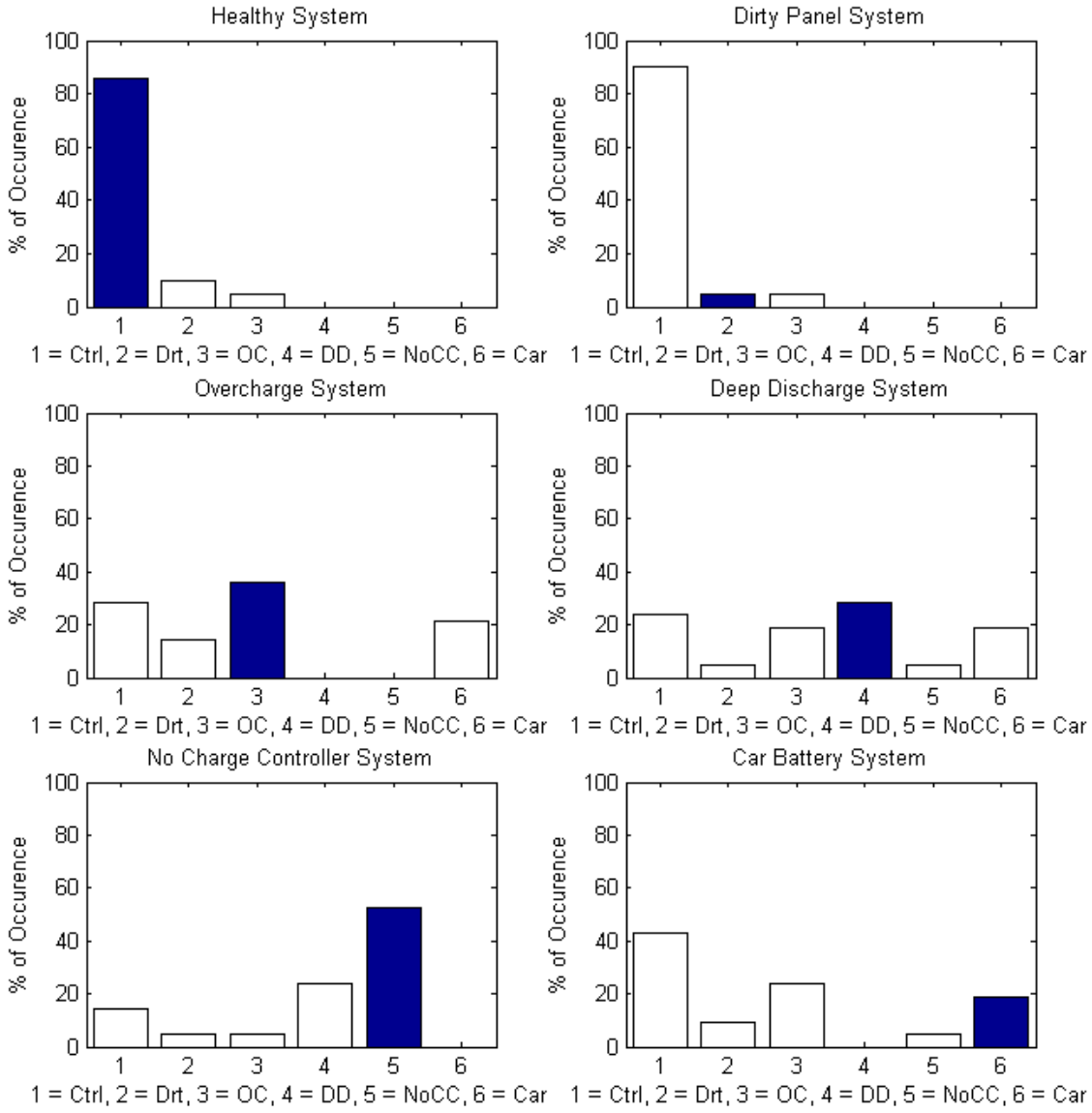

Figure 49: System Diagnoses for Single Metric Test: Average Curvature

5.2.5 **Single Metric Test: Maximum and Minimum Curvature**

The uses of maximum and minimum curvature alone were very inaccurate, as both tests yielded 36.5% and 19% correct diagnoses, respectively. Figure 50 shows low positive diagnosis, as only the No Charge Controller system was diagnosed correctly the majority of times. The overall misdiagnosis is no doubt due to the fluctuations in voltage patterns from day to day causing extreme deviation in these values. Maximum and minimum curvature could be averaged over a large sequence of days (greater than one week) to form a more accurate diagnosis.

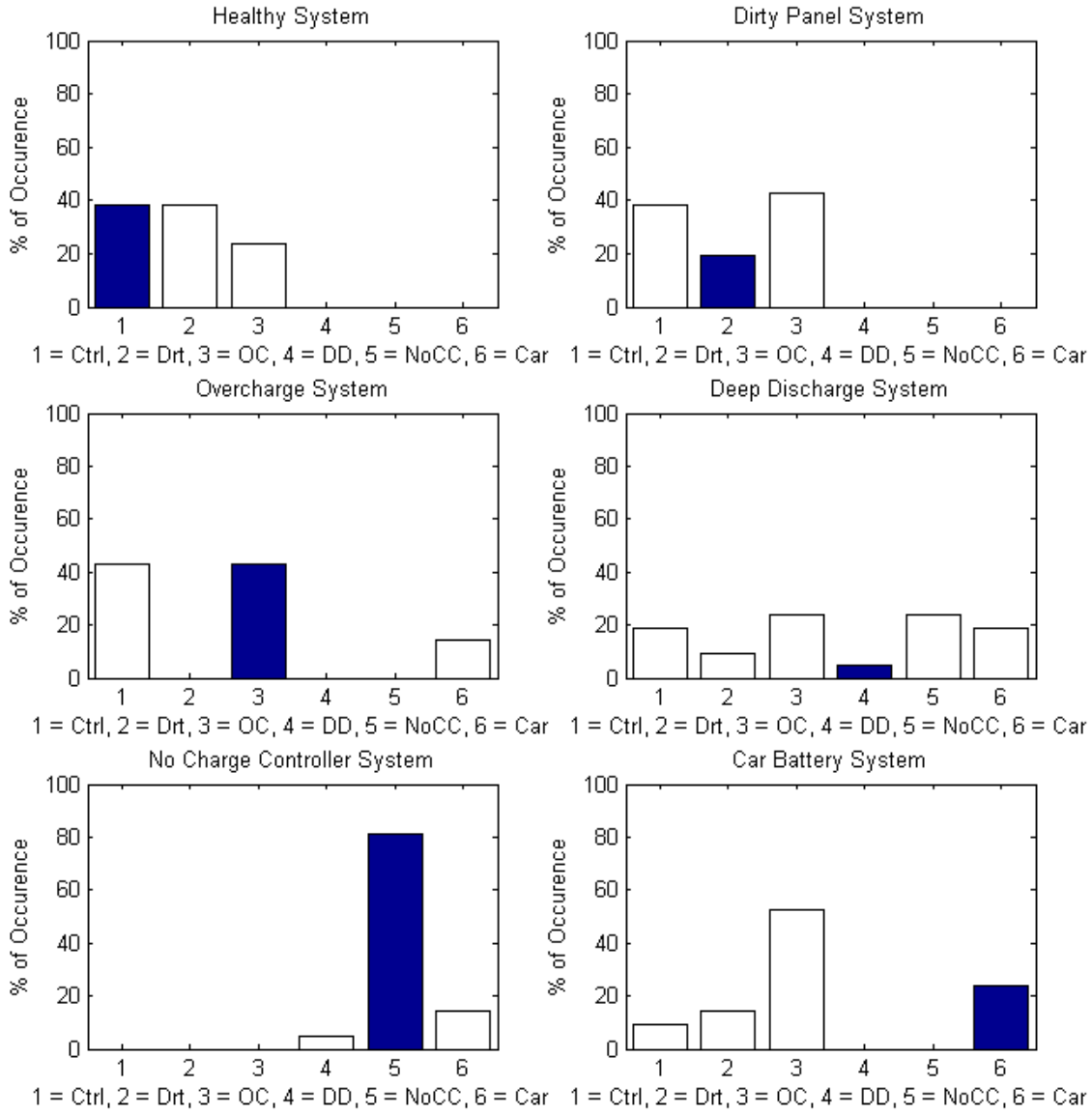

Figure 50: System Diagnoses for Single Metric Test: Maximum Curvature

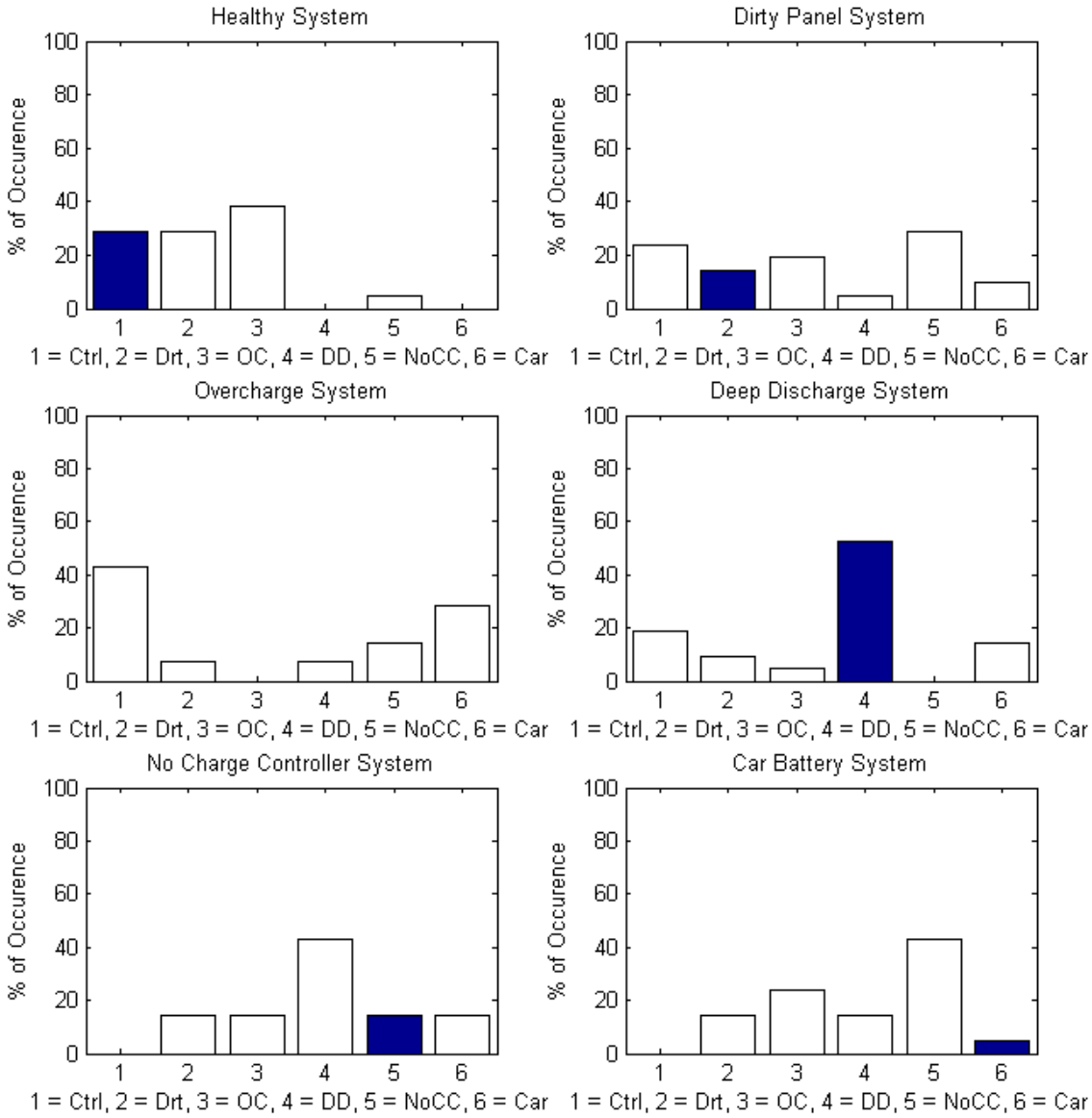

Figure 51: System Diagnoses for Single Metric Test: Minimum Curvature

5.2.6 **Single Metric Test: Average Discharge Slope**

Average discharge slope was also a highly variable parameter. Due to the similarity between certain discharge slopes (e.g. control and overcharge), it was difficult for the program to differentiate for proper diagnosis. Only 23% of daily voltage patterns

were correctly diagnosed overall. Figure 52 depicts the Control System as correctly diagnosed, but none of the common problems were diagnosed correctly. Due to seasonal change, the discharge slopes in the training data used to form target scores (from mid-November) were different than those in the test data (from December).

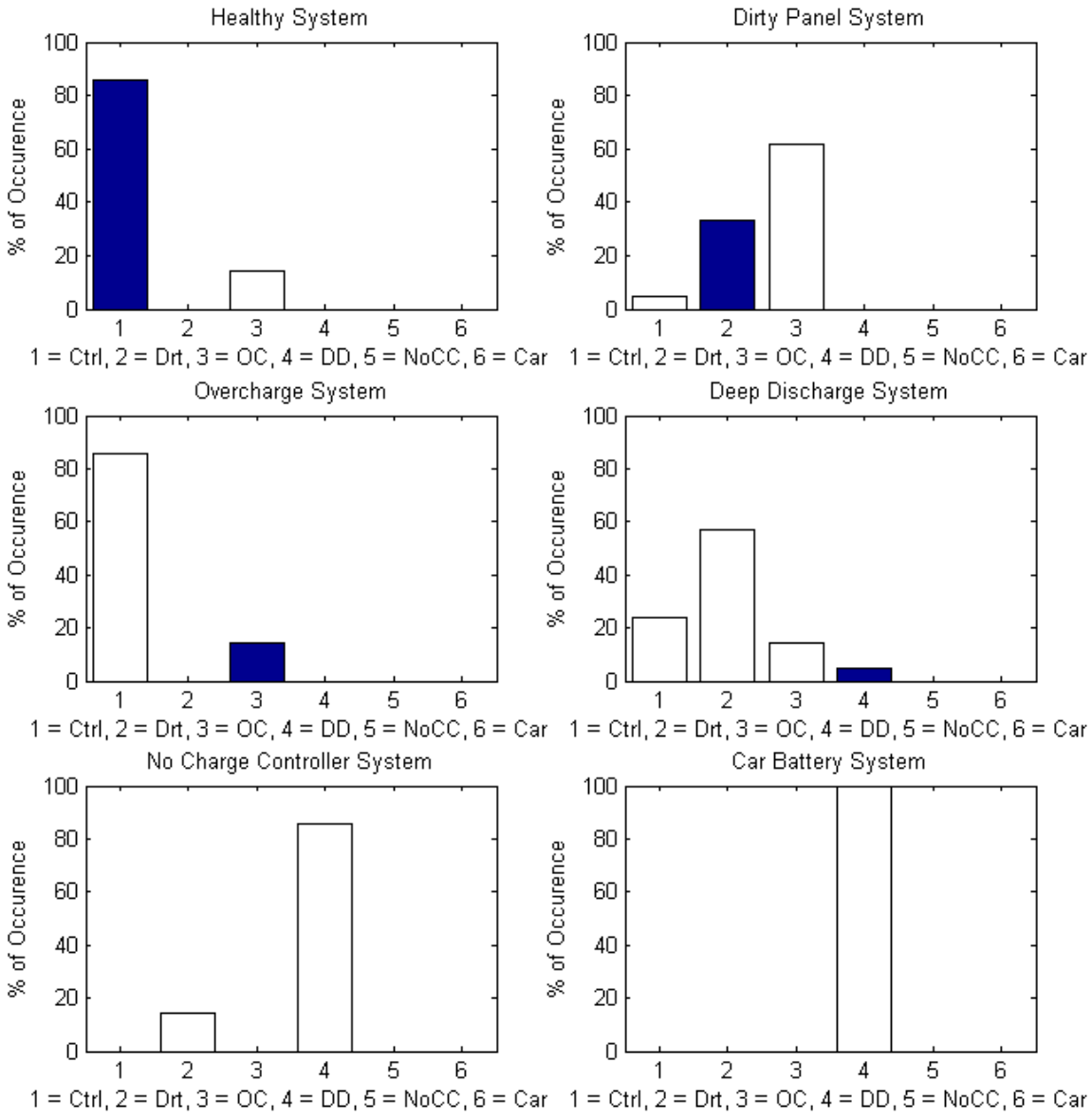

Figure 52: System Diagnoses for Single Metric Test: Average Discharge Slope

5.2.7 **Single Metric Test: Maximum Discharge Slope**

Finally, the test of maximum discharge slope was fairly inaccurate. 31.75% of daily voltage patterns were correctly diagnosed. The car battery was diagnosed well; however, the no charge controller system was overwhelmingly diagnosed as the car battery as well, indicating that there was little distinction between the two systems. The control system was diagnosed as a dirty panel system more often than the dirty panel was correctly diagnosed. Clearly, this test alone is not accurate enough to be used in a diagnosis tool, as is true with many of the other single metric tests.

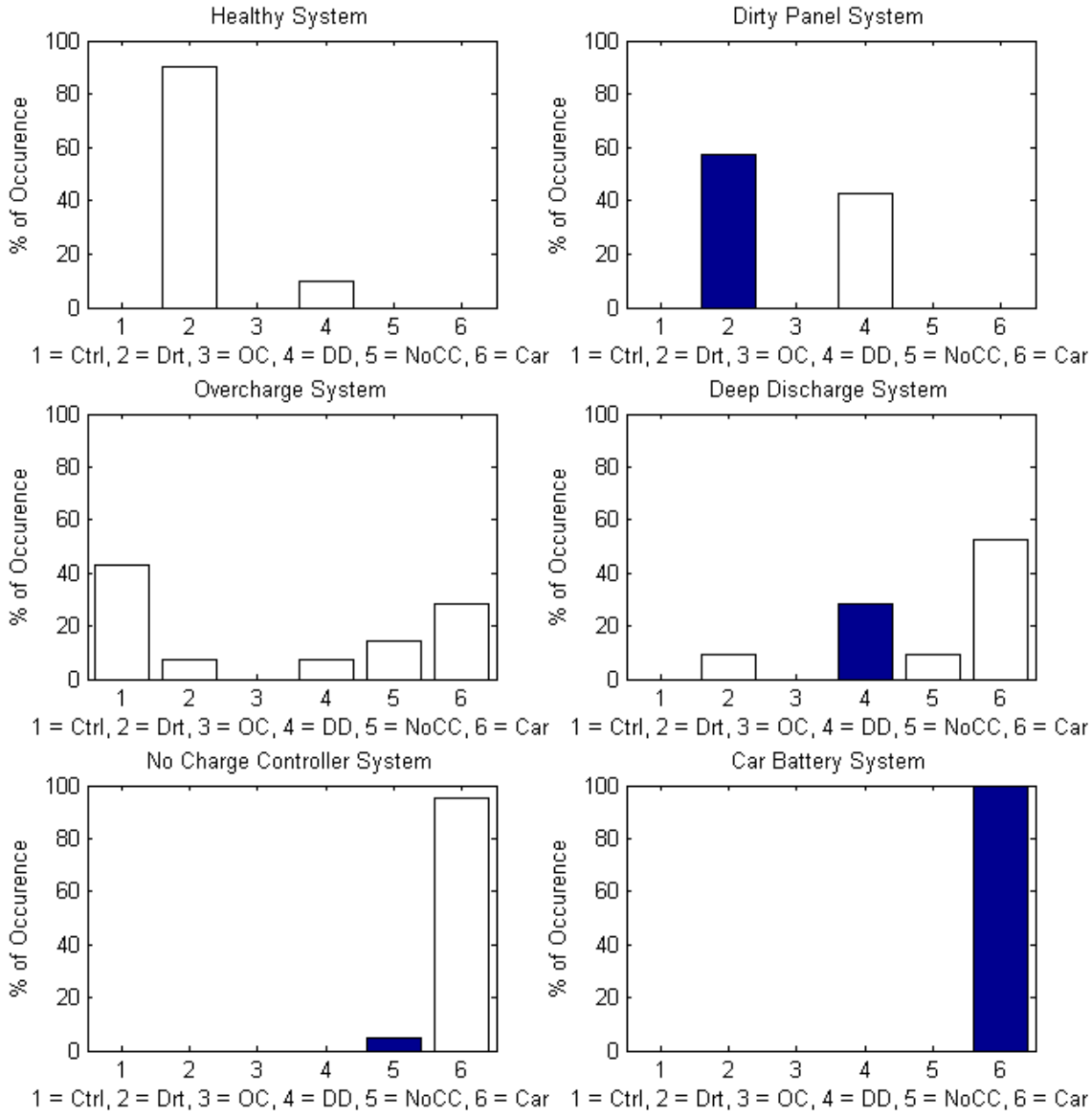

Figure 53: System Diagnoses for Single Metric Test: Minimum Discharge Slope

5.2.8 Single Metric Testing Conclusions

Individual parameters could not reliably detect problems to a sufficient degree. Although average voltage and average rotation are good indicators of system type, the use of several metrics in combination is hypothesized to be more accurate. Using a combination of weighted parameters, the reliable detection of most problems would be more likely.

5.2.9 **Combined Metric Test**

The combined metric test was less accurate than the baseline test. Using this detection algorithm, a 56% success rate was achieved using the standard test data. The dirty panel, overcharged system, and car battery system were correctly diagnosed 100% of the time. However, the control system was again mistaken for a dirty panel system. Also, the deep-discharged battery was mistakenly diagnosed as a car battery system. The features of the deep-discharged battery were highly unpredictable compared to the features of the other graphs, erratically exhibiting weak, low daytime voltage cycles. The reasons that the deep-discharged battery was incorrectly diagnosed include the fact that November data, used for model setup, had many low cycles due to cloudy or rainy days. Perhaps refinement of the weighting, removal of cloudy/rainy data, or use of additional statistical parameters would produce better results. A final option is to redesign the diagnostic test to evaluate a week-long (or longer) voltage time series rather than a single day's voltage time series. The combined metric test is, however, advantageous in realistic situations because it does not depend on specific baseline data. Unlike the other three tests used, this test can be outfitted on a system that has no prior voltage history.

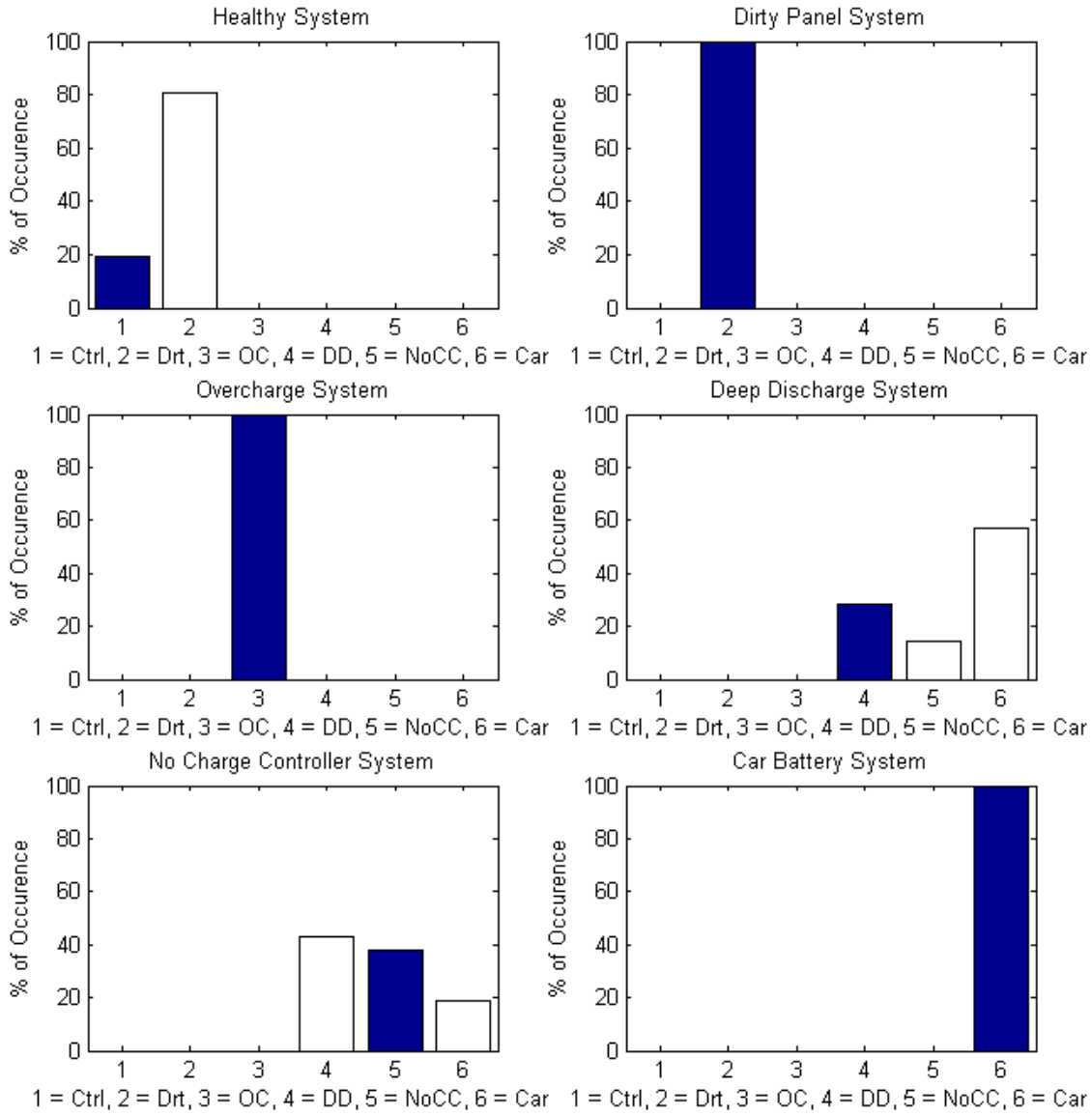

Figure 54: System Diagnoses using Combined Metric Test

5.2.10 **Least Squares Test**

When given our test data set, the Least Squares matching algorithm flawlessly diagnosed Dirty, Overcharged, and Deep Discharged systems, and performed nearly as well for the No Charge Controller system. For the Healthy/Control system, the diagnoses were about evenly divided between Control and Dirty, but slightly in favor of the correct diagnosis. For the system using a Car Battery, the diagnoses were all incorrect.

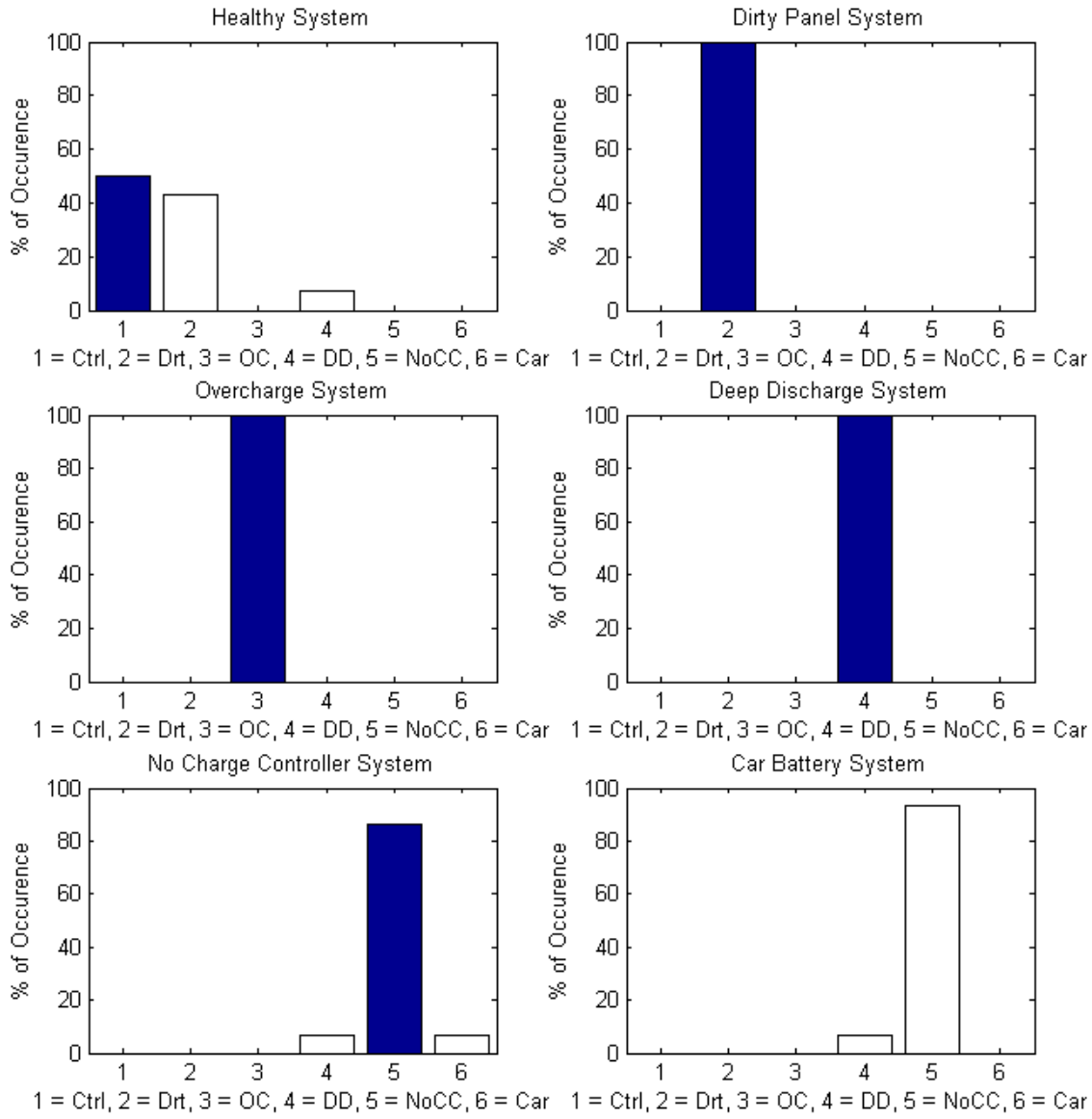

Figure 55: System Diagnoses using Least-Squares Test

The overwhelming majority of false diagnoses for the Car Battery system were for the No Charge Controller condition. Upon review of the mean baselines for these two problems, it is evident that they are very similar for their entire duration. In the vector sense, this equates to the two vectors being nearly parallel, and thus having very similar distances to any input vector. The distance between two n-dimensional vectors v1 and v2 is given by the following equation:

$$\sqrt{\sum_{i=1}^{n} |v_1(i) - v_2(i)|^2} \tag{5.1}$$

In this case, our test Car Battery data was slightly closer to the No Charge Controller vector for nearly every day in the test data.

5.2.11 **Gaussian Test**

When provided with the same set of test input data as the other matching methods, the Gaussian test performed admirably. It was able to correctly diagnose 100% of Dirty, Overcharge, Deep Discharge, and Car Battery days, 64% of Healthy/Control days, and 53% of No Charge Controller days. The series of bar charts in Figure 56 shows proportions of correct (black) and false (white) diagnoses from the test set.

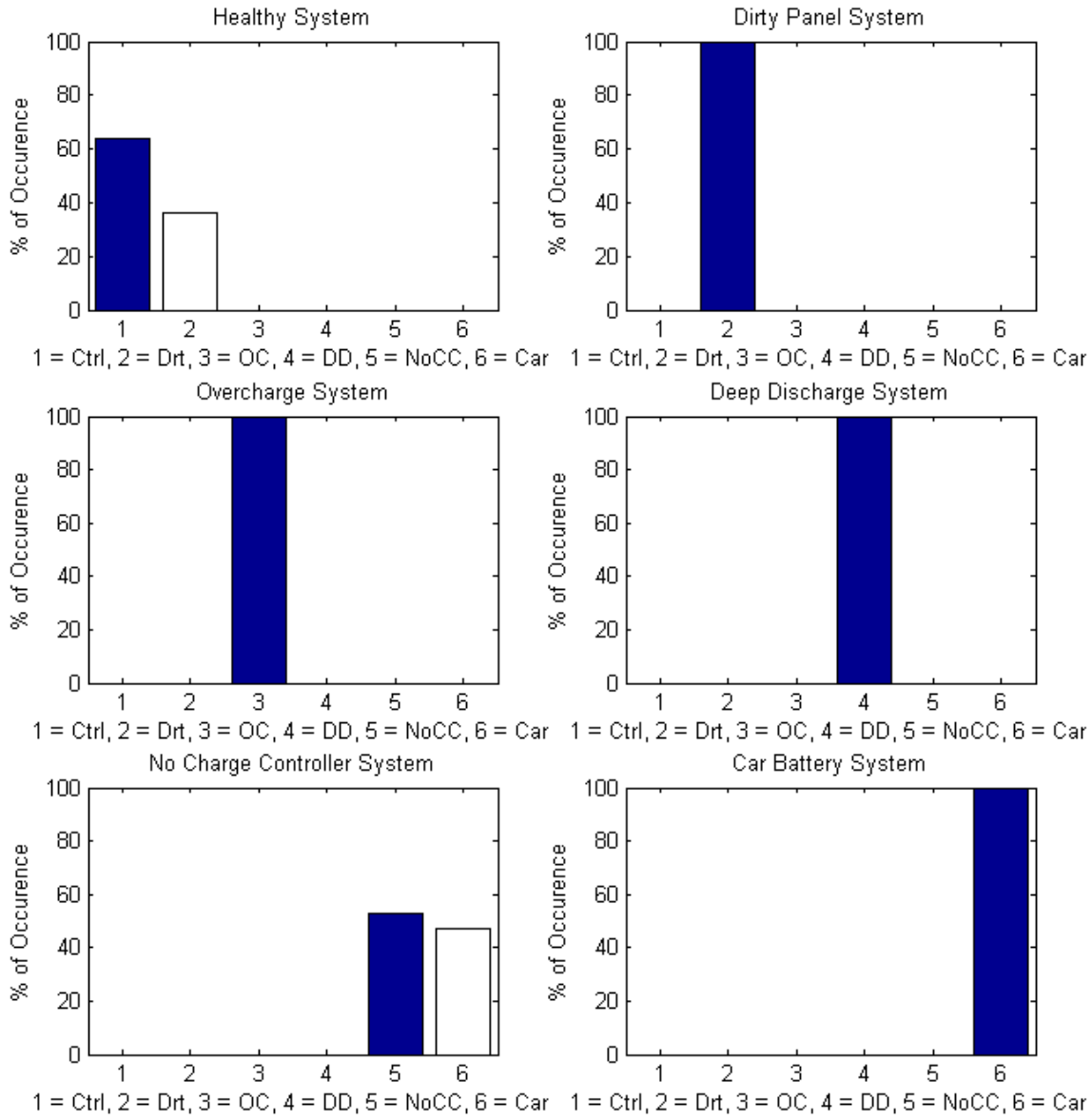

Figure 56: System Diagnoses using Gaussian Test

Chapter 6 Discussion

6.1 Comparison of Detection Programs

From the individual analyses, it is possible to make tentative conclusions about the effectiveness of each detection algorithm in real-world applications. Each test has advantages and disadvantages that affected its reliability for the simulations conducted in this research. A comparison of the percentage of correct diagnoses and the percentage of incorrect diagnoses for the four main detection algorithms is displayed in Figure 57.

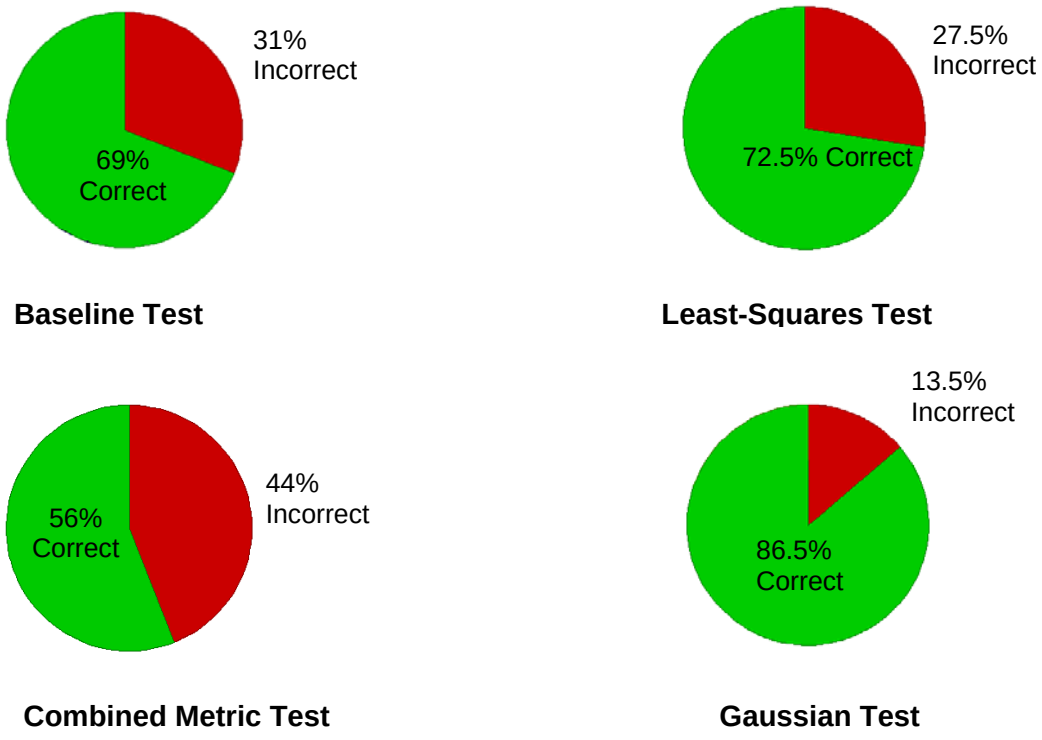

Figure 57: Percentage of Correct and Incorrect Diagnoses of Various Detection Methods

Results indicate that the Gaussian test had the greatest accuracy over the range of tested data, at 86.5%. The main factor which accounted for the success of the Gaussian test as compared to others was the application of a smooth weighting function. It was essentially a continuous, fine-resolution version of the Baseline test (which utilized an

envelope with a crisp boundary—see Section 4.2.1). The major difference between the Gaussian test results and the Least Squares test results was the ability to correctly identify the car battery system.

Although the Gaussian test was very accurate, further development could be undertaken to enhance its accuracy. The Gaussian test might be improved by allowing each data index point's Gaussian distribution to radiate in two dimensional space, rather than comparing only corresponding samples in time. Radial distribution (illustrated in Figure 58 would produce a baseline which has "thickness" in the horizontal dimension, and is therefore more resistant to phase shift in time. However, generating the new total distribution by overlapping many radial distributions would make the algorithm more complex.

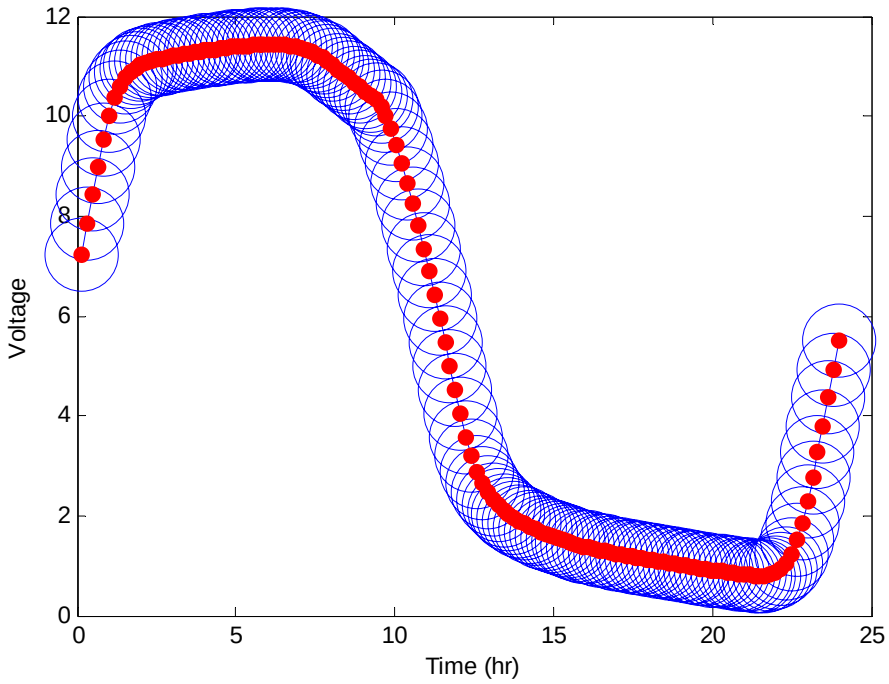

Figure 58: Illustration of a 2-D Radial Distribution

The Baseline test had 69% correct diagnoses. The advantage of this test lied in its simplicity. Voltage baselines can be easily formed by averaging sets of training data.

However, one disadvantage was its reliance on a set envelope rather than the distinctive features of each test. A major problem with the Baseline test was the misdiagnosis of healthy panels as dirty panels. The most likely reason for this failure is that the test did not account for seasonal change between the training data and the test data. The envelope set for this test was not able to compensate for seasonal changes. To solve this problem, different baselines could be used for different times of year, as was done for weather patterns (discussed earlier in Section 3.7), to mitigate misdiagnosis.

The Combined Metric test was the least accurate of the four main tests. Although this test took into account the important distinctive features of the voltage patterns, the variation in these parameters from day to day (especially curvature and discharge slope) severely weakened the effectiveness of the Combined Metric Test, leading to an overall accuracy of 56%. Rather, when data were averaged over several days, so that highly variable parameters such as curvature and discharge slope could be averaged, the test accurately diagnosed four out of the six systems with a 66% accuracy (Figure 59). The same problem as in the Baseline test, the misdiagnosis of healthy and dirty panel systems, occurred. The healthy systems exhibited steeper discharge slopes and lower average voltage than was expected because of seasonal change. Thus, the measured healthy system parameters resembled those of the dirty panel systems. A more robust program, taking into consideration time of year would be a simple and effective solution to this problem. Another issue that could have contributed to the inaccuracy of the Combined Metric test was the amount of filtering in the data. The test data were filtered with the aforementioned eight-point average filter. Depending on the amount of filtering, and the smoothness imparted to the curves, parameters such as curvature and discharge slope will

vary. Thus, future research attempting to use this method will benefit from a close inspection of the effects of filtering on these parameters.

The Least Squares test was the second-most effective, with 72.5% correct diagnoses. The only major misdiagnosis was that of the car battery system, typically misdiagnosed as a no charge controller system. This stems from the fact that the voltage patterns of the two systems are very similar overall. The least squares reconstruction of the car battery test data clearly yielded a correlation closer to that of the no charge controller system. However, this issue was not problematic in the Baseline, Combined Metric, and Gaussian tests. There was a distinctive separation between the No Charge Controller and Car Battery baselines just preceding the discharging slope (see Figure 32) because the baseline of the No Charge Controller test begins discharging earlier than the Car Battery system baseline. The Baseline and Gaussian tests were able to distinguish between the No Charge Controller data and the Car Battery data because the aforementioned baseline separation caused the No Charge Controller data to have a higher correlation with the No Charge Controller baseline, and the Car Battery data to have a higher correlation with the Car Battery baseline. In the Combined Metric test, this separation played a role in dictating the maximum and average curvature of the daily data, which also allowed for clear distinction and correct diagnosis. The Least Squares test did not identify this discrepancy because the approximation is less effective at detecting such minor discrepancies.

With regard to the parameters used in the Gaussian and Baseline matching algorithms, a more statistically valid model for the spread of each distribution would use

the standard error of the sample mean (SEM), rather than the sample standard deviation. The SEM is given by:

$$SE_{\bar{x}} = \frac{s}{\sqrt{n}} \tag{6.1}$$

s is the sample standard deviation (i.e. the sample based estimate of the standard deviation of the population), and n is the size (number of observations) of the sample.

Because this quantity is inversely related to the sample size (i.e. number of days of training data), a larger sample size yields a narrower distribution. As the sample size increases, the distribution becomes narrower and eventually converges to a single value: the true mean voltage at that time index for all systems afflicted with the same problem. Thus collecting more training data yields greater certainty as to the true shape of the voltage curve for each problem.

For use in a matching algorithm, the SEM can be multiplied by a scaling factor to change the algorithm's selectivity. While acquiring a large set of training data may yield a more accurate picture of the true voltage curve, it can also make the distribution so narrow as to exclude actual matches. Depending on the size of the training set, the scaling factor can be adjusted to maximize the percentage of correct diagnoses in a manner similar to the threshold proposed for the Least Squares test.

6.2 Limitations

Due to time constraints and lack of funding there are a few limitations we were unable to explore in our study. Although several trials were carried out, the effectiveness of the individual programs were only tested on two sizes of PV panels, two brands of charge controllers, and two different brands of batteries. Further testing on different types of photovoltaic systems in different conditions would be a practical method of validating

these results. These methods may have also been affected by variables for which we did not control, e.g. seasonal changes. Additional limitations are concurrent problems, variable load, and insect infestation.

6.2.1 **Seasonal Change**

We encountered several limitations conducting our study outdoors. For instance, the changes in season caused variation in sun light and precipitation levels. We tried to control for these changes through numerous repetitions within the study. However, future trials within a controlled environmental system could be conducted for further verification. Additionally, the effect temperature has on the solar panels and batteries was not explored and warrants further investigation. We hope that the next step in this research is in field trials of the pattern recognition system, to determine if the problems can still be identified even with all the uncontrolled variables found in a real-life setting.

6.2.2 **Concurrent Problems**

One limitation of our research was the inability to account for the existence of concurrent problems. We recognize the fact that more than one problem can affect a solar home system at any given time. However, Team SHINE was unable to factor this into our research and the detection algorithm we designed is only capable of detecting one problem at a time, since our baseline curves are derived from simulations of each problem individually. In each of our proposed detection schemes, the program selects which of the problems are affecting the system or decides that there is no problem.

One solution would be to combine the baseline curves derived from each of the problems into different combinations. This way, baselines for each problem would be obtained, but also for different problem combination. Unfortunately, the effects on

voltage from these problems are unlikely to be linear and cannot be easily combined. This method may be too simplistic and not applicable for actual solar home systems.

The most reasonable solution is to propose future research to determine the voltage output of these combinations of problems. We believe our experimental design was successful for the development of algorithms to detect single problems affecting solar home systems. One can develop similar experiments to simulate multiple problems on one system, and use these voltage outputs to create similar detection algorithms. Though limited time and resources have not allowed Team SHINE the opportunity to carry out these tests, the following is an example of an experiment for the detection of multiple problems affecting solar home systems.

One possible combination is the use of a car battery and at the same time overcharging the battery. This can be simulated by merging our two setups for each of these individual tests. The same basic control setup can be used (see Figure 8). Instead of a deep cycle battery, a 12V car battery can be used, just as in the Car Battery test. This system can then be overcharged by connecting it to a 15V panel, just as was done in the overcharge test. These data can then be logged and used to create baselines, as we did for each individual problem. For this example, the result would be a "car battery/overcharge" baseline. When looking at real data, this can then be a possible diagnosis in the detection algorithm.

This same process can be used for all combinations, even for more than two problems. For example, it is possible to have a system with an overcharging car battery and dust on the panel. Some combinations, however, will not need to be simulated because they are mutually exclusive. The car battery test by nature already has no charge

controller, so those would not need to be combined and tested. Another example is a system with both a dirty panel and overcharging, because these are not likely to happen in combination. For all of the relevant problem combinations, our same individual setups can be combined, allowing future researchers to broaden the scope of our diagnostic tool to concurrent problems.

6.2.3 **Variable Load**

Due to the many possible variations in usage of solar home systems, the experiment designed by Team SHINE chose to model the experiment in one standardized format for all data recording. The system was left with a steady load for all times during which it was utilizing the stored solar power. By designing the experiment in this manner, it ensured that regular baselines were found for the different stimulated common problems for accurate comparisons. The setup is based on the observation that it is typical for solar home systems in developing countries to power one light in a continuous manner. However, this may not be the way individuals make use of the power from the systems. Instead of continuously depleting the systems of stored power the usage could vary throughout the night depending on the needs of the users and this would alter the load on the system. Whether it is turning lights on and off, varying the number of lights operating in a home, or other such changes in power usage, these changes will affect the output recorded by our monitoring devices. The potential fluctuations or other changes of the voltage curves from these systems could challenge the ability of the monitoring system to accurately establish the common problem afflicting the given system. To address this potential problem adjustments would be made, and the testing may require the user to keep the light on during the entire testing period.

6.2.4 **Insect Infestation**

Insect infestation is a common problem in the developing world that could not be accounted for in this study. Due to the "insect's homing instinct to nest in warm and quietplaces" many of the components of solar home systems make ideal nesting places for insect (Lorenzo, 2001). Lorenzo et. al found that even covering a photovoltaic module connection box with a tight lid was not enough to prevent wasps from creating nests in the box. The authors stress the importance of making sure all components of the solar home system are water tight to prevent insects from building nests inside. Insect infestation can be detrimental to the system, because it increases the risk of the system short circuiting (Lorenzo, 2001). Additionally, insects can block sunlight from reaching the system by nesting on the photovoltaic panel. This decreases the voltage output from the panel and would reduce the amount of power available for the users. Although insect infestation is a serious issue in the developing world we were unable to simulate an infestation in our experiment. We had no way to create an insect infestation or to promote an infestation due to the fact that much of our equipment was located indoors, and would creating an insect infestation pose a health hazard. Possible future research could investigate how infestations affect voltage output by setting up the experiment in such a way that insects could nest in the equipment.

6.3 Expected Impact

Since the results of our study are algorithms and not a final product, it is impossible to predict the impact of our proposed final product. Overall, there are approximately 1.5 million solar home systems being used in the developing world

(Nieuwenhout, et al., 2004, p. 20). The most comprehensive literature study has shown 23% were functioning only partly and 15% had completely failed (Nieuwenhout, et al., 2004, p. 32). It is possible to estimate that approximately 570,000 solar home systems in developing countries are not healthy (345,000 malfunctioning and 225,000 failed). Though there is no way to determine the exact effects our diagnostic tool would have on these numbers, we may be able to make some rough estimates by looking at the accuracy of our detection scheme while also taking into account some figures concerning the occurrence of these problems.

To estimate the potential impact of our proposed diagnostic tool in the developing world, the following assumptions are made. To begin, we assume that users will have access to the proposed detection tool and employ it on their solar home systems. Though this is a best case scenario, our proposed product's success in a few implementations could cause its dissemination in many projects. We then need to assume that the user will regularly run the diagnostic test (through any of the means previously described). This is not completely plausible, as evidenced by the disregard many users have for the charge controller, but we are currently focusing on the merits of the device itself (Nieuwenhout et al., 2004, p. 35). We then assume the users would take the necessary steps to address the problem once it has been identified; for this reason we created a table of suggested user responses (See Table 4). Finally, we will assume that our detection algorithms would be as accurate in the field as they were in our experiment. While these are not perfectly realistic assumptions, they allow us to obtain some general numbers of our proposed detection method's possible impact.

Table 4: Suggested User Response Guide

Device Reading	Suggested Initial User Response	Suggested User Follow-up
"System is Healthy"	User does not need to take additional action.	Run diagnostic tool again according to normal, pre-determined schedule.
"Panel is Dirty"	Clean the surface of the photovoltaic panel to remove all sand or dust particles.	Run diagnostic tool immediately after panel is cleaned to ensure no other problem is occurring. Clean the panel during regular intervals in the future. Run diagnostic tool again according to predetermined schedule.
"Car Battery is Being Used"	If possible, read labels or past packaging to determine if car battery is being used. Run diagnostic tool again for a longer period (about one week) to confirm diagnosis.	If diagnosis confirmed, either purchase a deep cycle battery or use car battery for the duration of its lifetime. Run diagnostic test again when battery is replaced.
"System is Deep Discharged"	Ensure charge controller set points are set according to the manufacturer's suggestions.	If this cannot be done, set load disconnect higher and higher, until the tool no longer detects deep discharge as a problem. Run tool again according to predetermined schedule.
"System is Overcharged"	Ensure charge controller set points are set according to manufacturer's suggestions.	If this cannot be done, set load disconnect lower and lower until the tool no longer detects overcharging as a problem. Run tool again according to predetermined schedule.
"Charge Controller is Malfunctioning"	If system does not contain a charge controller, purchase and install one. If the charge controller's functions are bypassed, reverse this bypass. If neither of these are the case, user should monitor the load to see if it is ever disconnected by the load. If this does not occur, the charge controller should be replaced. If load disconnect is functioning but diagnosis remains the same, the disconnect set point should be adjusted until problem no longer occurs.	If new controller purchased or bypass reversed, diagnostic tool should be run immediately to ensure no other problems are occurring. Run tool again according to predetermined schedule.
"Can Not Make a Diagnosis"	Run the tool again until a different diagnosis can be made	Run tool according to predetermined schedule

Our most successful detection method was the Gaussian test, so we will use these results to obtain our estimates. Let us first consider at the dirty panel problem. The Gaussian test detected a dirty panel with 100% accuracy. We know that problems with the photovoltaic panel only account approximately 3% of malfunctioning or failed solar home systems (Nieuwenhout et al., 2004, p. 34). Because this figure includes

photovoltaic modules that are either broken or stolen, let us assume that dust accumulation accounts for only a third of this figure, 1%. Because our detection tool was 100% accurate in detecting the dirty panel problem, we can say that it would detect every instance of excessive dust accumulation. According to the original figure of 1.5 million solar home systems and assuming that 1% of them have dirty panels, our detection method could potentially address the problems of 15,000 solar home systems.

The overcharge and deep discharge tests also both had a 100% accuracy rate using the Gaussian method. Unfortunately, there are no conclusive figures as to the percentage of solar home system failures or malfunctions that resulted from either of these problems. However, we do have data from several implementations that show the percentage of systems in which the batteries have failed. In an Argentinian project, approximately 15% of batteries were malfunctioning three and a half years after implementation (Nieuwenhout et al., 2004, p. 36). In Indonesia, failure rates ranged from 0% to 16.1%, depending on the region, the mean failure rate being 6.1% (Nieuwenhout et al., 2004, p. 34). If we assume that these numbers are equivalent to the failure rates all over the developing world, we can say that anywhere from 91,500 (6.1% of 1.5 million systems) to 241,500 systems have problems with the battery. Because our two battery problems were detected with 100% accuracy, we predict that our system would save a number of systems somewhere within this range.

The Gaussian test was also able to detect the use of a car battery with 100% accuracy. Unfortunately, there are no aggregate figures that tell us how many car batteries are actually being used in developing countries. In a study in Brazil, eight of the fifteen (~53%) initially installed solar batteries were replaced with automotive batteries

(Reinders et al., 1999, p. 11). Another study showed that 19% of the solar home systems in Swaziland used automotive batteries (Nieuwenhout et al., 2001, p. 50). In Chad, Kenya, Zimbabwe, and Uganda, the use of car batteries ranged anywhere from 4.5% to 30% (Nieuwenhout et al., 1999, p. 38). Ignoring the Brazil data, because of the small sample size, we can make predictions based on this range of 4.5% to 30%. Anywhere from 67,500 to 450,000 car batteries are therefore being used in the developing world based on this range, and based on our tests our device would detect all of these.

The malfunctioning charge controller test was not identified with 100% accuracy using the Gaussian method, as it was detected only 55% of the time. A review of all literature has shown that charge controller are either missing, broken, malfunctioning, or bypassed 33% of the time (Nieuwenhout et al., 2004, p. 36). Again using the 1.5 million solar home systems figure, we can say that approximately 495,000 systems suffer from problems due to the charge controller. Because our detection rate is only 55%, we would expect to only detect approximately 270,000 of these.

Though these predictions are very rough and rely on several assumptions, they provide insight into the significant impact this kind of diagnostic tool can make (See Table 5). Based on these calculations, if the diagnostic tools are implemented everywhere, our device could detect problems on anywhere from 241,500 to 976,500 systems (many of these problems overlap, since there are only approximately 570,000 malfunctioning systems in the developing world) (Nieuwenhout, et al., 2004, p. 20)). We have confidence in the accuracy of our detection methods, and we believe that its use could spread quickly throughout the developing world, greatly reducing the failure rate of solar home systems and improving the quality of life in these areas.

The results of this research are important to the use of solar home systems in the developing world. As previously mentioned, the high failure rate of solar home systems leads to a loss of faith in the implementations of solar technology. Potential users may choose not to take the steps necessary to implement the system based on the failure rate and the potential high cost of repairs. The proposed detection tool will prevent failure of the system and promote proper maintenance which will restore users faith in the use of solar power. Additionally, preventing the need for major repairs on the system, such as replacing the battery, will greatly reduce the overall maintenance cost for the user. This is essential because cost is a major barrier when implementing solar home systems in the developing world.

Table 5: Expected Detection Rates

Problem	Number of Solar Home System with Given Problem	Number of Solar Home Systems Detected with Problem
Dirty Panel	15,000	15,000
Problems with Battery: Overcharging or Deep Discharging	91,500-241,500	91,500-241,500
Car Battery	67,500- 450,00	67,500-450,000
Malfunctioning Charge Controller	495,000	270,000

Our most successful detection method was the Gaussian test, so we will use these results to obtain our estimates. Let us first consider at the dirty panel problem. The Gaussian test detected a dirty panel with 100% accuracy. We know that problems with the photovoltaic panel only account approximately 3% of malfunctioning or failed solar home systems (Nieuwenhout et al., 2004, p. 34). Because this figure includes photovoltaic modules that are either broken or stolen, let us assume that dust

accumulation accounts for only a third of this figure, 1%. Because our detection tool was 100% accurate in detecting the dirty panel problem, we can say that it would detect every instance of excessive dust accumulation. According to the original figure of 1.5 million solar home systems and assuming that 1% of them have dirty panels, our detection method could potentially address the problems of 15,000 solar home systems.

The overcharge and deep discharge tests also both had a 100% accuracy rate using the Gaussian method. Unfortunately, there are no conclusive figures as to the percentage of solar home system failures or malfunctions that resulted from either of these problems. However, we do have data from several implementations that show the percentage of systems in which the batteries have failed. In an Argentinian project, approximately 15% of batteries were malfunctioning three and a half years after implementation (Nieuwenhout et al., 2004, p. 36). In Indonesia, failure rates ranged from 0% to 16.1%, depending on the region, the mean failure rate being 6.1% (Nieuwenhout et al., 2004, p. 34). If we assume that these numbers are equivalent to the failure rates all over the developing world, we can say that anywhere from 91,500 (6.1% of 1.5 million systems) to 241,500 systems have problems with the battery. Because our two

The Gaussian test was also able to detect the use of a car battery with 100% accuracy. Unfortunately, there are no aggregate figures that tell us how many car batteries are actually being used in developing countries. In a study in Brazil, eight of the fifteen (~53%) initially installed solar batteries were replaced with automotive batteries (Reinders et al., 1999, p. 11). Another study showed that 19% of the solar home systems in Swaziland used automotive batteries (Nieuwenhout et al., 2001, p. 50). In Chad, Kenya, Zimbabwe, and Uganda, the use of car batteries ranged anywhere from 4.5% to

30% (Nieuwenhout et al., 1999, p. 38). Ignoring the Brazil results (because of the small sample size) we can make predictions based on this range of 4.5% to 30%. Anywhere from 67,500 to 450,000 car batteries are therefore being used in the developing world based on this range, and based on our tests our device would detect all of these.

The malfunctioning charge controller test was not identified with 100% accuracy using the Gaussian method, as it was detected only 55% of the time. A review of all literature has shown that charge controller are either missing, broken, malfunctioning, or bypassed 33% of the time (Nieuwenhout et al., 2004, p. 36). Again using the 1.5 million solar home systems figure, we can say that approximately 495,000 systems suffer from problems due to the charge controller. Because our detection rate is only 55%, we would expect to only detect approximately 270,000 of these.

Though these predictions are very rough and rely on several assumptions, they provide insight into the significant impact this kind of diagnostic tool can make (See Figure 59). Based on these calculations, if the diagnostic tools are implemented everywhere, our device could detect problems on anywhere from 241,500 to 976,500 systems (many of these problems overlap, since there are only approximately 570,000 malfunctioning systems in the developing world). We have confidence in the accuracy of our detection methods, and we believe that its use could spread quickly throughout the developing world, greatly reducing the failure rate of solar home systems and improving the quality of life in these areas.

Chapter 7 Possible Implementations and Future Research

The algorithms created in this study can serve as an important basis for applications in solar home systems. The next step in future research would be to create a product that can be used in the field to detect the problems we have discussed concerning solar panels and batteries. When attached to an individual solar home system for a short period of time, this device could identify the problem and allow the user to address it before it causes long-term damage. In this section, we will propose several uses of such a tool and lay out the steps users can take to address each possible problem.

This proposed product would utilize our most successful detection algorithm: the Gaussian method. As discussed in previous sections, this method utilizes voltage patterns representative of each of the five problems we have discussed. These representative patterns would serve as the basis for our diagnostic tool. To test a given system, we can collect voltage data for that system for at least one day (since the detection algorithm relies on daily voltage patterns). The collection period can be longer than this, as the accuracy of the diagnosis would likely increase as the amount of voltage data increases.

Several methods can be utilized to collect this data and diagnose the problem. We devised four different options: (1) a stand-alone detection device with a separate data logger, (2) a charge controller with integrated detection algorithm (3) a detection device located on a central computer, and (4) a detection device accessible over the internet. The advantages and disadvantages of these will be discussed below.

7.1 Stand-alone Detection Device with Data Logger

This first method would consist of a single product that can be attached to the solar home system (which should consist of a load, battery, photovoltaic panel, and charge control). This product would consist of a data logger that could collect voltage data and a CPU that would contain our detection algorithms; these two elements would be integrated into one system. Similar to our process of testing the algorithms, this program would compare the given data to the representative problem patterns. The user would attach the product to his or her system and record voltage for a given period, at least one day. The greater amount of data collected, the more accurate the diagnosis.

The device would then send this voltage information to the CPU portion of the device, which would contain the day separation function, data filtering function, and the detection algorithm. The data would be separated into 24-hour periods (if more than 24 hours of voltage data is collected), filtered, and then diagnosed using the detection algorithm.

This product would then relay one of seven different results to the user: (1) System is Healthy, (2) Panel is Dirty, (3) Car Battery is Being Used, (4) System is Deep Discharged, (5) System is Overcharged, (6) Charge Controller is Malfunctioning, or (7) Can Not Make Diagnosis (though unlikely, this result is necessary in case the voltage pattern does not match that of a healthy system or any of the five problems). The results would be given to the user either in the form of a graphical display or using 6 different colored LED lights (one for each of the seven possible results).

The advantage of this type of system is that, because the two main components are combined, it would be much easier to use. Very little expertise is needed, and the only

instructions necessary are for attaching it to the system and interpreting the results. By having the logger and CPU in one unit, there is less chance for human error affecting the results. No intermediate step is needed for the user to take the raw data and input it into an algorithm. Additionally, since the device is not necessary for the system to function, the diagnostic device can be shared by members of a village. For example, each user in an area can check the health of their system with this device for a day or period of days, and then pass it on to another user. This would greatly reduce the cost of the device to the user, since it could be shared by a large amount of people. The ease of the system would likely encourage its use, which would also avoid long-term maintenance costs that would arise if these problems were not detected quickly.

The major downside to the device is its cost, even if this cost can be shared by multiple users. An entirely new product would have to be designed and manufactured, since there is no similar product on the market. Since the users of solar home systems in the developing world are poor, and because the products' benefits are long term, there may not be enough demand for such a device. Users may not see the benefit of investing in a product that does not improve the short-term functions of their solar home system. Since a data logger and CPU are not integral parts of a typical system, users may brush the product off as an unnecessary cost. Another downside is that the data will not be analyzed continuously. There is therefore a greater chance of false diagnoses, since the device will only be gathering data for a day or a period of several days (leaving it susceptible to short-term changes in weather patterns or use of the load).

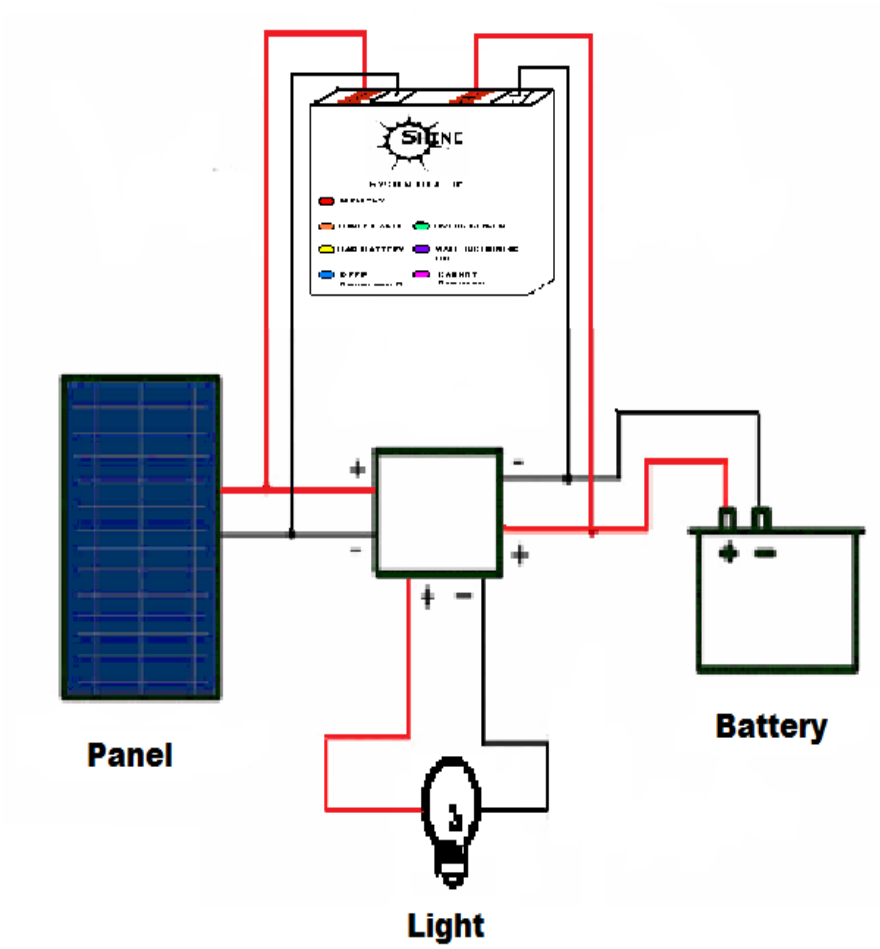

Figure 59: Diagram of Stand-Alone Detection Device with Data Logger

7.2 Charge Controller with Integrated Detection Algorithm

Another option would be a product in which the detection system is integrated within the charge controller. In this case, the computer program could read the voltage directly as it passes through the charge controller, allowing the problem to be diagnosed quickly. There would be no intermediate step of recording the voltage on a charge controller separately and then inputting it into the computer program.

This product would first require a slight alteration to our computer algorithm. Because no data logger will be involved, the program itself will be collecting the

recorded data while voltage runs through the charge controller. This means that the program will begin to detect once 24 hours of data has been collected. At this point, the program will then split the data into 24-hour periods, every time an additional day of data is collected. The program then filters the data, which it then inputs into the problem detection algorithm.

Because a charge controller is an important part of a solar home system, this device will be attached to the system for the entirety of its use and data will be collected continuously. The detection algorithm can also be altered for long-term monitoring. Rather than making a diagnosis on a day-to-day basis, as described in the previous section, the device should give a weekly diagnosis. Internally, the algorithm would choose one of the seven options mentioned above. Then, at the end of the week, the device would report the one result that is most common over that weekly period, using the LED system described in the previous method. Because this method takes more data into account, the accuracy of the diagnosis will be greater.

This method has several important advantages. First, it increases accuracy, as the greater amount of information would reduce the likelihood of false positives caused by changes in either weather or load. Second, because the system is included in a necessary component of a solar home system (the charge controller), there is a greater chance that users would purchase the product. A potential solar home system customer, or potential installer, will already need to purchase a charge controller. Our device could be marketed as a new type of charge controller with upgraded capabilities. Additionally, since every user would have their own device, there is less “wear and tear” or other potential conflicts that could occur for a product that is shared among members of a community.

At the top of the list of disadvantages for this product is that it could suffer from user bypass, just as in a typical charge controller. This would have even worse effects because, not only could damage be caused by having no controller, but there would also be no method of detecting other problems. Cost is also a significant disadvantage, as one of the biggest barriers to rapid deployment of solar home systems is the high upfront cost (Nieuwenhout, 2004, p.456). Although this product is first and foremost a charge controller, it is still essentially a new product. Just as in the previous method, the device would need to be developed and manufactured. It would inherently have a higher cost than other charge controllers, as it would need to contain a CPU with our programs and algorithms. Furthermore, because it cannot be shared among multiple users, the cost would be higher per person.

To alleviate the concern of user bypass of this product, one possibility is to pair this CPU-integrated charge controller with a solar panel also containing a CPU. The panel's CPU would shut down the solar home system if it is at risk of being damaged. The charge controller tool would still log and measure voltages to detect problems, but the panel would have a simpler CPU that could detect problems that could cause permanent irreversible damage. In this case, the panel CPU would stop the system from operating until the problem is addressed. One example would be if the system deep discharges for many days at a time; the system would cut off current flow to the battery (to prevent permanent failure) until the user decreases the load on the system or increases the available solar radiation to the panel. Users would therefore not only be alerted to, but also forced to maintain their systems properly. Even if the charge controller unit is bypassed or removed, the panel CPU will be a safeguard against blatant misuse of the

system. Over time, this could lead to better education about their solar home systems and an increasingly positive attitude toward solar power (due to fewer system failures). Unfortunately, there is a possibility of a negative reaction. Users may see this as too rigid a device that does not give them enough leeway to use their systems as they see fit. However, the expectation is that the positive effects of this device would outweigh any dissatisfaction over flexibility of use.

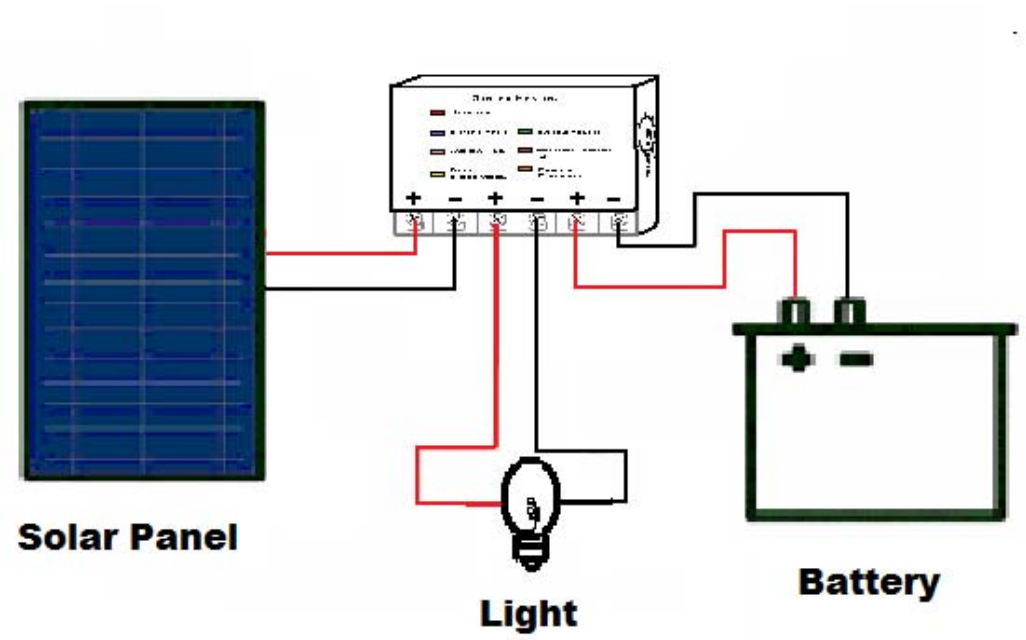

Figure 60: Diagram of Detection Device Contained within Charge Controller

7.3 Detection Device within a Central Computer

Another option would be for the data logger, computer algorithm, and charge controller to be separate components. A user could connect the data logger to their system and log a day or several days' worth of data, and then bring that data to a central computer, which would contain the 24-hour separation, data filtering programs, and detection algorithms. The central computer would then diagnose the system based on the given data.

For the user, this system would be a multi-step process. First the user attaches the data logger to his or her solar home system. Data can then be collected for a minimum of one day (again, the greater amount of data collected, the higher the accuracy of the diagnosis). Once the data has been collected, the user than takes this data logger to a computer that is located somewhere at the center of the community. This method is most applicable if a village has a central community center that may contain a computer (or at the very least, enough electricity capabilities to power a computer). The user can attach the data logger to the computer and upload the voltage data. Then, the program could be run to separate and filter the data, and then gives a diagnosis. The interface would then display the diagnosis, using one of the seven options mentioned in the past two methods.

Such a system would be convenient because data loggers are widely available and inexpensive. These could either be shared among community members, or used exclusively for each system. Additionally, only one central computer would be necessary, and everyone in a village could share it. Whenever a user expects that the system may not be working properly, he or she can collect data and bring it to this central location. This can also be done on a regular basis to ensure the health of the system.

This method does bring some disadvantages. First, the community would need to have a central site that either contains a computer, or which is capable of powering a computer. Also, because the user needs to take the data to this site, there are some time costs because of the travel involved. This also means that the problem may not be diagnosed as quickly, since the user needs to collect the data for a period and then bring it to the test site. Additionally, the user would need some training to use the program, even if the interface is simple. This method also requires that the program be taken to the site

of the community, most likely by the group that implements the system. Finally, because of the multiple steps in this process, there is a greater probability of human error.

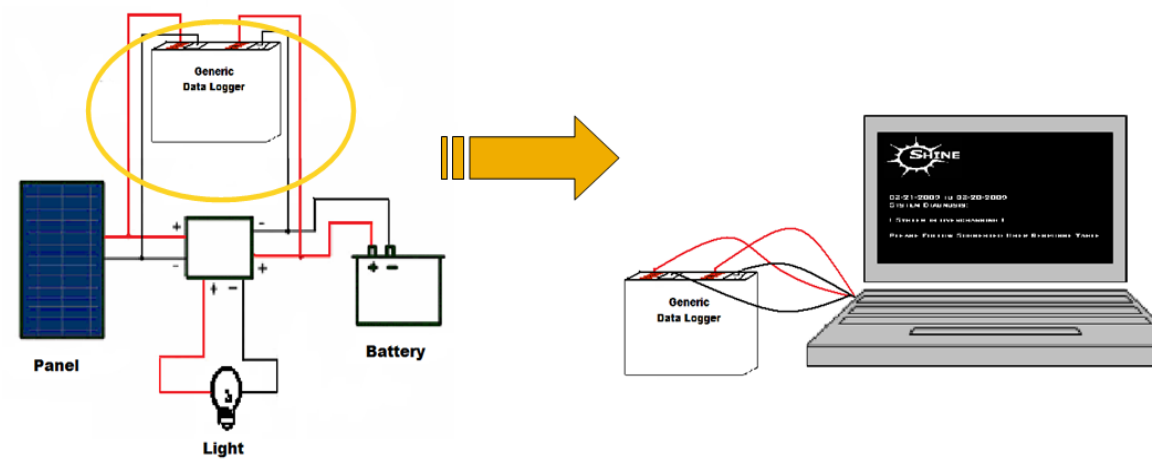

Figure 61: Diagram of Detection Device with Central Computer

7.4 Detection Device accessed through Internet

A final option is very similar to the previous one, except that the central computer would not need to include the diagnostic program. If the computer has internet access, then the voltage data can be compared to an online database that contains the separating, filtering, and detection programs.

The main advantage to this method is that implementers would not need to be sent to these remote locations to install this program onto a computer. Rather, the program could be accessed via the internet. The obvious problem is that most remote locations in the developing world would not have internet access. We see this method most applicable for more moderately developed regions. There are some green communities in the United States that utilize solar home systems. These areas are much more likely to have internet access, and it would be very convenient for this program to be accessed wirelessly.

7.5 Suggested User Responses

It is also important to consider how the user should respond to each possible problem scenario. While these detection methods are important for diagnosing common problems, it is up to the user to take steps to correct them. Some of these can be addressed rather simply, while some are more complex. Though the specifics of the solar home systems and village resources vary, we can provide some general recommendations for each problem.

A healthy system is obviously one that is not exhibiting any problems according to its voltage patterns. No further action should be taken except for future voltage measurements to ensure that the system remains healthy.

If the result is "Panel is Dirty," the subsequent steps are also fairly simple. The user needs to clean the surface of the panel, removing any dust, sand, or dirt particles. The photovoltaic panel should be in an accessible spot so that this cleaning can be done regularly. There is also the possibility that this diagnosis has been caused by other factors, such as several days of cloudy weather, or a damaged panel. The user should be informed of these possibilities; if the panel is damaged, it should be replaced. Once the problem has been addressed, the user should then collect voltage data from the system again to be sure that no other problem is occurring.

If the device detects "Car Battery is Being Used," there is no simple method to fix the problem. The user may not always know the type of battery that is being used in the system, and may not have any way to determine this. When this result is shown, it means that the battery will likely have a short lifetime. The user's only options are to purchase a new deep cycle battery (or modified car battery), or wait until the end of the lifetime of

the car battery to replace it. Before purchasing a new battery, the user should run the program for a longer period of time to confirm the diagnosis.

To address the result of "System is Deep Discharged," the steps are a bit more complex. The user should first check the charge controllers load connect and disconnect set-points. These points determine at which state of charge the battery should be connected and disconnected from the load. Ideally, the controller disconnects the load before the battery deep discharges and reconnects the load when the battery is within an adequate state of charge. The user should make sure that these values are set at the correct values recommended by the charge controller manufacturer. If this information is not available, and the deep discharge problem persists, then the load disconnect value should be set higher. The user should continue to monitor the system with the detection device until deep discharge is no longer detected as a problem. If it persists, then the disconnect value should be set higher and higher until the problem is no longer detected.

If the result "System is Overcharged" is detected, similar steps should be taken. The set-points should be checked and ensured that they match the manufacturer's suggestions. Again, if this information is unavailable, or if the problem persists, the user should adjust the set points. In this case, the disconnect set-point should be lowered. This way, more of a load can be used, draining more power from the battery, and preventing overcharging. Just as in deep discharge, the user should continue to monitor the voltage and adjust the set-points as needed. There is also the possibility that the system is not properly sized, and the panel's voltage is too high in comparison with the battery. If this is the case, either a battery with higher capacity or a panel with lower voltage should be purchased.

If “Charge Controller is Malfunctioning” is the diagnosis, then several steps should be taken. If the user does not have a charge controller or has bypassed its functions, then a charge controller should be purchased (or bypass reversed). If this is not the case, the user should determine whether the charge controller is functioning at all. He or she can do this by determining if the load is ever disconnected. This can be determined by a test performed by the user. The user should keep the load on during an extended period of time while covering up the panel, to keep light from reaching the panel. If the controller is functioning, the load should be cut off at a certain point to keep the battery from deep discharging. If this does not occur, a new controller should be purchased. If this is not the case, then the set points should be adjusted, just as if the system was overcharged or deep discharged, until the problem is no longer detected.

If the result is “Can Not Make Diagnosis,” then the algorithm cannot accurately detect whether the problem is healthy or exhibiting one of the problems. In this case, the user should use the detection device to continually monitor the system. This should be done until the product has enough data to predict one of the six other problems.

As explained in previous sections, this proposed product can have a significant impact in the use of solar home systems. Though each installation and village is different, we have proposed several methods of implementing our device, as well as suggestions for addressing each problem. Table 6 summarizes the comparison of the four different implementations discussed. Because these problems can be detected early, we expect to see that the failure rates would decrease (and the longevity of systems increase) when a detection device can be implemented.

7.6 Cost Analysis of Proposed Implementations

One can see that cost must be a significant factor in evaluating these proposed implementations, as high up-front costs are one of the major barriers to solar home system dissemination (Niewenhout et al., 2001, p.454). Here we discuss these barriers in costs for each of our proposed implementations, as well as discuss some ways to overcome these barriers. For both of the computer implementations, the additional costs would actually be quite low, but they rely on a high amount of already existing infrastructure (such as computers, internet access). This would be a valuable solution for more developed regions that already contain a computer and/or internet access. For the majority of solar home systems in regions without this type of resources, our other proposed implementations would be the sole options.

Determining the exact cost of creating the other two products would be out of the scope of this project, but it is expected to be significant. The charge controller itself only makes up 5% of the initial system cost (Instituto, 1998, p.14). In the U.S. they can be found commercially for approximately $10, and they would likely be less expensive for those in developing areas. The data logger is a bit more expensive, at about $75-100 in the U.S. Nonetheless, as this device would be shared among several users, this would likely be cheaper than a charge controller (per houshold). The issue is that a new product would need to be developed in order to incorporate our detection algorithm into these devices. This would require a large amount of funding for research and product development. To justify this, we must expect that users would be willing to buy the product. As we have seen with the case of charge controllers, even a product with long-

term benefits may be disregarded for short-term benefits (avoiding the cost of the new product).

One alternative possibility would be to have the implementers purchase the device, rather than the end user. Over 75% of implementations are large scale (over 100 systems) and about 1/3 of them are provided by non-commercial sources, such as governments and NGO's (Nieuwenhout, et al., 2001, p. 457). These are the types of organizations that these products would be marketed towards. Since their main goal is not profitability but sustainability of the project, they would have the highest interest in our product. Once the case is made that the failure reduction overrides this additional cost, we would expect to find significant interest in our project from these types of organizations. The long-term goal would be for these groups to initiate the use of our products; then, once their use proves to be effective, the use would spread through commercial routes.

Table 6: Proposed Implementation Types Compared (Green=positive, Yellow=moderate, Pink=negative)

Method	Cost	Infrastructure Necessary	Can be Shared	Necessary to System	Period of Data Collection	Travel Costs	Expertise Needed
Stand-Alone Product	Moderate	Little	Yes	No	Depends on if shared	None	Moderate
Integrated Product	Moderate	Little	No	Yes	Permanent	None	Low
Central Computer and Internet-Capable	Low	Significant	Yes	No	Depends on if shared	High	Moderate

7.7 Distributed Energy Systems

While the methods and software developed in this research were focused on small solar home systems, with the proper training data and perhaps a minimal amount of modification, they could be applied to most applications where batteries are used for bulk energy storage. In particular, distributed energy systems and electric automobiles will likely become prevalent in the coming decades, and both technologies rely heavily on the ability to store large amounts of energy.

In distributed energy systems, large banks of batteries are installed throughout the power grid along with DC-to-AC inverters and other equipment. During periods of high demand, the batteries supplement the grid by supplying power to nearby consumers. During periods of low demand, the batteries consume power in recharging. This allows power transmission equipment to be designed for the average demand rather than peak demand, improving the cost-efficiency of the system.

Figures 62 and 63 show two different ways of implementing the distributed energy principle, one where larger battery banks are connected to electrical substations, and another where each consumer has a smaller bank. Both configurations can in some sense be considered as larger scale replicas of solar home systems. The power source, batteries, and load are connected in parallel, and the charging and discharging of the batteries can be regulated in a similar way (with consideration given to the fact that the power grid is AC rather than DC, of course). However, the problems investigated in this project are not all applicable. Certainly, a power company would not likely use automotive batteries or bypass a charge controller, and if the banks are charged by the power grid, the presence of a dirty solar panel is not possible. The primary concern would

be with monitoring the batteries' discharge curves to detect when they are anything but healthy. A charge controller with incorrectly set thresholds could lead to overcharging or deep-discharging, and batteries wear out over time even with proper use.

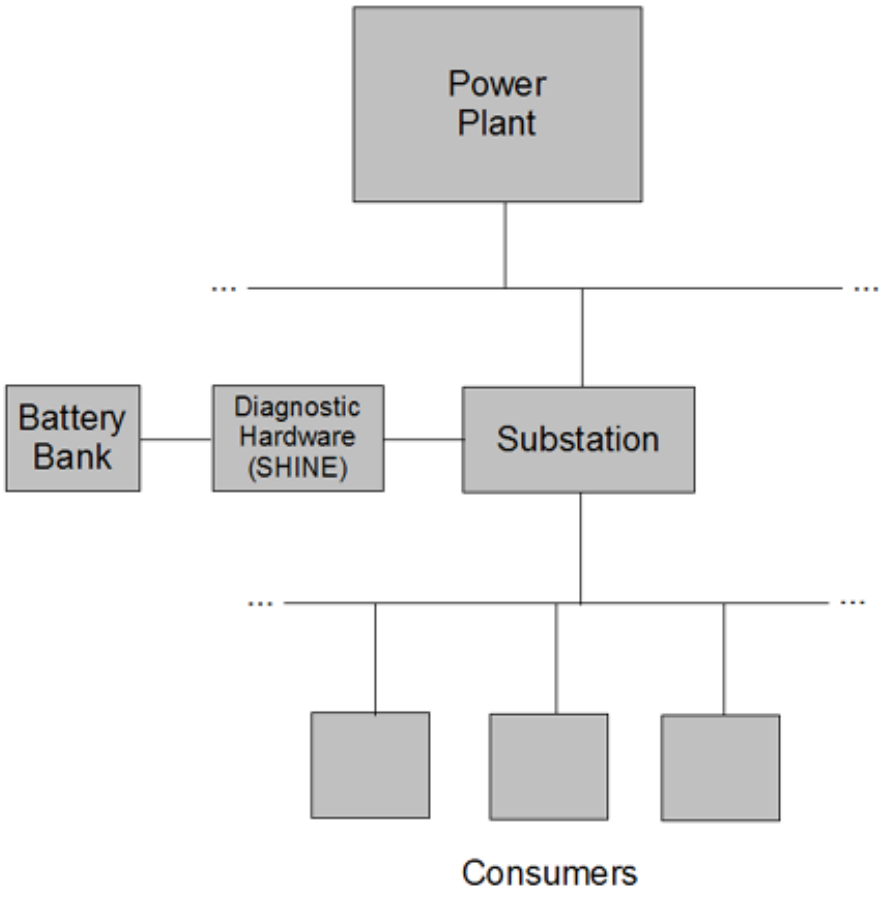

Figure 62: Diagram of Distributed System

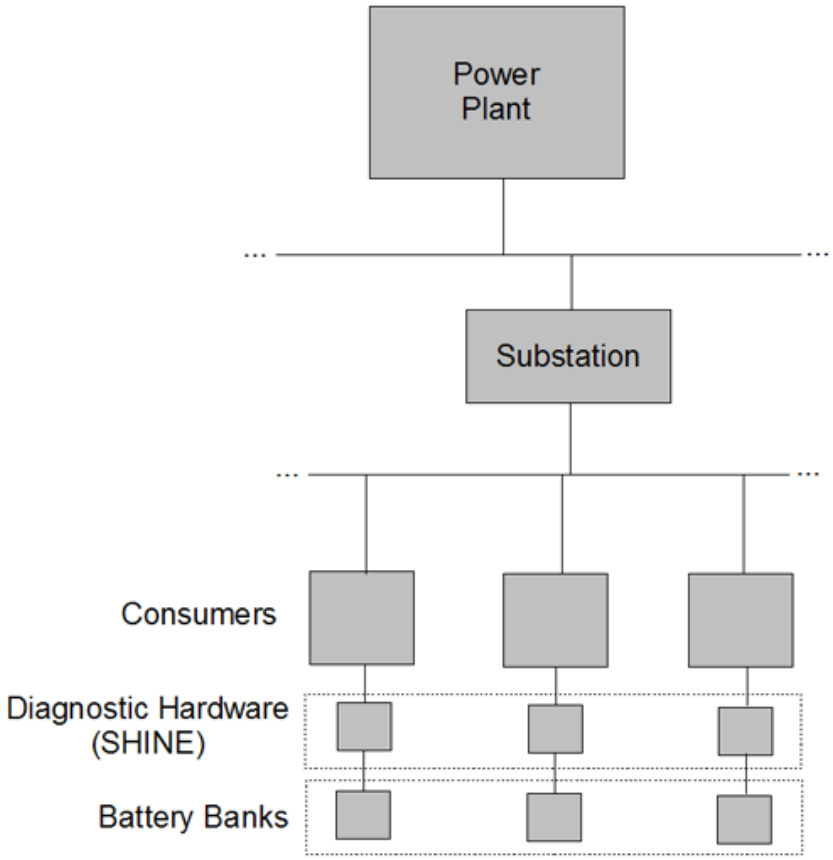

Figure 63: Diagram of Distributed System II

In both power grid and electric vehicle applications, reliability is a very high priority. Even brief power outages can cost businesses many thousands of dollars, and an automobile failure can leave the driver stranded. Thus it is highly desirable to be able to detect and address maintenance issues before a failure occurs. Installing a detection system such as ours could alert users to slowly developing problems or degradation of batteries due to normal use, allowing them to replace the batteries as often as necessary. This could also avert the scenario where a regular replacement schedule is implemented, enabling maximum use of the batteries over their lifespan.

Newer technologies such as ultracapacitors are being developed, but until they can attain the same energy density as any type of battery for the same price, batteries will

remain in widespread use. Thus it will be important for some time to be able to model their behavior and detect problems quickly, or even before they occur at all.

Chapter 8 References

Adiyabat, Amarbayar, and Kosuke Kurokawa. (1982). An optimal design and use of solar home system in Mongolia. *Japanese Journal of Applied Physics: Proceedings of the 3rd Photovoltaic Science and Engineering Conference held in Kyoto, Japan 19-21 May 1982* (pp. 2272-2275). Tokyo, Japan: Tokyo Publication Board.

Al-Hasan, Ahmad, and Adel Ghoneim. (2005). A new correlation between photovoltaic panel's efficiency and amount of sand dust accumulated on their surface. *International Journal of Sustainable Energy,* 124(4), 187-197.

Anthony, D., Rand, J., Moseley, P.T., Garche, J., & Parker, C.D. (2004). *Valve-Regulated Lead-Acid Batteries*. Amsterdam: Elsevier.

Armenta-Deu, C. (2003). Prediction of battery behavior in SAPV applications. *Renewable Energy,* 28(11), 1671-1684.

Baxter, R. (2006). *Energy Storage: A Nontechnical Guide.* Tulsa, OK: Pennwell Books.

Bergveld, H.J., Kruijt, W., & Notten, P. (2002). *Battery management systems : design by modelling*. Boston: Kluwer Academic.

Berndt, D. (1926). *Maintenance-free batteries: based on aqueous electrolyte lead-acid, nickel/cadmium, nickel/metal hydride : a handbook of battery technology.* Hertfordshire, England: Research Studies Press.

Bethel, Jim. (1997, June). *Least Squares Image Matching for CE604.* Purdue University, West Lafayette, Indiana.

Crompton, T. R. (2000). *Battery Reference Book*. Boston : Newnes.

Cui, M., J. Femiani, J. Hu, P. Wonka, and A. Razdan. (2008). Curve Matching for Open 2D Curves*. Pattern Recognition Letters*, 30, 1-10.

Dell, R., Anthony, D., & Rand, J. (2001). *Understanding Batteries*. Cambridge: Royal Society of Chemistry.

Diaz, Pablo and Eduardo Lorenzo. (2001). Solar home system battery and charge regulator testing. *Progression in Photovoltaics: Research and Application*, 9, 363-377.

Diaz, Pablo. (2007). Dependability analysis of stand-alone photovoltaic systems. *Progress in Photovoltaics*, 15(3), 245-264.

Drews, A., A.C. de Keizer, H.G. Beyer, W.G.J.H.M. van Sark, Dunlop, E. Lorenz, J. Betcke, James P., and Brian Farhi. (2001). Recommendations for Maximizing Battery Life in Photovoltaic Systems: A Review of Lessons Learned. *Solar Engineering: Proceedings of the International Solar Energy Conference held in*

Washington, D.C. 21-25 April 2001 (pp. 275-280). Washington, D.C.: American Society of Mechanical Engineers.

Energy Research Centre of the Netherlands. (2002). *Reliability of PVstand-alone systems for rural electrification Tackling the Quality in Solar Rural Electrification* (NNE5/2002/98). Madrid, Spain.

Farret, F & Simões, M.G. (2006). *Integration of Alternative Sources of Energy.* Denver: Wiley-IEEE.

Gaters Energy Products (1997). *Rechargeable Batteries Application Handbook*. Denver: Newnes

Gulski, E. (1995). Discharge Pattern Recognition in High Voltage Equipment. IEE Proceedings, 142, 51-61.

Gustavsson, Mathias and Daniel Mtonga. (2005). Lead-acid battery capacity in solar home systems- Field tests and experiences in Lundazi, Zambia. *Solar Energy*, 79, 551-558.

Hegazy, Adel. (2001). Effect of dust accumulation on solar transmittance through glass covers of plate-type collectors. *Renewable Energy*, 22(4),525-540.

Himann, Roselyn (2008). Light Up the World Foundation. Retrieved February 15, 2009, from Light up the World Foundation Web site: http://lutw.org/home.htm

Huacuz, Jorge M., Roberto Flores, Jaime Agredano, and Gonzales Munguia. (1995). Field Performance of Lead-Acid Batteries in Photovoltaic Rural Electrification Kits. *Solar Energy,* 55(4), 287-299.

Instituto de Energía Solar (1998). *Universal Technical Standard for Solar Home Systems* (Universidad Politécnica de Madrid, European Commission, Thermie B: SUP-995-96, EC-DGXVII). TaQSolRE Project. Retrieved Jan. 15, 2009, from http://www.taqsolre.net/doc/Standard_IngV2.pdf.

International Energy Agency. (1999). *Lead-Acid Battery Guide for Stand-Alone Photovoltaic Systems* (Report IEA-PVPS 3- 06:1999). Paris, France.

Kiehne, H.A. (2003). *Battery Technology Handbook*. New York: Marcel Dekker.

Knoke, D, Bohrnstedt, G, & Mee, A (2002). Statistics for Social Data Analysis. Belmont, CA: Wadsworth/Thomson Learning.

Krishnan, Sridhar and Ramalingam, Arunan (2006). Gaussian Mixture Modeling of Short-Time Fourier Transform Features for Audio Fingerprinting. *IEEE Transactions on Information Forensics and Security,* 1 (4), 457-463.

Landau, Charles (2002). Optimum orientation of solar panels. Retrieved November 29, 2008, from MACS Lab Incorporated Web site: http://www.macslab.com/optsolar.html

Lashway, Clin (1988). Effects of Failure and Maintenance on Photovoltaic System Performance. *Effects of failures and maintenance on photovoltaic system performance* (pp. 1116-1121). Las Vegas: IEEE.

Linden, D. & Reddy, T. (2002). *Handbook of Batteries.* New York: McGraw-Hill.

Lorenzo, E. and Labed, S. (2005). The battery voltage distribution: A possible tool for surveying the health of stand-alone pv systems. *Progress in Photovoltaics*,13(3), 251-260.

Lorenzo, Eduardo, Zilles, Roberto, Caamano-Martin, Estefania, . (2001). *Photovoltaic Rural Electrification. A Fieldwork Picture Book*. Progensa.

Lugue, A. & Hegedus, S. (2003). *Handbook of Photovoltaic Science and Engineering.* West Sussex, UK: John Wiley and Sons.

Mapako, M.C. (2005). Provision for long-term maintenance support for photovoltaic systems- Lessons from a Zimbabwean NGO. *Journal of Energy in Southern Africa*, 16(1), 21-26.

Mattera, F., D. Benchetrite, D. Desmettre, J.L. Martin, and E. Potteau. (2003). Irreversible sulphation in photovoltaic batteries. *Journal of Power Sources,* 116, 248-256.

Nieuwenhout, F., de Villers, T., Mate, N., and Aguilera, M.E (2004). *Reliability of PV stand-alone systems for rural electrification: a review* (Universidad Politécnica de Madrid, European Commission, TargetAction-C Contract No. NNE5/2002/98). TaQSolRE Project. Retrieved Jan. 15, 2009, from http://www.taqsolre.net/doc/TaQSolRe%20WorkPackage1-Year%201.pdf

Nieuwenhout, F.D.J., Dijk, A.L. van, Dijk, V.A.P. van, Lasschuit, P.E., Roekel, G.M. van, Arriaza, H., Hankins, M., Sharma, B.d., and Wade, H. (1999). *Monitoring and evaluation of solar home systems : experiences with applications of solar PV for households in developing countries.* (ECN Publication ECN-C--00-089). ECN Solar Energy, Retrieved February 25, 2009, from http://www.ecn.nl/publications/default.aspx?nr=c00089

Nieuwenhout, F.D.J., Martens, J.W., Lasschuit, P.E., Lafleur, M.C.C., and Cloin, J. (2001). *Life-cycle analysis and optimisation of solar home systems. Interim report over 2000 of ENGINE project 74556.* (ECN Publication ECN-C--01-057). ECN Solar Energy. Retrieved February 25, 2009, from http://www.ecn.nl/publications/default.aspx?nr=c01057

Niewenhout, F. (2004).Experience with Solar Home Systems in Developing Countries: A Review. *Progress in Photovoltaics*. *9*, 455-474.

Payne, J. (2003). *Understanding Boat Batteries and Battery Charging.* Dobbs Ferry, NY: Sheridan House, Inc.

Pearce, A (2007). Batteries Why and How they Fail. *Farmers Weekly*, *146(2)*, 64-65.

Reinders, A.H.M.E., Pramusito, Sudradjat, A., van Dijk, V.A.P., Mulyadi, R., and Turkenburg, W.C. (1999). Sukatani revisited: on the performance of nine-year-old solar home systems and street lighting systems in Indonesia. *Progress in Photovoltaics*. *3*, 1-47.

Robinson, Mark. Tilt and Angle Orientation of Solar Panels. Retrieved November 29, 2008, from The Energy Grid Web site: http://www.theenergygrid.com/grid/articles/paneltilt.html

Solar Electric Light Fund. (2008).Retrieved October 20, 2008, from Solar Electric Light Fund: Energy is a Human Right Web site: http://www.self.org/index.asp

Solar Energy International (2004). *Photovoltaics: Design and Installation Manual: Renewable Energy Education for a Sustainable Future.* Canada: New Society Publishers.

Spiers, David J. and Asko Rasinkoski. (1995). Predicting the service lifetime of lead/acid batteries in photovoltaic systems. *Journal of Power Sources*, 53, 245-253.

Stapleton, Geoff, Gunaratne, Lalith, Konings, Peter JM (2002). *The Solar Entrepreneur's Handbook*. Ulladulla, New South Wales: Global Sustainable Energy Solutions Pty Ltd.

Tenno, A., Tenno, R., & Suntio, T. (2002). Evaluation of VRLA battery under overcharging: model for battery testing. *Journal of Power Sources*, 111, 65-82.

Van der Plas, R.J. and M. Hankins. (1998). Solar Electricity in Africa: a reality. Energy Policy, 26(4), 295-305.

Vela, N. and Agulera, J. (2006). Characterisation of charge voltage of lead-acid batteries: Application to the charge control strategy in photovoltaic systems. *Progress in Photovoltaics*, 14(8),721-732.

W. Heydenreich, E. Wiemken, S. Stettler, P. Toggweiler, S. Bfinger, M. Schneider, G. Heilscher, and D. Heinemann. (2007). Monitoring and remote failure detection of grid-connected PV systems based on satellite observations. *Solar Energy*, 81, 548-564.

Woodworth, Joseph R., Michael Thomas, John Stephens, Steven Harrington, James Dunlop, and M. Ramu Swami. (1994). Evaluation of the batteries and charge controllers in small stand-alone photovoltaic systems. *Conference Record of the IEEE Photovoltaic Specialists Conference: Proceedings of the 24th IEEE Photovoltaic Specialists Conference held in Waikoloa, Hawaii 5-9 December 1994, (pp. 933-945)*

Xiaochun, Shi. Dalian Jiaotong. (2008). Comparison of Two Modern Pattern Recognition Methods. *International Conference on Intelligent Information Hiding and Multimedia Signal Processing (pp.351-53)*. Liaoning Province, China.

Yang, Hong, He Wang, Guangde Chen, and GuomingWu. (2006). Influence of the charge regulator strategy on state of charge and lifetime of VRLA battery in household photovoltaic systems. *Solar Energy*, 80(3), 281-287.

Zahedi, Ahmad and Hallenstain, Joe (2007) Effect of non-technical factors on the electricity cost of the photovoltaic (PV) systems. *The Ninth Arab International Conference on Solar Energy,* 209, 108-112.

Appendix A: Charge Controllers

Charge controllers come in many shapes, sizes, and price ranges. The least complex form of charge controllers are the 1 or 2 stage versions, which use relays or shunt transistors to control the voltage. They short or disconnect the panel when a certain voltage is reached. These charge controllers have been used for decades. They are cheap and reliable. (http://store.solar-electric.com/chco.html)

The next category is the 3-stage charge controller. This type of controller acts by charging in three stages: the bulk stage, the absorption stage, and the float stage. During the bulk phase of the charge cycle, the voltage sent to the battery rises to what is termed the "bulk level," and current to the battery is maximized. Next, in the absorption stage, the bulk voltage is maintained for a specific amount of time while the current lowers as the batteries charge up. After the absorption phase is the float stage, in which the voltage is lowered to float level, at which the batteries draw a small current until the next cycle begins. (http://www.freesunpower.com/chargecontrollers.php)

Many three stage controllers are equipped with "pulse width modulation," or PWM. PWM is the ability to change the length of the charging cycle based on the condition of the battery and the amount of current generated by the solar panel. (http://store.solar-electric.com/chco.html)

The most complex charge controllers include maximum power point tracking, or MPPT. This feature converts high voltage DC power into lower voltage DC power that optimizes the match between the panel and battery. This is claimed to provide 15 - 30% more power to the battery. **(**http://store.solar-electric.com/chco.html**)**

Appendix B: LabVIEW Data Collection Program

LabVIEW Data Collection Program: Overall Structure

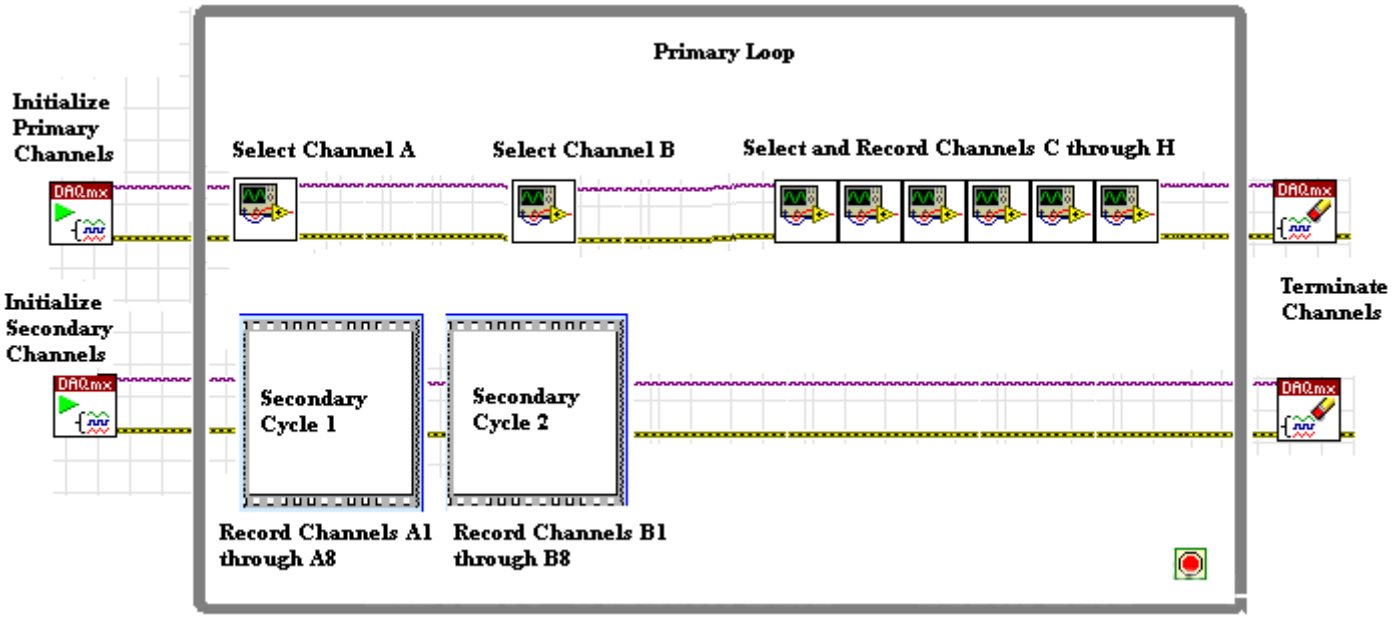

LabVIEW Data Collection Program: Select and Record Channels C through H

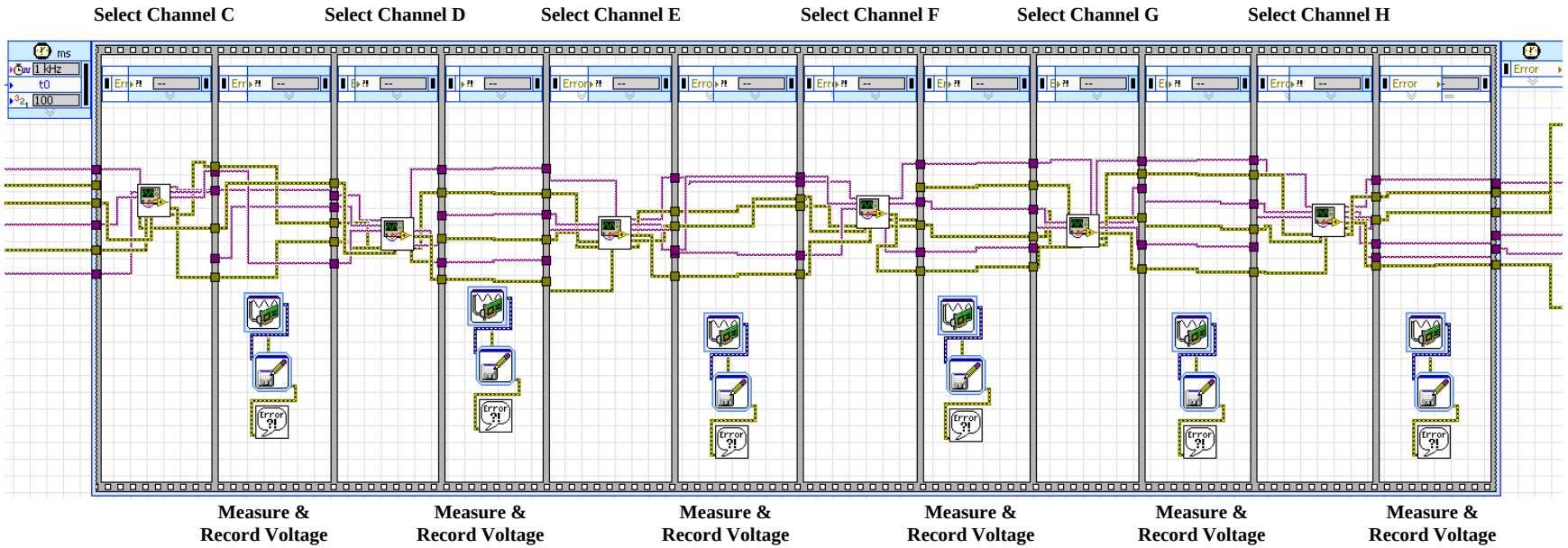

LabVIEW Data Collection Program: Secondary Cycle A

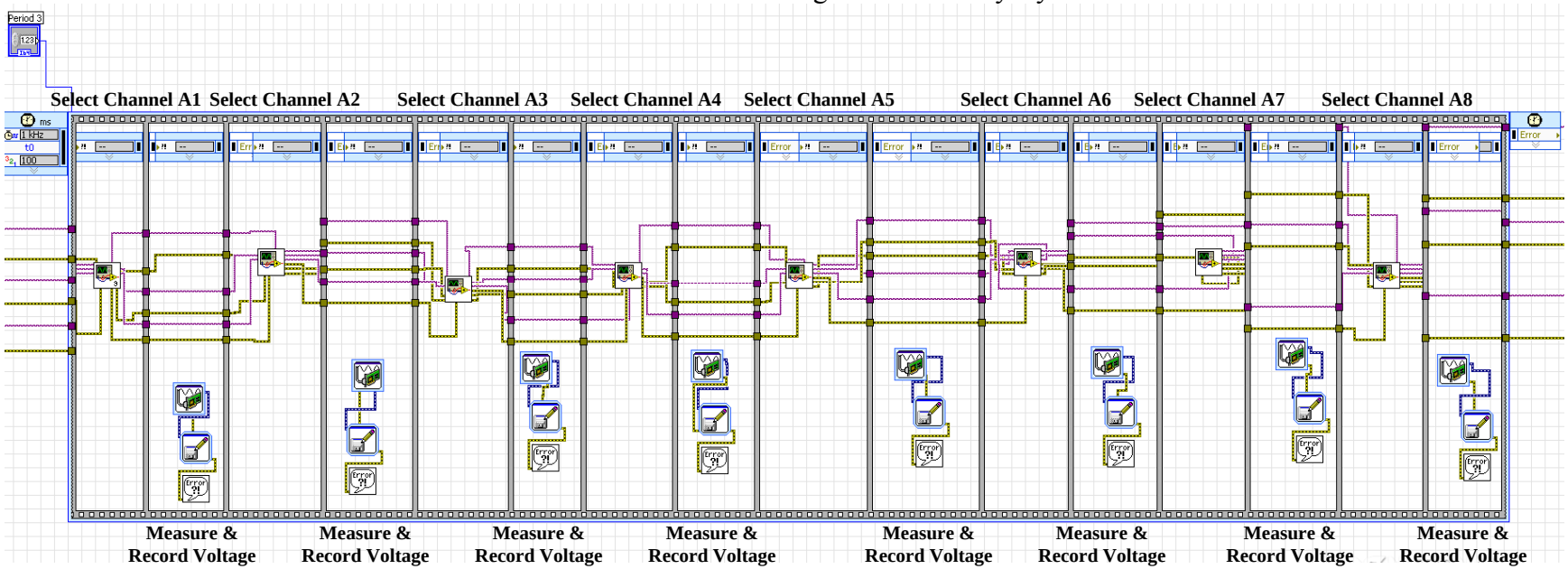

LabVIEW Data Collection Program: Secondary Cycle B

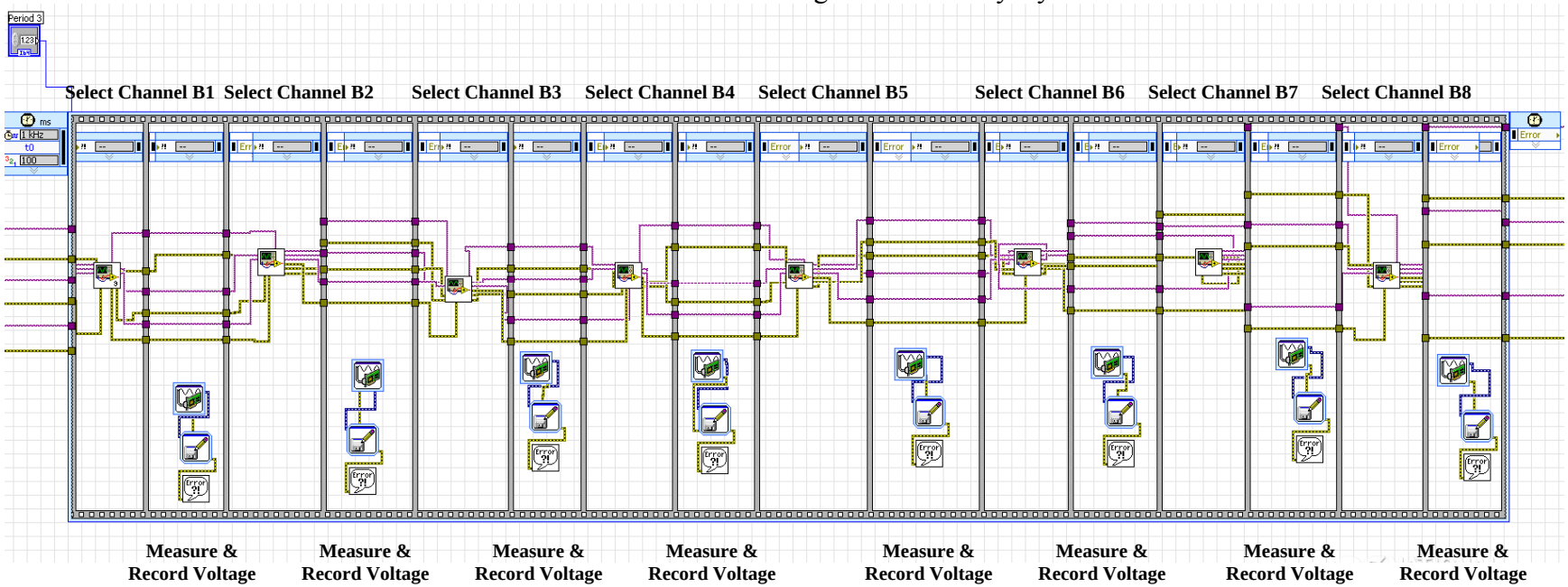

Appendix C: Example of Raw Data File: 24 Hour Period

LabVIEW Measurement
Writer_Version 0.92
Reader_Version 1
Separator Tab
Multi_Headings No
X_Columns Multi
Time_Pref Absolute
Operator SHINE
Date 2008/10/13
Time 17:12:27.510827
End_of_Header

Channels 4
Samples 1 1 1 1
Date 2008/10/13 2008/10/13 2008/10/13 2008/10/13
Time 17:12:27.510827 17:12:27.510827 17:12:27.510827 17:12:27.510827
X_Dimension Time Time Time Time
X0 0.0000000000000000E+0 0.0000000000000000E+0 0.0000000000000000E+0 0.0000000000000000E+0
Delta_X 1.000000 1.000000 1.000000 1.000000
End_of_Header

X_Value	Untitled	X_Value	Untitled 1	X_Value	Untitled 2	X_Value	Untitled 3	Comment
0.000000	0.682112	0.000000	13.565972	0.000000	11.521906	0.000000	11.363276	
570.129807	0.682112	570.129807	13.433342	570.129807	11.450489	570.129807	11.240891	
1169.772049	0.682112	1169.772049	13.208891	1169.772049	11.419882	1169.772049	11.200095	
1769.784826	0.682112	1769.784826	13.117070	1769.784826	11.399477	1769.784826	11.179698	
2369.977861	0.682112	2369.977861	13.086463	2369.977861	11.379072	2369.977861	11.159300	
2969.780334	0.682112	2969.780334	13.066059	2969.780334	11.368870	2969.780334	11.159300	
3569.783096	0.682112	3569.783096	13.045654	3569.783096	11.358667	3569.783096	11.138903	
4169.785858	0.682112	4169.785858	13.015047	4169.785858	11.358667	4169.785858	11.128704	
4769.788619	0.682112	4769.788619	12.994643	4769.788619	11.348465	4769.788619	11.128704	
5369.771352	0.661713	5369.771352	12.974238	5369.771352	11.348465	5369.771352	11.118505	
5969.784128	0.651514	5969.784128	12.964036	5969.784128	11.338262	5969.784128	11.118505	
6569.776875	0.651514	6569.776875	12.943631	6569.776875	11.328060	6569.776875	11.118505	
7169.779637	0.641314	7169.779637	12.902822	7169.779637	11.073000	7169.779637	10.598366	
7769.742341	0.641314	7769.742341	12.892619	7769.742341	10.981178	7769.742341	9.751866	
8369.785160	0.641314	8369.785160	12.882417	8369.785160	10.899559	8369.785160	8.782981	
8969.787921	0.641314	8969.787921	12.872215	8969.787921	10.777130	8969.787921	7.875288	
9569.740611	0.641314	9569.740611	12.872215	9569.740611	10.583285	9569.740611	7.140974	
10169.793445	0.641314	10169.793445	12.851810	10169.793445	10.205796	10169.793445	6.529046	
10769.786192	0.641314	10769.786192	12.851810	10769.786192	9.654866	10769.786192	6.029305	
11369.738882	0.641314	11369.738882	12.841608	11369.738882	8.991710	11369.738882	5.611155	
11969.761672	0.641314	11969.761672	12.831406	11969.761672	8.257137	11969.761672	5.274594	
12569.944693	0.641314	12569.944693	12.831406	12569.944693	7.614386	12569.944693	5.019625	
13169.777210	0.641314	13169.777210	12.821203	13169.777210	7.083861	13169.777210	4.825847	
13769.779971	0.641314	13769.779971	12.811001	13769.779971	6.624753	13769.779971	4.672865	
14369.762704	0.641314	14369.762704	12.800799	14369.762704	6.288074	14369.762704	4.550480	
14969.765466	0.641314	14969.765466	12.790596	14969.765466	5.971800	14969.765466	4.417896	
15569.768227	0.641314	15569.768227	12.790596	15569.768227	5.706537	15569.768227	4.295510	
16169.801032	0.641314	16169.801032	12.780394	16169.801032	5.492287	16169.801032	4.162926	
16769.763736	0.641314	16769.763736	12.780394	16769.763736	5.329048	16769.763736	4.030341	
17369.776512	0.641314	17369.776512	12.770192	17369.776512	5.176012	17369.776512	3.907956	
17969.779274	0.641314	17969.779274	12.759989	17969.779274	5.043381	17969.779274	3.805968	
18569.782035	0.641314	18569.782035	12.759989	18569.782035	4.941357	18569.782035	3.724377	
19169.784797	0.641314	19169.784797	12.749787	19169.784797	4.839333	19169.784797	3.652986	
19769.787559	0.641314	19769.787559	12.749787	19769.787559	4.747512	19769.787559	3.601992	
20369.780305	0.641314	20369.780305	12.739585	20369.780305	4.676095	20369.780305	3.561197	
20969.763038	0.641314	20969.763038	12.729382	20969.763038	4.614880	20969.763038	3.530600	

21569.785829	0.641314	21569.785829	12.729382	21569.785829	4.553666	21569.785829	3.489805
22169.758547	0.641314	22169.758547	12.719180	22169.758547	4.502654	22169.758547	3.449010
22769.761309	0.641314	22769.761309	12.719180	22769.761309	4.451642	22769.761309	3.418413
23369.724013	0.641314	23369.724013	12.708978	23369.724013	4.390428	23369.724013	3.377618
23969.756818	0.641314	23969.756818	12.698775	23969.756818	4.329213	23969.756818	3.336823
24569.759579	0.641314	24569.759579	12.698775	24569.759579	4.267999	24569.759579	3.316425
25169.722283	0.641314	25169.722283	12.688573	25169.722283	4.216987	25169.722283	3.285829
25769.755088	0.641314	25769.755088	12.678371	25769.755088	4.145570	25769.755088	3.255233
26369.757850	0.641314	26369.757850	12.678371	26369.757850	4.094558	26369.757850	3.234835
26969.760611	0.641314	26969.760611	12.668169	26969.760611	4.023141	26969.760611	3.204239
27569.763373	0.641314	27569.763373	12.657966	27569.763373	3.972129	27569.763373	3.183841
28169.766134	0.641314	28169.766134	12.657966	28169.766134	3.910915	28169.766134	3.163444
28769.768896	0.641314	28769.768896	12.647764	28769.768896	3.859903	28769.768896	3.132847
29369.761643	0.631115	29369.761643	12.637562	29369.761643	3.808891	29369.761643	3.112450
29969.764405	0.641314	29969.764405	12.637562	29969.764405	3.757879	29969.764405	3.092052
30569.757152	0.641314	30569.757152	12.627359	30569.757152	3.717069	30569.757152	3.071654
31169.769928	0.641314	31169.769928	12.627359	31169.769928	3.676260	31169.769928	3.051257
31769.762675	0.641314	31769.762675	12.617157	31769.762675	3.645652	31769.762675	3.030859
32369.765437	0.641314	32369.765437	12.606955	32369.765437	3.604843	32369.765437	3.010462
32969.758184	0.641314	32969.758184	12.596752	32969.758184	3.574236	32969.758184	2.979865
33569.851075	0.641314	33569.851075	12.596752	33569.851075	3.533426	33569.851075	2.939070
34169.763707	0.641314	34169.763707	12.586550	34169.763707	3.492616	34169.763707	2.888076
34769.756454	0.641314	34769.756454	12.586550	34769.756454	3.410997	34769.756454	2.745293
35369.759216	0.641314	35369.759216	12.576348	35369.759216	2.441769	35369.759216	2.082371
35969.761978	0.641314	35969.761978	12.576348	35969.761978	2.064280	35969.761978	1.643823
36569.764739	0.631115	36569.764739	12.566145	36569.764739	2.074483	36569.764739	1.603028
37169.717429	0.641314	37169.717429	12.555943	37169.717429	2.084685	37169.717429	1.603028
37769.760248	0.641314	37769.760248	12.555943	37769.760248	2.094888	37769.760248	1.603028
38369.763010	0.641314	38369.763010	12.545741	38369.763010	2.094888	38369.763010	1.592829
38969.725714	0.641314	38969.725714	12.535538	38969.725714	2.094888	38969.725714	1.592829
39569.758518	0.641314	39569.758518	12.525336	39569.758518	2.084685	39569.758518	1.582630
40169.771295	0.641314	40169.771295	12.515134	40169.771295	2.084685	40169.771295	1.582630
40769.733998	0.641314	40769.733998	12.515134	40769.733998	2.074483	40769.733998	1.582630
41369.786832	0.641314	41369.786832	12.504932	41369.786832	2.074483	41369.786832	1.572431
41969.789594	0.641314	41969.789594	12.504932	41969.789594	2.064280	41969.789594	1.572431
42569.792355	0.641314	42569.792355	12.494729	42569.792355	2.054078	42569.792355	1.572431
43169.915289	0.641314	43169.915289	12.484527	43169.915289	2.054078	43169.915289	1.562232
43769.978137	0.641314	43769.978137	12.484527	43769.978137	2.043875	43769.978137	1.562232
44369.930827	0.641314	44369.930827	12.474325	44369.930827	2.043875	44369.930827	1.552034
44969.793387	0.641314	44969.793387	12.464122	44969.793387	2.023471	44969.793387	1.552034
45569.946365	0.641314	45569.946365	12.464122	45569.946365	2.023471	45569.946365	1.541835
46169.909069	0.641314	46169.909069	12.453920	46169.909069	2.013268	46169.909069	1.541835
46770.082075	0.641314	46770.082075	12.443718	46770.082075	2.003066	46770.082075	1.541835
47369.904578	0.641314	47369.904578	12.433515	47369.904578	1.992863	47369.904578	1.531636
47969.917354	0.641314	47969.917354	12.433515	47969.917354	1.982661	47969.917354	1.531636
48569.940144	0.641314	48569.940144	12.433515	48569.940144	1.972459	48569.940144	1.521437
49169.912862	0.641314	49169.912862	12.423313	49169.912862	1.962256	49169.912862	1.521437
49787.771299	0.651514	49787.771299	12.413111	49787.771299	1.962256	49787.771299	1.521437
50371.110099	0.661713	50371.110099	12.413111	50371.110099	1.952054	50371.110099	1.531636
50970.411853	0.661713	50970.411853	12.423313	50970.411853	3.237556	50970.411853	2.551516
51570.044082	0.671913	51570.044082	12.474325	51570.044082	3.808891	51570.044082	3.234835
52170.036829	0.671913	52170.036829	12.606955	52170.036829	5.196417	52170.036829	4.948233
52769.869346	0.682112	52769.869346	12.872215	52769.869346	6.369693	52769.869346	6.386263
53369.982265	0.682112	53369.982265	12.811001	53369.982265	6.859409	53369.982265	7.059384
53970.125229	0.682112	53970.125229	13.086463	53970.125229	7.614386	53970.125229	8.171053
54569.967760	0.682112	54569.967760	13.249700	54569.967760	8.124506	54569.967760	9.068547
55175.838960	0.682112	55175.838960	13.321117	55175.838960	8.542805	55175.838960	9.894649
55770.013341	0.682112	55770.013341	13.290510	55770.013341	8.655031	55770.013341	10.251607
56370.046145	0.682112	56370.046145	13.219094	56370.046145	8.614221	56370.046145	10.343396
56970.028878	0.682112	56970.028878	13.290510	56970.028878	9.195758	56970.028878	11.128704
57569.971554	0.692312	57569.971554	13.423140	57569.971554	10.471058	57569.971554	11.444866
58169.964301	0.682112	58169.964301	13.637388	58169.964301	11.083202	58169.964301	11.720234

58770.037163	0.682112	58770.037163	13.708805	58770.037163	11.358667	58770.037163	11.638644
59369.919752	0.682112	59369.919752	13.810828	59369.919752	11.542310	59369.919752	11.638644
59969.952557	0.682112	59969.952557	13.821030	59969.952557	11.419882	59969.952557	11.567252
60570.095520	0.682112	60570.095520	13.974065	60570.095520	11.460691	60570.095520	11.628445
61170.088267	0.682112	61170.088267	14.167909	61170.088267	11.481096	61170.088267	11.618246
61770.141101	0.682112	61770.141101	14.331146	61770.141101	11.430084	61770.141101	11.567252
62369.923545	0.692312	62369.923545	14.637215	62369.923545	11.440286	62369.923545	11.597848
62969.916293	0.682112	62969.916293	14.953487	62969.916293	11.430084	62969.916293	11.557053
63569.939083	0.682112	63569.939083	15.126926	63569.939083	11.419882	63569.939083	11.516258
64169.921816	0.682112	64169.921816	15.402389	64169.921816	11.450489	64169.921816	11.557053
64770.124866	0.682112	64770.124866	15.698256	64770.124866	11.481096	64770.124866	11.587650
65369.967397	0.682112	65369.967397	15.820684	65369.967397	11.470894	65369.967397	11.567252
65969.900058	0.682112	65969.900058	15.983921	65969.900058	11.491298	65969.900058	11.587650
66569.872776	0.682112	66569.872776	16.096146	66569.872776	11.501501	66569.872776	11.557053
67169.875537	0.682112	67169.875537	16.024730	67169.875537	11.481096	67169.875537	11.506059
67769.928371	0.682112	67769.928371	16.147158	67769.928371	11.511703	67769.928371	11.536656
68369.931133	0.682112	68369.931133	16.136956	68369.931133	11.511703	68369.931133	11.506059
68969.903851	0.682112	68969.903851	15.983921	68969.903851	11.491298	68969.903851	11.424469
69569.916627	0.692312	69569.916627	16.249181	69569.916627	11.572918	69569.916627	11.516258
70169.849288	0.682112	70169.849288	16.208372	70169.849288	11.572918	70169.849288	11.516258
70769.922151	0.682112	70769.922151	16.187967	70769.922151	11.603525	70769.922151	11.526457
71369.934927	0.682112	71369.934927	16.065539	71369.934927	11.603525	71369.934927	11.526457
71969.847558	0.682112	71969.847558	15.932909	71969.847558	11.593322	71969.847558	11.485662
72569.770205	0.682112	72569.770205	15.728863	72569.770205	11.583120	72569.770205	11.475463
73169.762952	0.692312	73169.762952	15.779875	73169.762952	11.603525	73169.762952	11.495860
73769.775728	0.682112	73769.775728	15.749268	73769.775728	11.623930	73769.775728	11.485662
74369.778490	0.682112	74369.778490	15.504412	74369.778490	11.613727	74369.778490	11.444866
74969.831323	0.682112	74969.831323	15.453400	74969.831323	11.623930	74969.831323	11.495860
75569.763984	0.682112	75569.763984	15.351377	75569.763984	11.654537	75569.763984	11.526457
76169.766746	0.682112	76169.766746	15.218747	76169.766746	11.644334	76169.766746	11.516258
76769.769507	0.682112	76769.769507	15.106522	76769.769507	11.654537	76769.769507	11.536656
77369.962543	0.682112	77369.962543	14.973892	77369.962543	11.654537	77369.962543	11.516258
77972.218544	0.682112	77972.218544	14.902475	77972.218544	11.664739	77972.218544	11.536656
78569.827864	0.682112	78569.827864	14.841262	78569.827864	11.674942	78569.827864	11.546854
79169.770539	0.682112	79169.770539	14.841262	79169.770539	11.644334	79169.770539	11.516258
79769.763287	0.682112	79769.763287	14.810655	79769.763287	11.358667	79769.763287	10.996119
80373.261074	0.682112	80373.261074	14.943285	80373.261074	11.572918	80373.261074	11.465264
80969.818882	0.682112	80969.818882	14.820857	80969.818882	11.593322	80969.818882	11.485662
81569.761557	0.682112	81569.761557	14.698429	81569.761557	11.593322	81569.761557	11.475463
82169.724261	0.671913	82169.724261	14.892273	82169.724261	11.664739	82169.724261	11.577451
82769.767080	0.682112	82769.767080	14.586204	82769.767080	11.572918	82769.767080	11.465264
83369.769842	0.671913	83369.769842	14.718834	83369.769842	11.654537	83369.769842	11.567252
83969.722531	0.661713	83969.722531	14.504585	83969.722531	11.593322	83969.722531	11.485662
84569.765350	0.661713	84569.765350	14.494383	84569.765350	11.623930	84569.765350	11.516258
85169.768112	0.682112	85169.768112	14.076088	85169.768112	11.491298	85169.768112	11.312282
85769.720801	0.682112	85769.720801	14.127100	85769.720801	11.532108	85769.720801	11.363276
86369.773635	0.671913	86369.773635	13.923053	86369.773635	11.419882	86369.773635	11.169499

Appendix D: Data Format Conversion Program

```
clear all
close all

%-----------------------------------------------------------------
--------%
%READ FILES
A1=textread('testsetA1.lvm','','headerlines',21);
A2=textread('testsetA2.lvm','','headerlines',21);
A3=textread('testsetA3.lvm','','headerlines',21);
A4=textread('testsetA4.lvm','','headerlines',21);
A5=textread('testsetA5.lvm','','headerlines',21);
A6=textread('testsetA6.lvm','','headerlines',21);
A7=textread('testsetA7.lvm','','headerlines',21);
A8=textread('testsetA8.lvm','','headerlines',21);
Ba1=textread('testsetB1.lvm','','headerlines',21);
Ba2=textread('testsetB2.lvm','','headerlines',21);
C=textread('testsetC.lvm','','headerlines',21);
D=textread('testsetD.lvm','','headerlines',21);
E=textread('testsetE.lvm','','headerlines',21);
F=textread('testsetF.lvm','','headerlines',21);
G=textread('testsetG.lvm','','headerlines',21);
H=textread('testsetH.lvm','','headerlines',21);

%-----------------------------------------------------------------
--------%
%FIND SHORTEST vect
r=length(A1);
s=length(A2);
t=length(A6);
u=length(Ba1);
v=length(C);
w=length(D);
x=length(E);
y=length(F);
z=length(F);
za=length(G);
zb=length(H);
long=[r;s;t;u;v;w;x;y;z;za;zb];
stop=min(long);
%Because the program cycles from panel/battery to
%panel/battery, the amount of measurements may not match from
panel to
%panel. This is kind of a convoluted way to find the length of
each vector
%take the shortest one, and set the stop value for all the
vectors to that
```

```
time=H(1:stop,1);
%Should be the same for every matrix. H could be A1, A2, C,
whatever
filter16 = ones(16,1)./16;

Ctrl_I_1=filter(filter16, 1, A1(1:stop,2));
OC_B2_9=filter(filter16, 1, A1(1:stop,4));
NoCC_B1_5=filter(filter16, 1, A1(1:stop,6));
NoCC_P3_17=filter(filter16, 1, A1(1:stop,8));

Car_B2_12=filter(filter16, 1, Ba1(1:stop,2));
DD_B2_10=filter(filter16, 1, Ba1(1:stop,4));
Ctrl_B3_13=filter(filter16, 1, Ba1(1:stop,6));
Drt_B1_2=filter(filter16, 1, Ba1(1:stop,8));

OC_P3_15=filter(filter16, 1, C(1:stop,2));
DD_P3_16=filter(filter16, 1, C(1:stop,4));
Ctrl_B2_7=filter(filter16, 1, C(1:stop,6));
OC_B1_3=filter(filter16, 1, C(1:stop,8));

Drt_P3_14=filter(filter16, 1, D(1:stop,2));
Ctrl_P3_13=filter(filter16, 1, D(1:stop,4));
Drt_B2_8=filter(filter16, 1, D(1:stop,6));
DD_B1_4=filter(filter16, 1, D(1:stop,8));

Car_P3_18=filter(filter16, 1, E(1:stop,2));
NoCC_P1_5=filter(filter16, 1, E(1:stop,4));
DD_P2_10=filter(filter16, 1, E(1:stop,6));
OC_B3_15=filter(filter16, 1, E(1:stop,8));

Drt_P1_2=filter(filter16, 1, F(1:stop,2));
Car_P1_6=filter(filter16, 1, F(1:stop,4));
OC_P2_9=filter(filter16, 1, F(1:stop,6));
DD_B3_16=filter(filter16, 1, F(1:stop,8));

OC_P1_3=filter(filter16, 1, G(1:stop,2));
Ctrl_P2_7=filter(filter16, 1, G(1:stop,4));
NoCC_P2_11=filter(filter16, 1, G(1:stop,6));
NoCC_B3_17=filter(filter16, 1, G(1:stop,8));

DD_P1_4=filter(filter16, 1, H(1:stop,2));
Drt_P2_8=filter(filter16, 1, H(1:stop,4));
Car_P2_12=filter(filter16, 1, H(1:stop,6));
Drt_B3_14=filter(filter16, 1, H(1:stop,8));

Drt_I_8=filter(filter16, 1, A2(1:stop,2));
NoCC_I_17=filter(filter16, 1, A3(1:stop,2));
Car_I_6=filter(filter16, 1, A4(1:stop,2));
Car_B1_6=filter(filter16, 1, A5(1:stop,2));
Car_B3_18=filter(filter16, 1, A6(1:stop,2));
NoCC_B2_11=filter(filter16, 1, A7(1:stop,2));
```

```
Ctrl_P1_1=filter(filter16, 1, A8(1:stop,2));
Ctrl_B1_1=filter(filter16, 1, Ba2(1:stop,2));
clear A1 A2 A3 A4 A5 A6 A7 A8 Ba1 Ba2 C D E F G H
```

Appendix E: Day Separation Program

```
function [ndi, ndt] = separate24(data, times)

% [new_day_indices, new_day_times] = separate24(data, times)
%
% Reads in a vector of time-series voltage or current data and
returns
% sample indices for the beginning of each day
%
% If a vector of corresponding timestamps is provided, then a
vector
% containing the timestamps corresponding to the output samples
is also
% returned

if(nargin > 1)    % check to see if time vector specified
    times_flag = 1;
else
    times_flag = 0;
end

if(nargin > 2)    % idiot check
    error('Too many input arguments');
end

if(times_flag)
    if(length(times) ~= length(data))     % check vector
dimensions
        error('length(times) must equal length(data)');
    end
end

filter16 = ones(16,1)./16;
% daylength = 143;    % day length in (10 min) samples: 23 hrs,
50 min
thresh = 1e-4;    % threshold of daily_spikes value for new day

data_f16 = filter(filter16, 1, data);     % first noise filter
data_deriv = filter([1 -1], 1, data_f16);      % one-sample
differentiator
data_deriv_f16 = filter(filter16, 1, data_deriv);    % derivative
noise filter
daily_spikes = data_deriv_f16.^7;      % raise to a high odd
power to preserve
                                       % sign while exaggerating
peaks

new_day_counter = 0;
```

```
for i = 2:length(daily_spikes)
    prev = daily_spikes(i-1) - thresh;
    curr = daily_spikes(i) - thresh;

    if ((sign(prev) == -1) && (sign(curr) == 1))
        new_day_counter = new_day_counter + 1;
        new_day_indices(new_day_counter) = i - 1;

        if(times_flag)
            new_day_times(new_day_counter) = times(i-1);
        end

    end
end

ndt=(new_day_times/3600)';
ndi=new_day_indices';
```

Appendix F: Baseline Test (with weather consideration)

```
function [ctrl,drt,oc,dd,nocc,car] =
bsl_sd_weath_envelope(time,T,ndi)
close all

load blneandsd4.mat

%time in hours
time=time/3600;
f=1;

%Weather
weath=[0 0 1 1 0 0 0 0 0 1 0 0 2 0 1 1 0 0 0 0 0 0 1 2 2 1 1 2 0
0 0 2 2 0 1 0 0 0 1 1 2 0 0 0 0 0 0 0 0 0 0 0 1 0 2 0 1 1 2 2 0
0 0 1 1 0 0 2 1 1 0 0 2 0 1 0 1 0 1 1 0 0 0 1 1];

%Full cycle percentage calc
ctrl=0;
drt=0;
oc=0;
dd=0;
nocc=0;
car=0;

clear set bsl_ctrl1s bsl_drt1s bsl_oc1s bsl_dd1s bsl_nocc1s
bsl_car1s
figure
%Make a set of day indices
r=1;
for i=1:length(ndi)-1
    spc=ndi(i+1)-ndi(i);
    %Remove unwanted extra day slices and cut off earlier days
    if spc > 130 && spc < 150 && ndi(i) > 4131 && ndi(i) < 6008
%%ndi(i) > 7015 && ndi(i) < 10039
        set(r,1)=ndi(i);
        set(r,2)=ndi(i+1);
        set(r,3)=i;
        set(r,4)=weath(i);
        chart(r,:)=[set(r,3) set(r,4) set(r,1) set(r,2)];
        r=r+1;
    end
end

set

bsl_ctrl_s=bslsun(1:143,1);
bsl_drt_s=bslsun(1:143,2);
bsl_oc_s=bslsun(1:143,3);
bsl_dd_s=bslsun(1:143,4);
```

```
bsl_nocc_s=bslsun(1:143,5);
bsl_car_s=bslsun(1:143,6);

[bsl_ctrl_s bsl_drt_s bsl_oc_s bsl_dd_s bsl_nocc_s bsl_car_s]

sd_ctrl_s=sdsun(1:143,1);
sd_drt_s=sdsun(1:143,2);
sd_oc_s=sdsun(1:143,3);
sd_dd_s=sdsun(1:143,4);
sd_nocc_s=sdsun(1:143,5);
sd_car_s=sdsun(1:143,6);

bsl_ctrl_c=bslclo(1:143,1);
bsl_drt_c=bslclo(1:143,2);
bsl_oc_c=bslclo(1:143,3);
bsl_dd_c=bslclo(1:143,4);
bsl_nocc_c=bslclo(1:143,5);
bsl_car_c=bslclo(1:143,6);

sd_ctrl_c=sdclo(1:143,1);
sd_drt_c=sdclo(1:143,2);
sd_oc_c=sdclo(1:143,3);
sd_dd_c=sdclo(1:143,4);
sd_nocc_c=sdclo(1:143,5);
sd_car_c=sdclo(1:143,6);

bsl_ctrl_r=bslrain(1:143,1);
bsl_drt_r=bslrain(1:143,2);
bsl_oc_r=bslrain(1:143,3);
bsl_dd_r=bslrain(1:143,4);
bsl_nocc_r=bslrain(1:143,5);
bsl_car_r=bslrain(1:143,6);

sd_ctrl_r=sdrain(1:143,1);
sd_drt_r=sdrain(1:143,2);
sd_oc_r=sdrain(1:143,3);
sd_dd_r=sdrain(1:143,4);
sd_nocc_r=sdrain(1:143,5);
sd_car_r=sdrain(1:143,6);

for j=1:length(set)
    V=T(set(j,1):set(j,1)+142);
    disp('Day')
    disp(set(j,3))
    %Decide which baselines to use
    if weath(set(j,3))==0
        disp('Sunny')
        bsl_ctrl1=bsl_ctrl_s;
        bsl_drt1=bsl_drt_s;
        bsl_oc1=bsl_oc_s;
        bsl_dd1=bsl_dd_s;
        bsl_nocc1=bsl_nocc_s;
```

```
    bsl_car1=bsl_car_s;
    sd_ctrl1=sd_ctrl_s;
    sd_drt1=sd_drt_s;
    sd_oc1=sd_oc_s;
    sd_dd1=sd_dd_s;
    sd_nocc1=sd_nocc_s;
    sd_car1=sd_car_s;
elseif weath(set(j,3))==1
    disp('Cloudy')
    bsl_ctrl1=bsl_ctrl_c;
    bsl_drt1=bsl_drt_c;
    bsl_oc1=bsl_oc_c;
    bsl_dd1=bsl_dd_c;
    bsl_nocc1=bsl_nocc_c;
    bsl_car1=bsl_car_c;
    sd_ctrl1=sd_ctrl_c;
    sd_drt1=sd_drt_c;
    sd_oc1=sd_oc_c;
    sd_dd1=sd_dd_c;
    sd_nocc1=sd_nocc_c;
    sd_car1=sd_car_c;
elseif weath(set(j,3))==2
    disp('Rainy')
    bsl_ctrl1=bsl_ctrl_r;
    bsl_drt1=bsl_drt_r;
    bsl_oc1=bsl_oc_r;
    bsl_dd1=bsl_dd_r;
    bsl_nocc1=bsl_nocc_r;
    bsl_car1=bsl_car_r;
    sd_ctrl1=sd_ctrl_r;
    sd_drt1=sd_drt_r;
    sd_oc1=sd_oc_r;
    sd_dd1=sd_dd_r;
    sd_nocc1=sd_nocc_r;
    sd_car1=sd_car_r;
elseif weath(set(j,3))==3
    disp('Very Rainy')
    bsl_ctrl1=bsl_ctrl_r;
    bsl_drt1=bsl_drt_r;
    bsl_oc1=bsl_oc_r;
    bsl_dd1=bsl_dd_r;
    bsl_nocc1=bsl_nocc_r;
    bsl_car1=bsl_car_r;
    sd_ctrl1=sd_ctrl_r;
    sd_drt1=sd_drt_r;
    sd_oc1=sd_oc_r;
    sd_dd1=sd_dd_r;
    sd_nocc1=sd_nocc_r;
    sd_car1=sd_car_r;
end

%Control Check
```

```
    match=0;
    for i=1:length(V)
        if V(i) <= bsl_ctrl1(i)+f*sd_ctrl1(i) && V(i) >=
bsl_ctrl1(i)-f*sd_ctrl1(i)
            match=match+1;
        else
            match=match;
        end
    end
    pct_ctrl=match/length(V)*100;


    %Dirt Check
    match=0;
    for i=1:length(V)
        if V(i) <= bsl_drt1(i)+f*sd_drt1(i) && V(i) >=
bsl_drt1(i)-f*sd_drt1(i)
            match=match+1;
        else
            match=match;
        end
    end
    pct_drt=match/length(V)*100;


    %OverCharge Check
    match=0;
    for i=1:length(V)
        if V(i) <= bsl_oc1(i)+f*sd_oc1(i) && V(i) >= bsl_oc1(i)-
f*sd_oc1(i)
            match=match+1;
        else
            match=match;
        end
    end
    pct_oc=match/length(V)*100;


    %Deep Discharge Check
    match=0;
    for i=1:length(V)
        if V(i) <= bsl_dd1(i)+f*sd_dd1(i) && V(i) >= bsl_dd1(i)-
f*sd_dd1(i)
            match=match+1;
        else
            match=match;
        end
    end
    pct_dd=match/length(V)*100;


    %Malfunctioning or lack of a charge controller Check
```

```
    match=0;
    for i=1:length(V)
        if V(i) <= bsl_nocc1(i)+f*sd_nocc1(i) && V(i) >=
bsl_nocc1(i)-f*sd_nocc1(i)
            match=match+1;
        else
            match=match;
        end
    end
    pct_nocc=match/length(V)*100;


    %Car Battery Check
    match=0;
    for i=1:length(V)
        if V(i) <= bsl_car1(i)+f*sd_car1(i) && V(i) >=
bsl_car1(i)-f*sd_car1(i)
            match=match+1;
        else
            match=match;
        end
    end
    pct_car=match/length(V)*100;

    %Make a figure and plot the day's data
    if weath(set(j,3))==0
        plot(time(1:length(V)),V(1:length(V)),'b','Linewidth',3)
    elseif weath(set(j,3))==1
        plot(time(1:length(V)),V(1:length(V)),'m','Linewidth',3)
    elseif weath(set(j,3))==2
        plot(time(1:length(V)),V(1:length(V)),'g','Linewidth',3)
    elseif weath(set(j,3))==3
        plot(time(1:length(V)),V(1:length(V)),'k','Linewidth',3)
    end
    hold on
    axis([0 24 0 16])
    xlabel('Time (hrs)')
    ylabel('Voltage (V)')


    %Correlate
    tot=[pct_ctrl pct_drt pct_oc pct_dd pct_nocc pct_car];
    if max(tot) < 30
        disp 'The correlations are too low for system type to be
determined.'
        disp ' '
    elseif max(tot)==pct_ctrl
        disp 'The battery is from a healthy system.'
        disp ' '

plot(time(1:length(V)),bsl_ctrl1(1:length(V)),'k','Linewidth',3)
```

```
        plot(time(1:length(V)),bsl_ctrl1(1:length(V))-
f*sd_ctrl1(1:length(V)),'k:')

plot(time(1:length(V)),bsl_ctrl1(1:length(V))+f*sd_ctrl1(1:length
(V)),'k:')
        ctrl=ctrl+1;
    elseif max(tot)==pct_drt
        disp 'The battery is from a dirty system.'
        disp ' '
        plot(time(1:length(V)),bsl_drt1(1:length(V)),'g')
        plot(time(1:length(V)),bsl_drt1(1:length(V))-
f*sd_drt1(1:length(V)),'k:')

plot(time(1:length(V)),bsl_drt1(1:length(V))+f*sd_drt1(1:length(V
)),'k:')
        drt=drt+1;
    elseif max(tot)==pct_oc
        disp 'The battery is from a overcharged system.'
        disp ' '
        plot(time(1:length(V)),bsl_oc1(1:length(V)),'r')
        plot(time(1:length(V)),bsl_oc1(1:length(V))-
f*sd_oc1(1:length(V)),'k:')

plot(time(1:length(V)),bsl_oc1(1:length(V))+f*sd_oc1(1:length(V))
,'k:')
        oc=oc+1;
    elseif max(tot)==pct_dd
        disp 'The battery is from a deep discharged system.'
        disp ' '
        plot(time(1:length(V)),bsl_dd1(1:length(V)),'r')
        plot(time(1:length(V)),bsl_dd1(1:length(V))-
f*sd_dd1(1:length(V)),'k:')

plot(time(1:length(V)),bsl_dd1(1:length(V))+.3*sd_dd1(1:length(V)
),'k:')
        dd=dd+1;
    elseif max(tot)==pct_nocc
        disp 'The battery is from a malfunctioning or lack of a
charge controller system.'
        disp ' '
        plot(time(1:length(V)),bsl_nocc1(1:length(V)),'r')
        plot(time(1:length(V)),bsl_nocc1(1:length(V))-
f*sd_nocc1(1:length(V)),'k:')

plot(time(1:length(V)),bsl_nocc1(1:length(V))+f*sd_nocc1(1:length
(V)),'k:')
        nocc=nocc+1;
    elseif max(tot)==pct_car
        disp 'The battery is from a car battery system.'
        disp ' '
        plot(time(1:length(V)),bsl_car1(1:length(V)),'r')
```

```
        plot(time(1:length(V)),bsl_car1(1:length(V))-
f*sd_car1(1:length(V)),'k:')

plot(time(1:length(V)),bsl_car1(1:length(V))+f*sd_car1(1:length(V
)),'k:')
        car=car+1;
    end
    M(j) = getframe;
end
ctrl=ctrl/length(set)*100;
drt=drt/length(set)*100;
oc=oc/length(set)*100;
dd=dd/length(set)*100;
nocc=nocc/length(set)*100;
car=car/length(set)*100;
chart=chart
movie(M,1,2)
%Final Decision
tot=[ctrl drt oc dd nocc car];
if max(tot) < 30
    disp 'The correlations are too low for system type to be
determined.'
    disp ' '
    %end
elseif max(tot)==ctrl
    disp 'HEALTHY SYSTEM'
    disp ' '
elseif max(tot)==drt
    disp 'DIRTY PANEL'
    disp ' '
elseif max(tot)==oc
    disp 'OVERCHARGED BATTERY'
    disp ' '
elseif max(tot)==dd
    disp 'DEEP DISCHARGED BATTERY'
    disp ' '
elseif max(tot)==nocc
    disp 'MALFUNCTIONING OR LACK OF A CHARGE CONTROLLER'
    disp ' '
elseif max(tot)==car
    disp 'USING A CAR BATTERY'
    disp ' '
end
```

Appendix G: Combined Metric Test

```
function [ctrl drt oc dd nocc car]=stats_daily(time,T,ndi)
close all

%Weather
weath=[0 0 1 1 0 0 0 0 0 1 0 0 2 0 1 1 0 0 0 0 0 0 1 2 2 1 1 2 0
0 0 2 2 0 1 0 0 0 1 1 2 0 0 0 0 0 0 0 0 0 0 0 0 1 0 2 0 1 1 2 2 0
0 0 1 1 0 0 2 1 1 0 0 2 0 1 0 1 0 1 1 0 0 0 1 1];

clear set

%Make a set of day indices
r=1;
for i=1:length(ndi)-1
    spc=ndi(i+1)-ndi(i);
    %Remove unwanted extra day slices and cut off earlier days
    if spc > 130 && spc < 150 && ndi(i) > 7015 && ndi(i) < 10039
        set(r,1)=ndi(i);
        set(r,2)=ndi(i+1);
        set(r,3)=i;
        set(r,4)=weath(i);
        r=r+1;
    end
end

clear sum rotsum ktot dydxsum dc_slope dydxmax Kmax K
sum=zeros(140,length(set));
rotsum=zeros(140,length(set));
ktot=zeros(140,length(set));
dydxsum=zeros(length(set),1);

for j=1:length(set)
    V=T(set(j,1):set(j,2));
    for rr=3:140
        sum(j)=sum(j)+V(rr);
        r(rr,j)=atand(V(rr)/(time(rr)/3600));
        rotsum(j)=rotsum(j)+r(rr,j);
        dydx2(rr-1,j)=(V(rr-1)-V(rr-2))/((time(rr-1)-time(rr-
2))/3600);
        dydx(rr,j)=(V(rr)-V(rr-1))/((time(rr)-time(rr-1))/3600);
        d2ydx2(rr,j)=(dydx(rr,j)-dydx2(rr-1,j))/((time(rr)-
time(rr-1))/3600);
        k(rr,j)=d2ydx2(rr,j)/(1+dydx(rr,j)^2)^(3/2);
        ktot(j)=ktot(j)+k(rr,j);
        if rr>=41 && rr<76
            dydxsum(j)=dydx(rr,j)+dydxsum(j);
        end
    end
    [dydxmax(j),Idydx]=min(dydx(41:76,j));
```

```
    avg(j)=sum(j)/140;
    rot(j)=rotsum(j)/140;
    K(j)=ktot(j)/140;
    dc_slope(j)=dydxsum(j)/(76-41);
    [Kmax(j),Imax]=max(k(1:140,j));
    [Kmin(j),Imin]=min(k(1:140,j));
    Kmax(j)=mean([k(Imax-1,j),k(Imax,j),k(Imax,j)]);
    Kmin(j)=mean([k(Imin-1,j),k(Imin,j),k(Imin,j)]);
    figure; axis([0 24 0 14]);hold on
    plot(time(1:140)/3600,V(1:140),'b','Linewidth',3)
    plot(time(Imax)/3600,V(Imax),'go','Linewidth',2);
    plot(time(Imin)/3600,V(Imin),'ko','Linewidth',2);
    plot(time(Idydx+41)/3600,V(Idydx+41),'mo','Linewidth',2);
    plot(time(41)/3600,V(41),'rx','Linewidth',3);
    plot(time(76)/3600,V(76),'rx','Linewidth',3);
    line([0,15*cosd(rot(j))],[0,15*sind(rot(j))],'Color','c')
    line([time(Idydx+41)/3600-
2,time(Idydx+41)/3600+2],[V(Idydx+41)-
dydxmax(j)*2,dydxmax(j)*2+V(Idydx+41)],'Color','r')
end

disp('      day    weather      avg       rot         K      Kmax
Kmin   dydxmax  dc_slope')
stats=[set(:,3) set(:,4) avg' rot' K'  Kmax' Kmin' dydxmax'
dc_slope'];

ctrl=0;
drt=0;
oc=0;
dd=0;
nocc=0;
car=0;

for l=1:length(set)
    score(l,1:9)=abs(stats(l,1:9))
    Tscore=-5*score(l,3)-
.3*score(l,4)+800*score(l,5)+4*score(l,6)+3*score(l,7)+5*score(l,
8)+5*score(l,9)
    match=[-52.5 -34.5 -69.9 72.3 51.5 19.5]
    less=abs(Tscore-match)
    pick=min((less))

    if pick==less(1)
        disp 'HEALTHY SYSTEM'
        disp ' '
        ctrl=ctrl+1;
    elseif pick==less(2)
        disp 'DIRTY PANEL'
        disp ' '
        drt=drt+1;
    elseif pick==less(3)
        disp 'OVERCHARGED BATTERY'
```

```
        disp ' '
        oc=oc+1;
    elseif pick==less(4)
        disp 'DEEP DISCHARGED BATTERY'
        disp ' '
        dd=dd+1;
    elseif pick==less(5)
        disp 'MALFUNCTIONING OR LACK OF A CHARGE CONTROLLER'
        disp ' '
        nocc=nocc+1;
    elseif pick==less(6)
        disp 'USING A CAR BATTERY'
        disp ' '
        car=car+1;
    end
end

ctrl=ctrl/length(set)*100;
drt=drt/length(set)*100;
oc=oc/length(set)*100;
dd=dd/length(set)*100;
nocc=nocc/length(set)*100;
car=car/length(set)*100;

%Final Decision
tot=[ctrl drt oc dd nocc car];
disp 'Final Decision:'
if max(tot) < 0
    disp 'The correlations are too low for system type to be
determined.'
    disp ' '
elseif max(tot)==ctrl
    disp 'HEALTHY SYSTEM'
    disp ' '
elseif max(tot)==drt
    disp 'DIRTY PANEL'
    disp ' '
elseif max(tot)==oc
    disp 'OVERCHARGED BATTERY'
    disp ' '
elseif max(tot)==dd
    disp 'DEEP DISCHARGED BATTERY'
    disp ' '
elseif max(tot)==nocc
    disp 'MALFUNCTIONING OR LACK OF A CHARGE CONTROLLER'
    disp ' '
elseif max(tot)==car
    disp 'USING A CAR BATTERY'
    disp ' '
end
```

Appendix H: Least Squares and Gaussian Tests

```
function diagnose_commonBaselines(Vpanel, Vbatt, Ibatt, method,
normFlag)

% diagnosis = diagnose(Vpanel, Vbatt, Ibatt, method, FSFilterFlag)
%
% Given Vpanel and Vbatt (plus optional Ibatt) from a system with an
% unknown problem, this function returns the most probable diagnosis.
% (1 for Healthy, 2 for Dirty panel, etc)
%
% Ibatt currently won't affect the results, as we have insufficient
% training data.
%
% Method:
% 1 for Least Squares
% 2 for Gaussian baseline matching
% 3 for No-baseline method (not currently implemented here)
%
% normFlag - Use Normalized data sets; 1 = on, 0 = off
% Pre-filters Vbatt by subtracting out the time-domain average of the
% baseline signals. If used, the filtered Vbatt will be compared to a
set
% of baselines with the same average signal subtracted.


day_length = 143;   % 143*(10min/sample) = 23 hrs 50 min
                    % Note that if this is changed, baseline sets will
have
                    % to be recompiled to match

min_day_length = 140; % threshold below which to discard a day's data
new_day_offset = -2;  % |offset| < day_length
decision_margin = 10;  % should be > 0; lower number -> more selective


% check inputs
if(nargin ~= 5)
    error('Too many or too few input arguments');
end

% compare lengths of Vbatt and Vpanel, truncate if necessary
if(length(Vbatt) < length(Vpanel))
    Vpanel = Vpanel(1:length(Vbatt));
elseif(length(Vbatt) > length(Vpanel))
    Vbatt = Vbatt(1:length(Vpanel));
end

% get new day indices
new_day_indices = separate24(Vpanel);

% check for errors by flagging "days" with length < min_day_length
for i = 2:length(new_day_indices)
    if(new_day_indices(i) - new_day_indices(i-1) < min_day_length)
        new_day_indices(i-1) = -1;
        continue
```

```
    end
end

% then discard those indices
i = 1;
while 1
    if(new_day_indices(i) == -1)
        new_day_indices = [new_day_indices(1:i-1)
new_day_indices(i+1:length(new_day_indices))];
        continue
    end
    i = i + 1;
    if(i > length(new_day_indices))
        break
    end
end

% if offset would cause invalid reference, throw out first day
if(new_day_indices(1) - new_day_offset < 1)
    new_day_indices = new_day_indices(2:length(new_day_indices));
end

% apply offset
new_day_indices = new_day_indices - new_day_offset;

% discard last partial day
new_day_indices = new_day_indices(1:length(new_day_indices)-2);  %was -
1, but failed sometimes

num_days = length(new_day_indices);

if(num_days == 0)
    error('No usable days found in input vector')
end

% rearrange battery data into a matrix; each column is a day
daysMatrix = zeros(day_length,num_days);  % day_length + 1?
for i = 1:num_days
    daysMatrix(:,i) =
Vbatt(new_day_indices(i):new_day_indices(i)+day_length-1);
end

% Load Baseline Data
[LSbaselines, ProbFields, MeanBaseline] = loadBaselines(daysMatrix,
num_days, normFlag, method);  %daysMatrix passed so that the average
                                                        %curve can be
superimposed on PDF

% LSbaselines = [LSbaselines ones(day_length+1,1)];  % add column for
DC
% offset

totals = zeros(1,6);

switch method
    case 1 % Least Squares
        % compare each day in unknown set to LSbaselines
```

```
        for i = 1:num_days
            if(normFlag)
                daysMatrix(:,i) = daysMatrix(:,i) - MeanBaseline;
%Normalize, if requested
            end
            coeffs(:,i) = LSbaselines\daysMatrix(:,i);
            relative(:,i) = (coeffs(1:6,i)./mean(coeffs(1:6,i))).^2;

            % k = find(relative(:,i) > decision_margin);   % use
decision margin
            k = find(coeffs(:,i) == max(coeffs(:,i)));      % simple
maximum (force decision)

            if(length(k) ~= 1)
                %         diagnosis(i) = 'Indeterminate';
                problem_type(i) = 0;
            else
                problem_type(i) = k;

                totals(k) = totals(k)+1;
            end
        end

        %figure; hist(problem_type,1:6);

        figure;
        percentages = totals./num_days;
        bar(percentages)
        axis([0.5 6.5 0 1])

        title('Problem type vs. Relative Frequency');
        xlabel('1 = control, 2 = dirty, 3 = OC, 4 = DD, 5 = NoCC, 6 =
Car');
        coeffs
        relative


    case 2 % Gaussian Baseline
        scores = zeros(num_days,6);
        for day = 1:num_days
            if(normFlag)
                daysMatrix(:,day) = daysMatrix(:,day) - MeanBaseline;
%Normalize, if requested
            end
            for problem = 1:6   %test all problems
            %for problem = [5 6]    %test particular problems
                for sample = 1:day_length  % +1?
                    %Find closest matching voltage index (ceiling)
                    v_index = round((abs(daysMatrix(sample,day)-
ProbFields(problem).Vmin)/(ProbFields(problem).Vmax-
ProbFields(problem).Vmin))*ProbFields(problem).GridRes);
%                   for v_index = 1:ProbFields(problem).GridRes+1
%                         if(ProbFields(problem).Vgrid(v_index) >
daysMatrix(sample,day))   %VERY SLOW
%                             break
%                         end
%                   end
```

```
                    scores(day,problem) = scores(day,problem) +
ProbFields(problem).ProbField(v_index,sample);
                end
            end
        end

        scores
        %total_scores = sum(scores)  %column-wise sum--that is, sum
across all days in question

        totals = zeros(1,6);

        %for each day
        for i = 1:num_days
            %find highest scoring problem
            current_problem = find(scores(i,:) == max(scores(i,:)));
            %increment the total for that day
            totals(current_problem) = totals(current_problem) + 1;
        end



        percentages = totals./sum(totals);

        figure; bar(percentages);

        axis([0.5 6.5 0 1])

        title('Problem type vs. Score');
        xlabel('1 = control, 2 = dirty, 3 = OC, 4 = DD, 5 = NoCC, 6 =
Car');

    case 3
        disp('No-baseline matching not yet available in this function')

end



%-------------------------------------------------
% Helper Function to load baseline data

function [baselines, ProbFields, MeanBaseline] =
loadBaselines(daysMatrix, num_days, normFlag, method)

if method == 2

%-------------------------------------------------
% Prepare probability field and supporting data

for problem = 1:6

    dim_StatBaselines = 143;

    mu = baselines(:,problem);
    sigma = SunnyStDevs(:,problem);
```

```
    %Generate series of voltages on which to evaluate gaussian PDF
    ProbFields(problem).GridRes = 500;
    %Vmin = min(mu)-4;
    %Vmax = max(mu)+4;

    if(normFlag)
        Vmin = -10;
        Vmax = 10;
    else
        Vmin = 0;
        Vmax = 20;
    end

    Vgrid = Vmin:(Vmax - Vmin)/ProbFields(problem).GridRes:Vmax;
    ProbFields(problem).Vgrid = Vgrid;
    ProbFields(problem).Vmin = Vmin;
    ProbFields(problem).Vmax = Vmax;

    ProbFields(problem).ProbField =
zeros(length(Vgrid),dim_StatBaselines(1));


    for i = 1:length(mu)
        %Generate Gaussian PDF for each sample
        ProbFields(problem).ProbField(:,i) =
(1/(sigma(i)*sqrt(2*pi)))*exp(-((Vgrid - mu(i)).^2/(2*sigma(i)^2)));
    end

    switch problem
        case 1
            type = 'Control';
            figure;
        case 2
            type = 'Dirty';
        case 3
            type = 'Overcharge';
        case 4
            type = 'Deep Discharge';
        case 5
            type = 'No CC';
        case 6
            type = 'Car Battery';
    end

    %subplot(2,3,problem);
    figure;
    imagesc(1:dim_StatBaselines(1),Vgrid,ProbFields(problem).ProbField)
    set(gca,'Ydir','normal')

    %title([type ' ' num2str(dim_StatBaselines(2)) '-day
distribution'])
    title(['Compared with ' type ' baseline distribution'])
    xlabel('Sample')
    ylabel('Voltage')

    hold on
    if(normFlag && problem == 1)
```

```
        for i = 1:num_days
            daysMatrix(:,i) = daysMatrix(:,i) - MeanBaseline;
%Normalize, if requested
        end
    end
    plot(mean(daysMatrix'),'m','linewidth',3)
    hold off

end

else
    ProbFields = 0;
end
```